

**SYSTEMS ANALYSIS OF β -BLOCKERS AND β -ADRENERGIC
RESPONSIVENESS IN CARDIAC MYOCYTES**

A Dissertation Presented to the Faculty of
The School of Engineering and Applied Science
University of Virginia

In Partial Fulfillment
of the Requirements for the Degree of
Doctor of Philosophy in Biomedical Engineering

by

ROBERT KWESI ADUAMA AMANFU
DECEMBER 2013

APPROVAL SHEET

This dissertation is submitted in partial fulfillment of the requirements for the degree of
Doctor of Philosophy in Biomedical Engineering

Robert Kwesi Aduama Amanfu

Author

This dissertation has been read and approved by the Examining Committee:

Jeffrey J. Saucerman, Ph.D.

Dissertation Advisor

Jason A. Papin, Ph.D.

Committee Chair

Brent A. French, Ph.D.

Kevin A. Janes, Ph.D.

Chris M. Kramer, M.D.

Accepted for the School of Engineering and Applied Science:



Dean, School of Engineering and Applied Science

DECEMBER

2013

晋蓉原

非

Abstract

Heart failure, the inability of the heart to provide adequate blood flow to meet the body's demand, is one of the leading causes of hospitalization and mortality in the United States. β -adrenergic receptor blockers (β -blockers) are commonly used to treat chronic heart failure but the biological mechanisms governing the efficacy of β -blockers is poorly understood. This impedes the design of improved and personalized heart failure therapies.

The β_1 -adrenergic receptor pathway has a dominant role in the regulation of heart contractility. Elevated catecholamine release, a hallmark of heart failure, has been shown to desensitize the β -adrenergic pathway causing an inability to increase contractility and cardiac output in response to acute stress. Two conflicting theories commonly postulated are that β -blockers are effective by either inhibiting the harmful consequences of sustained stimulation or maintaining the beneficial aspects of β_1 -adrenergic receptor pathway activation.

The focus of this dissertation is to quantitatively examine how cardiac β -adrenergic signaling is modulated by β -blockers, receptor polymorphisms and altered expression of pathway components. This was done via the following 3 aims: 1) test the hypothesis that the β -blocker propranolol both inhibits and maintains β_1 -adrenergic signaling in normal cardiac myocytes, 2) test the hypothesis that β_1 -adrenergic signaling is differentially modulated by clinically relevant β -blockers and receptor polymorphisms 3) test the hypothesis that integration of human heart failure patient transcriptional profiles with mechanistic computational models is sufficient to predict reduced β -adrenergic responsiveness.

The complexity of the β -adrenergic receptor pathway coupled with the influence of receptor polymorphisms makes it difficult to intuit the effect of β -blockers on observed cardiac physiology. We began by using a systems pharmacology approach to test the hypothesis that both proposed mechanisms for β -blocker efficacy can occur concurrently. To do this, a published computational model of the β_1 -adrenergic receptor pathway developed in our group was extended to include detailed receptor interactions. Model predictions, validated with Ca^{2+} and FRET imaging of isolated rat cardiac myocytes, surprisingly suggest that β -blockers can both inhibit and maintain signaling depending on the magnitude of receptor stimulation. In addition, these responses are modulated by receptor polymorphisms. To comprehensively investigate how alterations to the β -adrenergic signaling pathway contribute to the loss of adrenergic responsiveness in heart failure, we mapped differential gene expression in heart failure onto protein species in the computational model. Etiology-specific computational models were able to capture altered features of Ca^{2+} signaling in failing human myocytes. Together, this body of work provides insight into how β -adrenergic signaling is altered in heart failure and the impact of β -blockers. We discovered significant patient population-specific differences in response to β -blockers and alterations to the β_1 -adrenergic receptor pathway. Evaluating the mechanisms for these differences, with the help of computational models, is an important step towards designing personalized heart failure therapies.

Acknowledgements

This thesis is a reflection of the tremendous support of advisors, colleagues, friends and family. Foremost, I thank my advisor Jeffrey Saucerman for the opportunity to learn about the field of systems biology. Jeff is a terrific mentor who strikes the perfect balance between active management and allowing scientific freedom. In the same breath, I thank my committee members: Jason Papin, Brent French, Kevin Janes and Chris Kramer. Their constructive critique and support was crucial in developing the story presented in this thesis.

Other collaborators in the Saucerman lab provided key contributions to specific aspects of this project. Renata Polanowska-Grabowska and Lindsay McLellan supplied materials and cells used in Chapters 3-5. Undergraduates Jason Muller (Chapter 3), Sean Meredith and Ryan Connolly (Chapter 4) helped develop some of the methods utilized. Past and present members of the lab provided crucial feedback on the project including Jason Yang, Karen Ryall, Eric Greenwald, Anthony Soltis, Brooks Taylor, Lulu Chu and Sa Ra Park.

Finally, on a personal note, I thank my parents whose sacrifices bear fruition in the ensuing pages. I will forever be indebted

Table of Contents

Abstract	iv
Acknowledgements	v
Table of Contents	vi
List of Figures	ix
List of Tables.....	xii
List of Abbreviations.....	xiii
1. INTRODUCTION	1
1.1 β -adrenergic receptor signaling controls cardiac performance	1
1.2 β -adrenergic receptor de-sensitization is a hallmark of heart failure.....	2
1.3 Conflicting theories of the mechanism of β -blocker function.....	4
1.4 Scope of the dissertation	8
2. CARDIAC MODELS IN DRUG DISCOVERY AND DEVELOPMENT.....	10
2.1 Introduction.....	10
2.2 Therapies targeted against arrhythmias	11
2.3 Therapies targeted against ischemia and metabolic disorders.....	21
2.4 Therapies targeted against signaling disorders	24
2.5 Future directions	32
3. AUTOMATED IMAGE ANALYSIS OF CARDIAC MYOCYTE Ca^{2+} SIGNALING.....	36
3.1 Introduction.....	36
3.2 Materials and methods.....	37
3.2.1 Data acquisition.....	37
3.2.2 Automated cell segmentation	40
3.2.3 Ca^{2+} signal analysis.....	40
3.3 Results	42
3.3.1 CCD-based imaging of Ca^{2+} transients	42

3.3.2	<i>Ventricular myocyte shape analysis</i>	44
3.4	Discussion	49
4.	MODELING THE EFFECT OF β_1-ADRENERGIC RECEPTOR BLOCKERS AND POLYMORPHISMS ON CARDIAC MYOCYTE CALCIUM HANDLING	51
4.1	Introduction	51
4.2	Methods and materials	53
4.2.1	<i>Computational modeling of β-blockers</i>	53
4.2.2	<i>Isolation and culture of rat cardiac myocytes</i>	54
4.2.3	<i>Camera-based Ca^{2+} imaging of myocytes</i>	56
4.2.4	<i>FRET imaging of cardiac myocytes</i>	57
4.3	Results	58
4.3.1	<i>Validation of β_1-adrenergic model with extended ternary complex receptor model</i>	58
4.3.2	<i>Propranolol inhibits and maintains the β-adrenergic response depending on the magnitude of receptor stimulation</i>	60
4.3.3	<i>β-blockers differ in their ability to inhibit and maintain β-adrenergic responsiveness</i>	63
4.3.4	<i>Metoprolol and carvedilol differ in their ability to maintain β-adrenergic responsiveness</i>	68
4.3.5	<i>Receptor polymorphisms are differentially modulated by diverse β-blockers</i>	70
4.4	Discussion	72
4.4.1	<i>Mechanisms of β-blocker efficacy in heart failure</i>	72
4.4.2	<i>Metoprolol and carvedilol have distinct mechanisms of action</i>	73
4.4.3	<i>Pharmacogenomic targeted treatment with β-blockers</i>	74
4.4.4	<i>Limitations and Considerations</i>	75
4.4.5	<i>Conclusions</i>	76
5.	INTEGRATION OF HUMAN TRANSCRIPTOME AND SYSTEMS MODELS TO ANALYZE ADRENERGIC RESPONSIVENESS IN HUMAN HEART FAILURE	77
5.1	Introduction	77
5.2	Materials and methods	79
5.2.1	<i>Computational model of β_1-adrenergic signaling and EC coupling in rabbit mouse ventricular myocytes</i>	79
5.2.2	<i>Gene-protein parameter mapping</i>	81
5.2.3	<i>Gene expression data</i>	84
5.2.4	<i>Simulation conditions</i>	84
5.2.5	<i>Sensitivity analysis</i>	85
5.2.6	<i>Statistical analysis</i>	85
5.3	Results	85
5.3.1	<i>Validating computational models of human heart failure</i>	85

5.3.2	<i>Single gene-protein-parameter perturbations identify therapeutic targets for restoring adrenergic responsiveness</i>	87
5.3.3	<i>Model outputs predict patient clinical measures</i>	89
5.4	Discussion	92
5.4.1	<i>Genes contributing to altered β_1-adrenergic signaling and EC coupling</i>	95
5.4.2	<i>Computational models can relate patient transcriptional profiles to clinical measures</i>	96
5.4.3	<i>Limitations and Considerations</i>	97
5.4.4	<i>Conclusions</i>	98
6.	SUMMARY AND CONCLUSIONS	99
6.1	Contribution to understanding of the mechanisms of β-blocker efficacy in heart failure	99
6.2	Contributions to understanding how altered expression of β_1-adrenergic pathway components causes the heart failure phenotype	100
6.3	Contributions to live-cell imaging of signaling networks in cardiac myocytes	101
6.4	Limitations	102
6.5	Future directions	103
	APPENDIX	105
	CV	109
	REFERENCES	112

List of Figures

Figure 1.1: β -adrenergic receptor signaling pathway	3
Figure 1.2: Conflicting theories explaining β -blocker efficacy in heart failure	6
Figure 1.3: Timeline; β -blocker treatment in heart failure	7
Figure 2.1: Cardiac ventricular action potential and electrocardiogram	13
Figure 2.2: Schematic of cardiac electrophysiology and contraction	15
Figure 2.3: Schematic of β -adrenergic, α -adrenergic and Ang receptor signaling network.	25
Figure. 3.1: Flow diagram for the proposed method	38
Figure 3.2: Automated image segmentation	41
Figure 3.3: Analysis of the effects of down-sampling PMT data.	43
Figure 3.4: Raw fluorescent intensity values for Ca^{2+} transients obtained from 4 ventricular myocyte ROIs	45
Figure 3.5: Histogram of cell size and shape features calculated from automated segmentation of 176 myocytes	46
Figure 3.6: Correlation plots	48
Figure 4.1: Model of β_1 -adrenergic signaling and EC coupling with extended ternary complex model (ETCM)	55
Figure 4.2: Experimental validation of coupled β_1 -adrenergic signaling and EC coupling model	59
Figure 4.3: Propranolol both inhibits and maintains β_1 -adrenergic-mediated regulation of Ca^{2+} transients	61
Figure 4.4: Propranolol both inhibits and maintains the β_1 -adrenergic-mediated Ca^{2+} and PKA response following 24 hour ISO pre-treatment	62

Figure 4.5: Ligand binding affinity and inverse agonism both predicted to influence ligand cAMP sensitivity	64
Figure 4.6: Predicted effect of propranolol on kinetics of selected model state variables	65
Figure 4.7: Predicted effect of metoprolol on kinetics of selected model state variables	66
Figure 4.8: Predicted effect of carvedilol on kinetics of selected model state variables	67
Figure 4.9: Metoprolol and carvedilol differentially influence β_1 -adrenergic responsiveness	69
Figure 4.10: β_1 AR-Arg389 polymorphism responds differently to β -blockers	71
Figure 5.1: Model schematic	80
Figure 5.2: Etiology-specific computational models capture altered features of Ca^{2+} signaling in failing human myocytes	86
Figure 5.3: Single gene-protein-parameter perturbations of computational model based on idiopathic cardiomyopathy patient gene profiles	88
Figure 5.4: Single gene-protein-parameter perturbations of computational model based on hypertrophic cardiomyopathy patient gene profiles	90
Figure 5.5: Single gene-protein-parameter perturbations of computational model based on ischemic cardiomyopathy patient gene profiles	91
Figure 5.6: Gene expression-based models model predict patient-specific adrenergic responsiveness	93

Figure 5.7: Gene-expression based models predict patient clinical measures.

94

List of Tables

Table 2.1: Examples of cardiac computational models used to investigate the effect of drugs and therapies.	12
Table 5.1: Gene-protein-parameter mapping: signaling module	82
Table 5.2: Gene-protein-parameter mapping: EC coupling module	83

List of Abbreviations

AC	adenylyl cyclase
β -AR	β -adrenergic receptor
β_1 -AR	β_1 -adrenergic receptor
β ARK	β -adrenergic receptor kinase
CaM	calmodulin
CaMKII	Ca ²⁺ /calmodulin protein kinase II
cAMP	cyclic adenosine monophosphate
CAR	carvedilol
CFP	cyan fluorescent protein
EC	excitation-contraction
ECC	excitation-contraction coupling
ETCM	extended ternary complex model
FRET	Forster resonance energy transfer
FSK	forskolin
GPP	guanosine 5'-[β,γ -imido] triphosphate
IBMX	3-isobutyl-1-methylxanthine
ISO	isoproterenol
MET	metoprolol
PRO	propranolol
PKA	protein kinase A
PLB	phospholamban
SERCA	sarcoplasmic reticulum Ca ²⁺ ATPase

1. Introduction

1.1 β -adrenergic receptor signaling controls cardiac performance

Heart failure is a condition in which cardiac output is not sufficient to supply the body's tissues with enough blood¹. Approximately 5 million Americans have the disease and although death rates have declined, the disease burden remains high with an estimated 20% of all hospital admissions of persons older than 65 due to heart failure². The disease is a clinical syndrome that represents the final pathway of a myriad of diseases that affect the heart² including myocardial infarction and hypertension. Despite the varying etiologies and disease progression, key clinically observed symptoms include fatigue, breathlessness and exercise intolerance. Along with ACE inhibitors, aldosterone receptor blockers and diuretics, β -adrenergic receptor blockers (β -blockers) represent the front line treatment for heart failure³.

The β -adrenergic receptors are a family of G-protein coupled receptors found in cardiac, airway smooth muscle and adipose tissue. They are characterized by seven transmembrane spanning domains forming a ligand binding pocket⁴. Three isoforms of the β -adrenergic receptor (β_1 , β_2 and β_3) have been found in the mammalian heart however, the β_1 and β_2 -adrenergic receptor isoforms are the most abundant (75:25)⁵. Binding of the catecholamines epinephrine or norepinephrine, the endogenous agonists, results in the coupling of the β -adrenergic receptors to the guanine nucleotide binding protein G_s , with the subsequent release of the $G_{\alpha s}$ subunit following hydrolysis of guanosine triphosphate. $G_{\alpha s}$ then activates the membrane anchored effector enzyme adenylyl cyclase. Activation of adenylyl cyclase converts adenosine triphosphate into the second messenger 3'-5'-cyclic adenosine monophosphate (cAMP). cAMP causes the

dissociation of the regulatory and catalytic subunits of protein kinase A (PKA) allowing PKA's catalytic subunit to phosphorylate various protein targets including L-type calcium channel, phospholamban (inhibitor of the ryanodine receptor- RyR) and troponin I (TnI). Phosphorylation of the L-type calcium channel and phospholamban results in increased calcium flux; phosphorylation of troponin increases the calcium sensitivity of the cardiac myocyte contractile apparatus⁶. The net result of classical β -adrenergic receptor activation in the heart is increased myocyte beating rate, contractility (inotropy), relaxation and the modulation of cell metabolism (Figure 1.1). The β -adrenergic receptor pathway is optimized for short term needs but sustained stimulation results in a less optimal response⁷. To compensate for reduced cardiac output in heart failure, there is increased catecholamine release to stimulate the β -adrenergic receptor pathway⁸. Sustained stimulation has detrimental long term consequences including apoptosis and hypertrophy^{9,10}.

1.2 β -adrenergic receptor de-sensitization is a hallmark of heart failure

Signal transduction needs an off switch to ensure the precise regulation of cell function, and in the case of β -adrenergic receptor signaling, halt the harmful consequences of chronic pathway activation¹¹. There are multiple negative feedback systems that curtail β -adrenergic receptor signaling. These include the activation of phosphodiesterases (PDE's) which degrade cAMP, thus halting signaling at an early

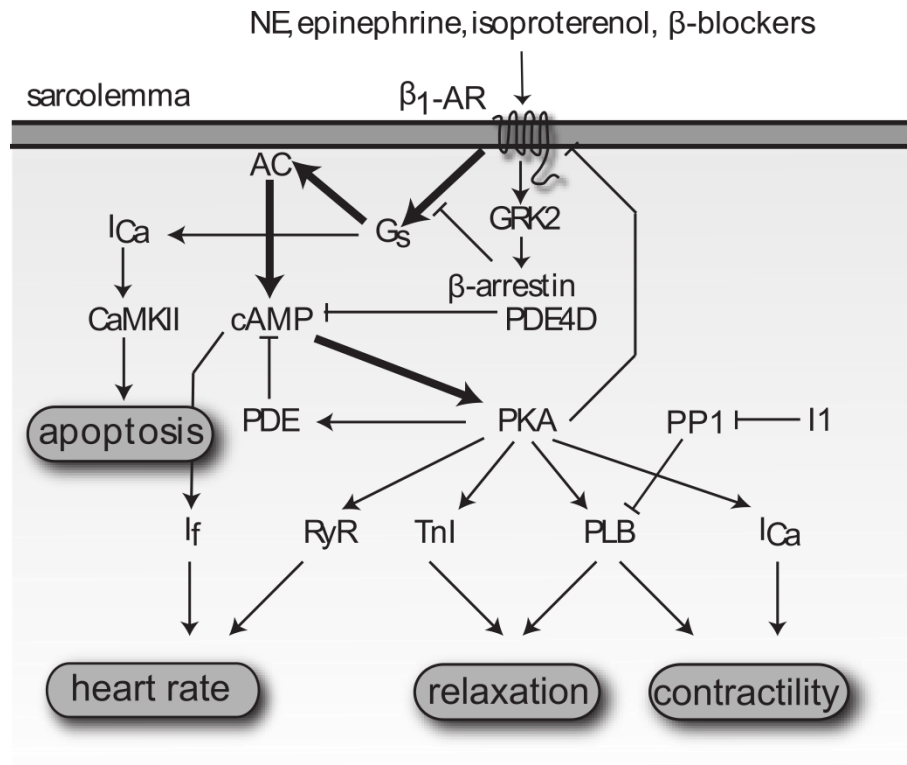


Figure 1.1: **β -adrenergic receptor signaling pathway**. Pathway is characterized by multiple negative feedback mechanisms including phosphodiesterases (PDE4) and phosphatases like PP1.

stage¹². Phosphatases (for example PP1) also dephosphorylate proteins activated by PKA mediated phosphorylation¹³. Desensitization, defined here as the inability of the receptor to activate downstream components in the presence of a stimulus, is another mechanism. Desensitization occurs via receptor uncoupling (acute response) and down-regulation (chronic response)⁴. Phosphorylation of the receptor by G-protein receptor kinase 2 (GRK2), and to a lesser degree PKA, leads to receptor uncoupling. The phosphorylated receptor is then bound by β -arrestin resulting in the dissociation of G_s protein thereby halting activation of adenylyl cyclase and hence further signaling¹⁴. Down-regulation, which occurs slowly (taking hours to days), is due to altered expression of signaling pathway components. The most prominent altered protein is the β_1 -adrenergic receptor, which is downregulated 50% in heart failure patients¹⁵. Other altered pathway components include sarcoplasmic reticulum Ca^{2+} ATPase (SERCA)¹⁶, GRK2¹⁷, PP1¹⁸ and the PP1 inhibitor I1³⁰. These changes in the signaling network blunt the intended inotropic effect of chronic elevated catecholamine release. In an end-stage failing heart, 50-60% of the total β -adrenergic signal transducing potential is lost¹⁹.

1.3 Conflicting theories of the mechanism of β -blocker function

The adoption of β -blockers as standard treatment for heart failure faced early resistance because they were believed to be contraindicated. Studies began to slowly confirm that blockade of the β -adrenergic receptor could increase cardiac function in heart failure leading to the eventual acceptance of β -blockers²⁰. However, the biological mechanisms governing the counterintuitive success of β -blockers are poorly understood^{3,21,22}. Two conflicting theories commonly postulated are that β -blockers are effective by either

inhibiting the deleterious consequences of sustained stimulation or maintaining β_1 -adrenergic receptor signaling (Figure 1.2)²³. The inhibition hypothesis is supported by clinical and experimental evidence that β -blockers help prevent or reverse the cardiac remodeling that leads to heart failure²⁴. Conversely, the maintenance hypothesis is given credence by clinical evidence that β -blockers increase β_1 -adrenergic receptor levels²⁵ and exercise tolerance²⁶. First generation β -blockers like propranolol are non-selective for the different β -adrenergic isoforms (Figure 1.3). They were replaced with second generation compounds; examples include bisoprolol and metoprolol, which selectively target the β_1 -adrenergic receptor¹⁹. This was done to reduce the contraindication of non-selective blockers in asthmatics and to target the more abundant β_1 -adrenergic receptor. Third generation β -blockers were developed with ancillary properties like vasodilation (achieved through antagonism of the α -adrenergic receptors) to additionally treat hypertension¹⁹. Carvedilol, a third generation compound, is however more selective for the β_1 -adrenergic receptor at moderate doses²⁷. Carvedilol, bisoprolol and metoprolol have all shown significant efficacy in reducing mortality in heart failure patients²⁸⁻³⁰. There is a greater diversity of properties among the 17 FDA approved β -blockers beyond just receptor specificity³¹. This diversity complicates attempts to determine which β -blockers are efficacious in the treatment of heart failure. One important property is the ability of β -blockers to behave as inverse agonists³². Inverse agonism is the ability of a ligand to reduce the basal level of signaling following receptor binding³³. This property necessitates the classification of ligands as a continuum ranging from agonists to inverse agonists.

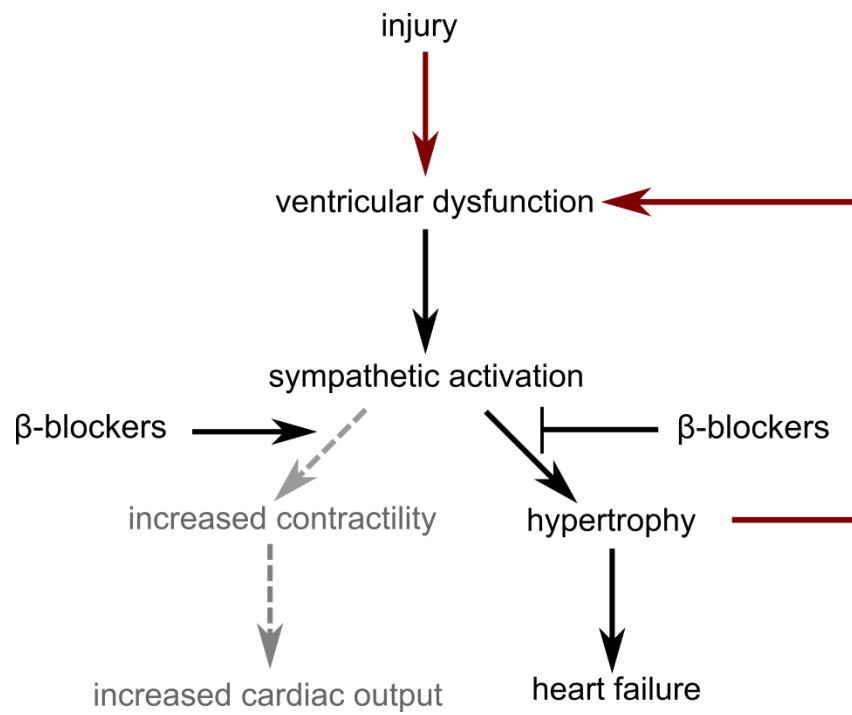


Figure 1.2: **Conflicting theories explaining β -blocker efficacy in heart failure.**

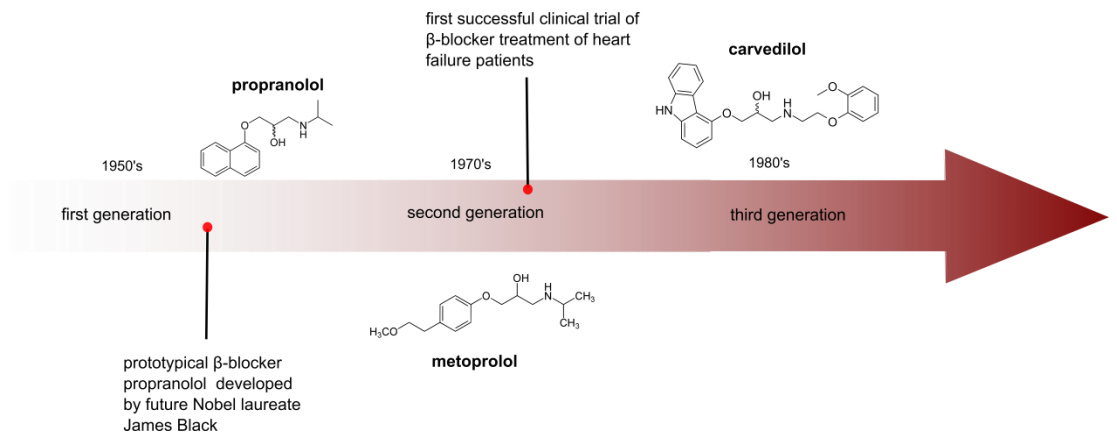


Figure 1.3: Timeline; β -blocker treatment in heart failure

Inverse agonism may explain differences in drug efficacy and mode of action in conditions where β_1 -adrenergic receptor antagonism alone is not a sufficient explanation³⁴.

Genetic differences among patients also impacts β -blocker efficacy³⁵. A common polymorphism of the β_1 -adrenergic receptor is the glycine for arginine substitution at amino acid 389³⁶. *In vitro* experiments in cell expression systems show that the β_1 Arg389 variant has a higher fold increase in adenylyl cyclase after receptor stimulation but is desensitized the most^{36,37}. Carvedilol, bisoprolol and metoprolol have equal affinity for both receptor variants³⁸ *in vitro* but carvedilol has a larger effect on receptor conformation of the β_1 Arg389 variant³⁹. This suggests potential compound-specific phenotypes for the β_1 -adrenergic receptor polymorphisms⁷. The complexity of the β -adrenergic receptor pathway coupled with the influence of receptor polymorphisms makes it difficult to intuit the effect of β -blockers on observed cardiac physiology. Computational models are however ideally suited for this task. *The focus of this dissertation is to quantitatively examine how cardiac β -adrenergic signaling is modulated by β -blockers, receptor polymorphisms and altered expression of pathway components.*

1.4 Scope of the dissertation

The objective of this dissertation was to develop a systems level understanding of β -adrenergic signaling in the context of β -blockers, receptor polymorphisms and pathway remodeling using mechanistic computational models and *in vitro* live cell imaging. This required significant extension of existing computational models, mapping of human

genomic data onto computational models, and the development of a novel Ca^{2+} imaging technique. Computational modeling allows perturbation and observation of pathway components in a manner that is impossible with current experimental approaches. Ca^{2+} and PKA imaging experiments in cardiac myocytes was used to test model predictions and helped modify model assumptions. This interplay between computational modeling and experimental validation allowed a comprehensive study of the potential mechanisms governing β -blocker efficacy.

In Chapter 2, we will discuss how cellular models of electrophysiology, cell signaling and metabolism have been used to investigate therapies for cardiac diseases. Chapter 3 will present a method for high-throughput measurement, automated cell segmentation and signal analysis of Ca^{2+} transients in isolated adult ventricular myocytes. The modeling of β -blockers will be explored in Chapter 4 where it's impact on β_1 -adrenergic signaling and receptor polymorphisms will be investigated. In Chapter 5, alterations in the β_1 -adrenergic signaling pathway in disease will be studied by mapping differential gene expression in various human cardiomyopathies onto the protein species present in a computational model of β_1 -adrenergic signaling and excitation contraction coupling. Finally, Chapter 6 summarizes the work and provides a perspective on its contribution towards understanding mechanisms governing β -blocker efficacy and the use of systems analysis to understand adrenergic responsiveness in heart failure.

2. Cardiac models in drug discovery and development

2.1 Introduction

Computational modeling has played an important role in understanding heart physiology and pathology since the first model of the cardiac action potential 50 years ago⁴⁰. These models have been invaluable in understanding an organ whose function is the result of a complex system of nonlinear feedback loops that span single ion channels, cardiac cells and the whole heart⁴¹. Despite its remarkable robustness, the heart is afflicted by various diseases that are complex and multifaceted⁴². Heart disease remains the leading cause of premature death in developed societies. Approximately 2300 Americans die of cardiovascular disease each day, an average of one death every 38 seconds⁴³. The failure of many therapies targeting cardiac arrhythmia⁴⁴, contrasted with the success of counter-intuitive therapies like β -blockers in heart failure⁴⁵, highlights the difficulty in developing therapies for cardiovascular disease. A common cause of drug withdrawal from the market is due to their propensity to cause fatal cardiac arrhythmia⁴⁶ resulting in significant financial loss⁴⁷ and complicating new drug development⁴⁸.

Computational modeling can serve as a useful tool for developing new therapies, evaluating current treatment of cardiovascular diseases and predicting drugs with adverse cardiovascular consequences. This idea is beginning to gain traction with the formation of the preDICT project, a consortium of pharmaceutical companies and academic institutions charged with the mission to model, simulate and predict the impact of pharmacological compounds on heart rhythm⁴⁹. Computational modeling has also been identified as a key component of the Critical Path Initiative, a project launched by the US

Food and Drug Administration to improve drug and medical device development⁵⁰. The Critical Path Initiative lists six broad areas where innovation is needed including harnessing bioinformatics. Clinical trial simulation using *in silico* disease models was identified as a specific scientific opportunity to aid in this endeavor⁵¹. This represents a shift in the drug approval process from requiring only empirical evidence to an increased emphasis on mechanistic understanding of drug action⁵².

Models now exist for many aspects of cellular cardiac biology including electrophysiology, metabolism and signaling networks. These processes do not function in isolation, and there are significant efforts to integrate these models to simulate heart function in increasing detail⁵³. This chapter will discuss how models at cellular and tissue scales of cardiac biology can be used to assess current therapies, test therapies in development and suggest new targets (Table 2.1).

2.2 Therapies targeted against arrhythmias

Modeling the electrical activity of the heart (cardiac electrophysiology) is perhaps the most advanced area of cardiac computational biology, and it has been the most successful in drug development⁵⁴. The role of cardiac electrophysiology is to coordinate the mechanical pumping of the heart in a process called excitation-contraction coupling⁵⁵. The key emergent property of cellular electrophysiology is the action potential, which reflects an intricate interplay between an array of ion channels (Figure 2.1). Fast activating sodium channels in the cell membrane are the first to open when a

Table 2.1: Examples of cardiac computational models used to investigate the effect of drugs and therapies.

Target	Pathology	Drug/Treatment	Reference
I_{Na}	LQT3	mexiletine	70
I_{Na}	LQT3	ranolazine	78
I_{Kr}	acquired LQTS	E-4031	82
I_{Kr}	LQTS	sotalol (pro-arrhythmic)	87
I_{Kr}	LQTS	NS1643	89
I_{K-ATP}	ischemia	pinacidil	104
I_{Na-H}	ischemia	blocker of Na-H exchanger	106
$I_{Na(f,L)}$	ischemia	blocker of late sodium channel	108
Cr, Adenine, exchangeable P	heart failure	elevating all 3 pools	114
CaMKII	T-wave alternans	CaMKII inhibitor	122
CaMKII	myocardial infarct	CaMKII inhibitor	126
AC	heart failure	AC overexpression	131
CaMKII	heart failure	inhibition of CaMKII phosphorylation of RyR	135
β -adrenergic receptor	LQT1	β -adrenergic receptor blocker	137
β -adrenergic receptor	LQT3	propranolol	140
LCC	LQT8	reduction of LCC current	143
α -adrenergic receptor	pathological hypertrophy	α -adrenergic receptor blocker	148

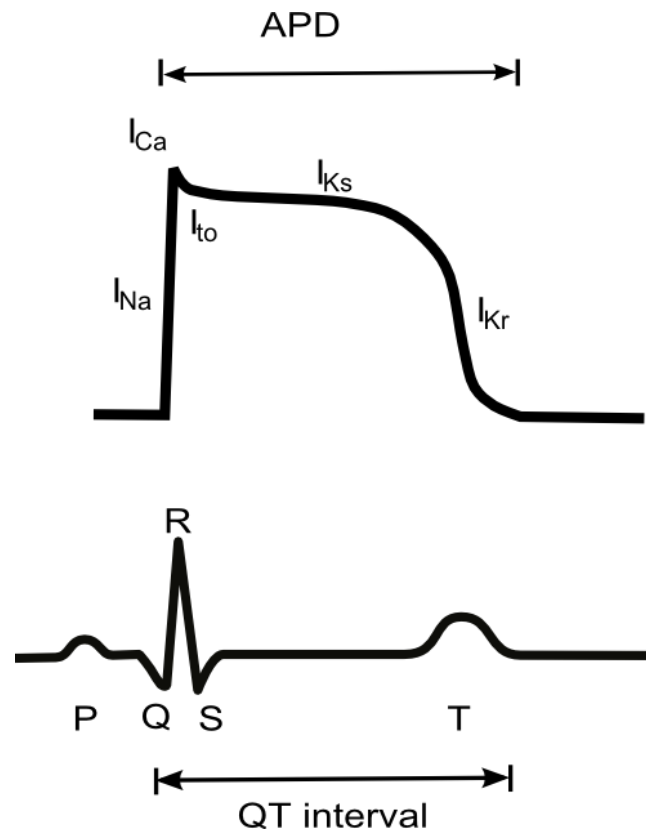


Figure 2.1: **Cardiac ventricular action potential and electrocardiogram.** Predominant ion fluxes at different phases of the action potential are indicated. APD, action potential duration.

cardiac myocyte is slightly depolarized above a threshold. Increased sodium current (I_{Na}) strongly depolarizes the membrane, which activates L-type calcium channels (LCC) to increase calcium current (I_{Ca}). This influx of calcium induces ryanodine receptors to release an even larger amount of calcium from the sarcoplasmic reticulum, specialized calcium stores, into cytosolic space; a process called calcium-induced calcium release (CICR). It is this rise in cytosolic calcium that activates a myocyte's contractile machinery (Figure 2.2). Relaxation occurs when calcium is re-sequestered into the sarcoplasmic reticulum by the sarcoplasmic reticulum calcium ATPase (SERCA) and the cell's membrane potential is repolarized by potassium currents.

There are multiple channels with different properties that carry the repolarizing potassium current including the transient outward potassium current (I_{to}), which influences the early repolarization phase, and the delayed rectifier potassium currents (i.e. I_{Ks} and I_{Kr} .) Alterations in the orchestrated changes in ion flow can cause severe pathology. One such example is Long QT syndrome (LQTS), a family of diseases (LQT1-8) characterized by prolonged action potential duration (APD), which is measured as an increased QT interval on an electrocardiogram⁵⁶. LQTS is caused predominantly by either a reduction of potassium current or an increase in sodium current. This can occur due to genetic mutations or drugs acting on channels that carry both currents. Without treatment, 13% of individuals carrying gene mutations that cause LQTS will suffer cardiac arrest or sudden death due to ventricular tachycardia⁵⁷.

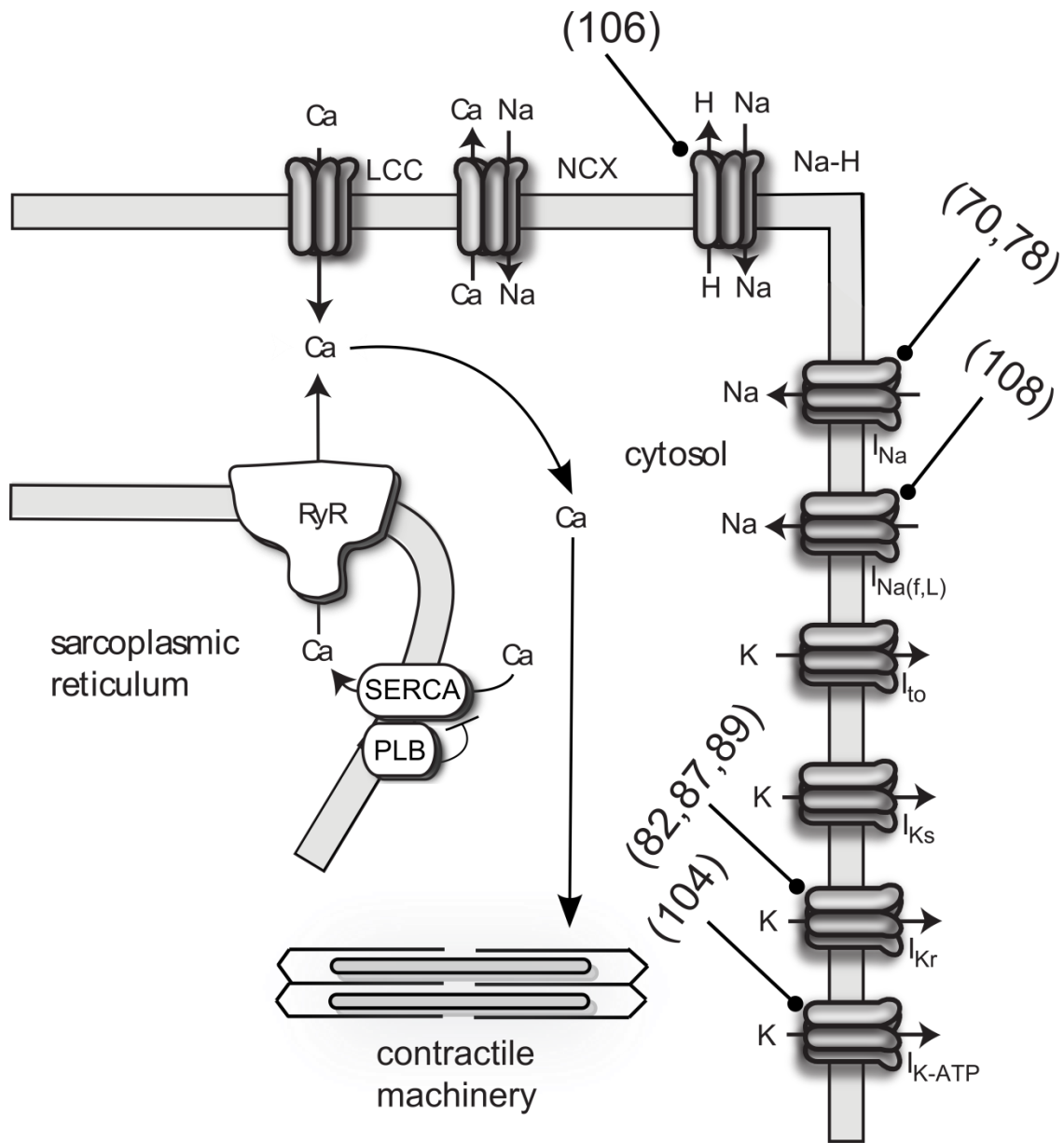


Figure 2.2: **Schematic of cardiac electrophysiology and contraction.** Targets of computational models are indicated with blunt arrows (references in parenthesis). $I_{Na(f,L)}$, late sodium current; I_{K-ATP} , ATP dependent potassium current; PLB, phospholamban; NCX, sodium-calcium exchanger.

Understanding the mechanistic bases of arrhythmias and applying such knowledge to improve therapy is a great challenge in cardiac electrophysiology⁵⁸.

The earliest computational model of cardiac electrophysiology by Noble was based on the Hodgkin-Huxley model for the neuron action potential, predating the discovery of the calcium current⁴⁰. The first ventricular cell model, developed using experimental data from a variety of mammals, was published in 1977 by Beeler and Reuter and included the effect of intracellular calcium dynamics on the action potential⁵⁹. Luo and Rudy subsequently developed biophysically detailed models of a guinea pig ventricular myocyte by taking advantage of improved measurement of ionic currents from patch clamping^{60,61}. By replacing the description of the calcium current in the Luo-Rudy models with detailed models of the L-type calcium channel and ryanodine receptor, Jafri et al.⁶² were able to mechanistically represent calcium-induced calcium release. A notable feature of the Jafri-Rice-Winslow model was the inclusion of Markov state models of the L-type calcium channel and ryanodine receptor. This is a departure from Hodgkin and Huxley's approach which used phenomenological descriptions of ion channel function⁶³. Ion channels are composed of protein subunits whose conformational changes "gate" ionic currents, causing shifts between inactive, closed or open states⁶⁴. The probability of a channel being in a certain state often depends on the previous state⁶⁵. Experimental observations of channel gating and aspects of channel structure can be replicated by modeling this channel property as a probabilistic Markov process⁶⁶.

Markov models can simulate the molecular basis of arrhythmias caused by mutations in ion channels and the effect of pharmaceutical compounds⁶⁶. There is evidence that drug binding affinity is often determined by the conformational state of the

ion channel⁶⁷. This level of drug-channel interaction is important when developing drugs for patients suffering from LQT3, the most lethal subtype of LQTS⁶⁸. LQT3 is caused by mutations in the gene SCN5A, which encodes the α -subunit for the sodium channel. One such mutation results in deletion of three amino acid residues in the channel protein (Δ KPQ mutants) which causes a small persistent current during the plateau phase of the action potential, delaying repolarization⁶⁹. Clancy et al.⁷⁰ examined the mechanisms of drug block of the sodium channel by modifying Markov models of both the wild type and the Δ KPQ mutant channels⁷¹. The Δ KPQ channel model was able to simulate the experimentally observed faster recovery from inactivation compared to the wild-type channel. By including additional model states for drug binding, they investigated the drugs mexiletine (an open state blocker) and lidocaine (an inactivation state blocker). The model predicted that lidocaine induces a rightward shift in voltage-dependent sodium channel availability, consistent with experimental data. The Markov models for SCN5A were then integrated with the Luo-Rudy model of the ventricular action potential. Simulations suggested that low doses of mexiletine can shorten the action potential duration in LQT3 without affecting the peak sodium current, which underlies the action potential upstroke. Conversely, lidocaine was predicted to have a lesser effect on action potential duration but blocked the peak current at high doses. This study illustrated how specific mechanisms of drug action can have a significant impact on cellular physiology.

Electrophysiology models have now been developed for a variety of animal species, allowing representation of species-specific propensity for arrhythmia and other aspects of pathophysiology⁶³. The scarcity of human data, due to the lack of non-invasive techniques, increases the need for computational models of the human heart to gain

further insight into cardiac disease⁷². Models of the human ventricular myocyte have been developed by Priebe et al.⁷³, ten Tusscher et al.⁷⁴, Iyer et al.⁷⁵ and Grandi et al.⁷⁶. Like most models in biology, these models are constrained by limited available experimental data and each has specific applications for which their use is appropriate. The ten Tusscher-Noble-Noble-Panfilov (TNNP) model has the advantages of being based mostly on data obtained from human ventricular myocytes and is less complex due to the use of Hodgkin-Huxley-type equations for ion channels⁷⁷. Fredj et al.⁷⁸ replaced the sodium channel equations in the TNNP model with the Clancy-Rudy SCN5A Markov model⁷¹ to investigate the potential therapeutic effect of ranolazine, an antianginal drug, on LQT3 human patients with Δ KPQ mutant sodium channels. *In vitro* experiments with a cell line expressing mutant channels confirmed their hypothesis that ranolazine is a use-dependent blocker that reduces sustained sodium current without affecting peak current. Simulations with the model containing the mutant Δ KPQ sodium channel showed a decrease in ventricular cell action potential duration in the presence of ranolazine. This suggests its potential as a treatment for LQT3 arrhythmias.

The rapid delayed rectifier potassium current (I_{Kr}) is encoded by the Human Ether-a-go-go Related Gene (hERG) and its mutations cause LQT2⁷⁹. Drugs that inhibit this repolarizing potassium current prolong action potential duration and the QT interval (causing acquired LQTS), which can increase the risk to develop arrhythmia⁸⁰. hERG channels can exist as heteromers consisting of hERG 1a and 1b or as homomers of hERG1a. Despite evidence that the hERG 1a/b heteromers underlie the cardiac repolarizing current⁸¹, little is known about how hERG hetero/homomers differ and how the hERG 1b subunit influences channel properties (especially in the context of

pharmaceutical channel block). *In-vitro* experiments by Sale et al. showed that hERG heteromers have a quicker transition to an open state than hERG homomers⁸². This suggests that an open channel blocker should be more effective against hERG heteromers but paradoxically, experimental results showed that hERG homomers were more inhibited by open channel block. To explain this mechanistically, the authors turned to the TNNP model, replacing the original I_{Kr} model with a Markov model that represents both hERG heteromers and homomers. They discovered that the additional channel gating mode of hERG 1a homomers results in more complete block by the open channel blocker E-4031, thus increasing the risk for acquired LQTS.

One of the challenges of understanding arrhythmia and developing effective therapies is linking molecular mechanisms from single cell to tissue levels⁷². A cross-section of the ventricular wall reveals at least three different cell types: epicardial, endocardial and midmyocardial⁸³. These cells have different electrophysiological characteristics due to the differential expression of various channel proteins⁸⁴ including the repolarizing potassium currents⁸⁵. This heterogeneity results in tissue level characteristics including delay of repolarization across the ventricular wall or transmural dispersion of repolarization⁸⁶. Drugs that delay repolarization produce a substrate for reentrant arrhythmias⁸³. The electrical signal measured transmurally across the wall reflects properties of the whole body electrocardiogram with respect to QT interval and T wave morphology⁴². This tissue heterogeneity can be modeled in its most basic form by using a 1D cable electrophysiology model. This consists of a string of cells with changes made to channel expression in order to simulate the different ventricular cell types⁴². Brennan et al.⁸⁷ used a 1D fiber model to investigate sotalol, an anti-arrhythmic drug that

targets I_{Kr} . They developed a Markov model of human hERG to represent the binding kinetics of sotalol⁸⁸, which was then included in the TNNP human myocyte model. Single cell simulations indicated that sotalol prolongs action potential duration, similar to experimental data obtained from human ventricular tissue, and is thus pro-arrhythmic. By inserting the modified ventricular models into a fiber model, the authors showed that sotalol increased T-wave dispersion and amplitude (all pro-arrhythmia markers), linking molecular properties of sotalol with observed tissue level phenomena. A similar approach was used by Pietersen et al. to investigate NS1643, a hERG channel opener⁸⁹. NS1643 causes an increase in channel conductance⁹⁰ and a depolarizing shift in voltage dependency of inactivation⁹¹ which is anti-arrhythmic at the cellular level. Predicting whether NS1643 can be pro-arrhythmic at the tissue level or which of its effect on channel conductance and inactivation is crucial is difficult. Using simulations of a string of 100 human ventricular cells, the authors determined that NS1643 can be pro-arrhythmic at the tissue level (by increasing the vulnerable window for reentry) with the effect on channel inactivation having a larger contribution. However, simulations suggest that at low external potassium concentrations, the effect on channel conductance is more pronounced and increases the drug's anti-arrhythmic properties by causing a greater reduction of the action potential duration. This indicates a specific condition (hypokalemia) in which the drug would be more beneficial in preventing arrhythmia and illustrates how models can be used to explain drug effects in different experimental conditions. Electrophysiology models can also be used in screening lead compounds as demonstrated by Mirams et al. where a variety of ventricular action potential models were used to predict the arrhythmogenic risk of 31 drugs⁹². Using drug IC_{50} values and

therapeutic concentrations to calculate channel properties under drug influence, the authors identified simulation of action potential duration prolongation as an improved measure of potential risk for Torsade-de-Pointes arrhythmias. The study is also a good example of the utility of collaboration between academia and industry in leveraging computational modeling for drug discovery.

2.3 Therapies targeted against ischemia and metabolic disorders

Computational models of cardiac metabolism have been built to investigate the changes in the metabolic state of a myocyte during pathological conditions like myocardial ischemia⁹³ and heart failure⁹⁴, and its effect on cardiac electrophysiology. Deficiencies in energy input and waste removal results in alterations to the cardiac action potential, contributing to failure of contraction⁹⁵. This condition is most pronounced during ischemia, the block of blood flow to the heart, and is a major trigger for arrhythmias⁹⁶. The heart consumes more energy than any other organ⁹⁷. To acquire this energy, it uses fatty acids and glucose to produce adenosine triphosphate (ATP) in the mitochondria, which is then shuttled to the contractile machinery through the utilization of creatine⁹⁸. When ischemia occurs after complete cessation of blood flow, the concentration of oxygen drops drastically (anoxia) resulting in decreased production of ATP⁹⁹. This is accompanied by elevated extracellular potassium concentration and increased blood acidity¹⁰⁰. Electrophysiological changes during the initial stages of ischemia are extremely rapid, making it difficult to study experimentally⁹³. The large number of simultaneous perturbations to the ischemic myocyte and the difficulty

developing *in vitro* models of ischemia also emphasize the need for computational models in this area.

Expanding on the Luo-Rudy model, Shaw et al.⁹⁹ studied the ionic mechanisms underlying changes in the action potential in acute ischemia. By increasing the extracellular potassium concentration and changing the channel properties of the ATP sensitive potassium current, L-type calcium current and the sodium current, the authors were able to replicate the shortened action potential and conduction failure seen experimentally during ischemia.

The ATP-sensitive potassium channel plays a key role in the effects of ischemia on the heart¹⁰¹. The effects of potassium channel openers in ischemia are controversial with conflicting views on whether they are protective or arrhythmogenic^{102,103}. Trenor et al.¹⁰⁴ used a model of the ATP-sensitive potassium channel¹⁰⁵, incorporating the effect the potassium channel opener pinacidil, and integrating it with the Luo-Rudy model. The single cell model was able to replicate the experimentally observed reduction in action potential duration due to pinacidil. To study the effects of pinacidil in acute regional ischemia, the authors implemented a two-dimensional virtual heart tissue model. They noticed that the effect of pinacidil was strongly dose-dependent and had a strong anti-arrhythmic effect at high doses.

Ch'en et al.¹⁰⁶ opted to concentrate on the effects of acidosis and ATP depletion in ischemia. They incorporated equations describing ATP hydrolysis and intracellular pH into the DiFrancesco-Noble action potential model¹⁰⁷. The combined model, despite its limited scope, was able to correctly simulate ischemia-induced sodium overload (due to activation of the sodium-hydrogen exchanger, which causes calcium overload through

activation of the sodium-calcium pump) seen experimentally. From their simulations, the authors suggested that cardiac arrhythmia can be attenuated by blocking the sodium-hydrogen exchanger. The cardiac action potential is also influenced by a late sodium current which is small but may contribute significantly to sodium/calcium overload during ischemia. Simulations performed by Noble et al.¹⁰⁸ suggest that blocking the late sodium current in conditions where the action potential is prolonged (e.g. with drugs affecting hERG) would be protective against arrhythmia.

The link between metabolism and calcium handling in a myocyte was modeled by Michailova et al.¹⁰⁹. Specifically, they investigated the effect of calcium and magnesium buffering by ATP and ADP and included ATP regulation of ion transporters. However, they did not explicitly simulate mitochondrial activity¹¹⁰. An integrated cardiac cell model that linked electrophysiology and contraction with mitochondrial energy generation was developed by Cortassa et al.¹¹¹. This model was composed of an earlier model of cardiac mitochondrial metabolism which matched experimental data obtained from rat mitochondria¹¹². Another biophysically detailed model of cardiac mitochondria was developed by Beard et al.¹¹³ and was used by Wu et al.¹¹⁴ to investigate the evolution of the metabolic state in pathological hypertrophy, a precursor to heart failure. Heart failure, the inability of the heart to supply the body with enough blood¹¹⁵, is characterized by a complex blend of changes to normal function including reduced mitochondrial ATP synthesis⁹⁴. The model is able to correctly predict the drop in cytoplasmic inorganic phosphate concentration seen in moderate left ventricular hypertrophy. They explored possible metabolic therapies by changing levels of creatine, adenine and exchangeable phosphate and discovered that altering levels of creatine alone was not sufficient,

consistent with experimental studies¹¹⁶. Their simulations suggest elevating levels of all three metabolites could be a beneficial metabolic therapy.

2.4 Therapies targeted against signaling disorders

Modeling of disorders of cell signaling networks in myocytes is still in its infancy⁷² despite the fact that drugs targeting cardiac signaling pathways are among the most heavily prescribed¹¹⁷. Intracellular signaling pathways manage cellular processes like cell growth and contractility¹¹⁸. A unifying feature of some signaling pathways in myocytes is the ubiquity of calcium as a second messenger¹¹⁹. In addition to its role in contraction, calcium can also signal through Ca/calmodulin dependent protein kinase (CaMKII), a serine/threonine protein kinase, which is activated when bound by the calcium/calmodulin complex (Figure 2.3). CaMKII regulates cardiac gene expression through phosphorylation of transcription factors like CREB and HDAC¹²⁰ but also has an important role in calcium mobilization through phosphorylation of proteins like ion channels¹²¹. By modeling the influence of CaMKII on calcium handling, Livshitz et al.¹²² were able to show its potential effect on T wave alternans. T wave alternans are beat-to-beat variations in the amplitude of the T wave of the electrocardiogram and is associated with dispersion of repolarization, ventricular arrhythmia and sudden death¹²². This is hypothesized to originate from variation in action potential duration at the cellular level coupled with variation in calcium transient amplitude.

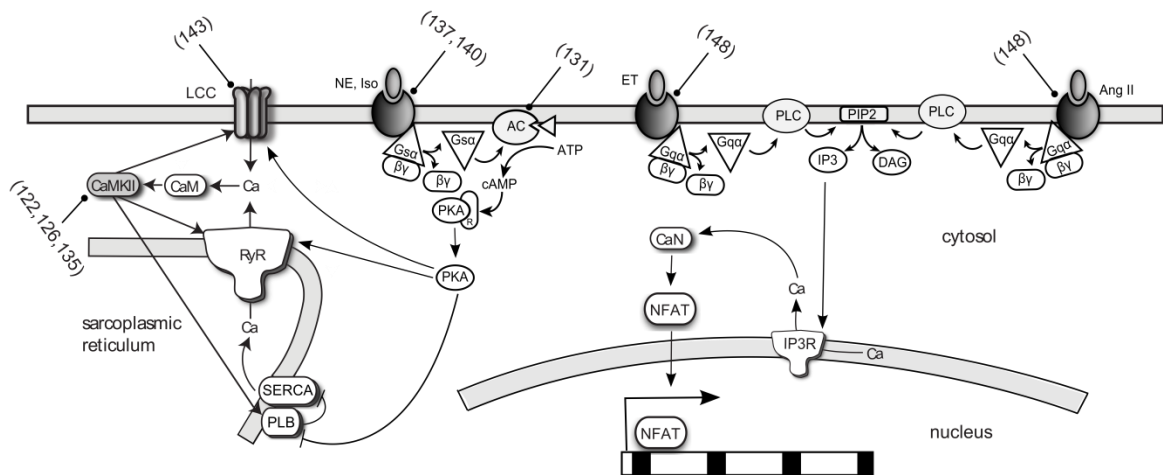


Figure 2.3: Schematic of β -adrenergic, α -adrenergic and Ang receptor signaling network. Targets of computational models are indicated with blunt arrows (references in parenthesis). AC, adenylyl cyclase; CaM, calmodulin; CaN, calcineurin; ET; endothelin ; NE, norepinepherine; IP3R, IP3 receptor; Iso, isoproterenol.

Livshitz et al. reformulated the CICR kinetics in the Hund-Rudy model¹²³, a canine ventricular action potential model that includes the CaMKII regulatory pathway. Their model was able to reproduce the experimentally observed frequency-dependent activation of CaMKII and the effect of CaMKII inhibition on calcium transients. Further simulations showed that increased CaMKII activity causes increased alternans. They identify combined CaMKII inhibition and modulation of repolarizing currents as a possible intervention for suppressing T wave alternans.

CaMKII can auto-phosphorylate in order to retain kinase activity in the absence of calcium¹²⁴. Oxidation can also cause persistent activation independent of auto-phosphorylation¹²⁵. Levels of reactive oxygen species, hydrogen peroxide and superoxide are elevated following myocardial infarction resulting in increased levels of oxidated CaMKII. In order to ascertain the impact of oxidative activation of CaMKII following a myocardial infarct, Christensen et al.¹²⁶ used the Hund-Rudy model with the inclusion of an oxidized active state for CaMKII in addition to the calcium and autophosphorylation-mediated active states. Their cardiac fiber model described two regions of the epicardium: the normal and the border zone. The border zone of a myocardial infarct is the region of the epicardium that survives a transmural infarct and is often the site of reentrant excitation, which causes ventricular tachycardia¹²⁷. Enhanced CaMKII activity was predicted to increase recovery from inactivation of the sodium channel which promotes reduced conduction velocity, a marker for increased risk of arrhythmia¹²⁸. Based on their simulations, one may anticipate that inhibition of CaMKII or upstream redox pathways in the infarct border zone could reduce re-entrant arrhythmia and ventricular tachycardia¹²⁹.

Extracellular stimuli for essential processes reach the cell via primary messengers, including catecholamines and hormones, and activate a diverse array of cellular receptors on the plasma membrane¹¹⁸. These include β -adrenergic receptors, a family of G-protein coupled receptors found predominantly in cardiac, airway smooth muscle and adipose tissue. Binding of the catecholamines epinephrine or norepinephrine results in the coupling of the receptor to the guanine nucleotide binding protein G_s , with the subsequent release of the $G_{s\alpha}$ subunit following hydrolysis of guanosine triphosphate. $G_{s\alpha}$ then activates adenylyl cyclase resulting in the production of cyclic AMP. Cyclic AMP causes the dissociation of the regulatory and catalytic subunits of protein kinase A (PKA). This allows PKA's catalytic subunit to phosphorylate various protein targets including L-type calcium channel, phospholamban (inhibitor of SERCA), ryanodine receptor (RyR) and troponin. The key result of classical β -adrenergic receptor activation in the heart is increased cardiac output¹³⁰. Saucerman et al.¹³¹ developed a model describing the β_1 -adrenergic receptor pathway, the most dominant receptor isoform, integrated with the Luo-Rudy model and modified for the rat ventricular myocyte. The model was able to reproduce the experimentally observed temporal response to β_1 -adrenergic stimulation including cAMP production, PKA activity and phospholamban phosphorylation. It then served as a platform for investigating possible therapeutics for heart failure where desensitization of the β -adrenergic receptor system occurs¹³². Their model predicted that adenylyl cyclase overexpression, which can be achieved through gene therapy, increased the generation of cyclic AMP which in turn increased the β_1 -adrenergic response with minimal side effects compared with β_1 -adrenergic receptor or G_s overexpression. They

also suggested that a hypothetical drug that increases the affinity of G_{sa} and adenylyl cyclase could be effective.

CaMKII is overexpressed in heart failure¹³³ and its activity appears to contribute to some aspects of β -adrenergic signaling¹³⁴. Soltis et al.¹³⁵ investigated the consequences of integrated β -adrenergic and CaMKII signaling by developing a combined model of both pathways and their regulation of excitation-contraction coupling. The model was validated against key experimental readouts including CaMKII-mediated phosphorylation of the ryanodine receptor and phospholamban and effects of CaMKII on Ca dynamics such as I_{Ca} facilitation and acceleration of relaxation. Their model predicted that increased CaMKII expression coupled with β -adrenergic stimulation is pro-arrhythmogenic due to a synergy of PKA and CaMKII effects on I_{Ca} , RyR, and phospholamban. CaMKII-mediated increase in RyR phosphorylation played a key role and was necessary to predict spontaneous delayed after-depolarizations during β -adrenergic signaling. Thus blocking the ability of CaMKII to phosphorylate the RyR could be a potential therapy in such conditions.

Patients with LQT1 are susceptible to sudden cardiac death during β -adrenergic stimulation due to mutations in KCNQ1, a gene that encodes the repolarizing potassium current I_{Ks} ⁵⁶. One particular KCNQ1 mutation observed clinically is KCNQ1-G589D, which disrupts the channel's ability to form a signaling complex with PKA and phosphatase 1, mediated by the scaffolding protein yotiao¹³⁶. Saucerman et al.¹³⁷ investigated the whole-cell and tissue-level consequences of this disruption by integrating the Saucerman-McCulloch model of β -adrenergic signaling with a model of the rabbit ventricular myocyte integrated into a heterogenous 3D ventricular wedge model. The

functional consequences of β -adrenergic signaling predicted by the model agreed with literature from rabbit ventricular myocytes including kinetics and dose response to isoproterenol, enhanced current through the KCNQ1 channel, and decreased action potential duration. Single cell model simulations suggested that the KCNQ1 mutation promotes early after depolarization (triggers for arrhythmia) only in the context of β -adrenergic stimulation. This effect was amplified at the tissue level with the appearance of T-wave abnormalities in simulated ECG's, including dispersion of repolarization and T-wave inversion. Thus these simulations helped explain the *in vivo* consequences of KCNQ1 mutation and why β -blockers are effective for LQT1 patients. Indeed, a subsequent clinical report illustrated remarkably similar "Himalayan" T-waves in an LQT1 patient, who was subsequently treated with a β -blocker and implantation of a cardioverter-defibrillator¹³⁸.

In another subtype of the LQT syndrome, LQT3, it is unclear whether activation of the β -adrenergic system is beneficial or deleterious¹³⁹. In order to investigate this discrepancy, Ahrens-Nicklas et al.¹⁴⁰ incorporated a description of the human SCN5A- Δ KPQ mutation associated with LQT3 into a modified version of the Luo-Rudy¹⁴¹ and used the Saucerman-McCulloch model of β -adrenergic signaling to predict phosphorylation levels of channels for I_{Ks} and I_{Ca} . This allowed the investigation of the pharmacology of LQT3 mutant channels in the context of a human-like action potential. The tissue effect of the various pharmacological agents was observed by performing transmural fiber simulations. In order to model the effects of β -blockade, decreased phosphorylation of I_{Ks} and I_{Ca} channels were predicted based on the decreased cyclic AMP production seen with the β -blocker propranolol. In addition, the authors

incorporated the separate sodium channel blocking effects of propranolol into a Markov model of the Δ KPQ sodium current. Computational modeling allowed the authors to investigate various β -blocker levels and pacing protocols that have produced apparently contradicting results in published experiments. Isoproterenol decreased action potential duration and suppressed early after depolarization for all 3 ventricular cell types (endocardial, midmyocardial and epicardial). The fiber simulations showed that transmural dispersion of repolarization was decreased in the model following isoproterenol stimulation consistent with *in vivo* observations¹³⁹. An important observation was that this beneficial effect of isoproterenol was pacing-pattern dependent, explaining the discrepancies observed *in vivo*. Low doses of propranolol increased transmural dispersion and action potential duration, worsening the LQT3 phenotype. However, the high doses of propranolol had the opposite effect on the LQT3 phenotype which suggested to the authors that this beneficial effect was due to increased late sodium current blockage.

Timothy syndrome is a form of long QT syndrome (LQT8) caused by a mutation in the CACNA1C gene that encodes for the α_{1C} -subunit of the L-type calcium channel⁵⁶. This mutation eliminates voltage-dependent inactivation of the channel, thus leaving it open⁵⁶. The resulting susceptibility to arrhythmia is ultimately deadly and patients rarely survive past 3 years¹⁴². Sung et al.¹⁴³ investigated the influence of β -adrenergic stimulation on arrhythmogenesis in Timothy Syndrome by making modifications to the Markov model of the L-type calcium current in a modified version of the Luo-Rudy model¹⁴⁴. β -adrenergic modulation of various ion channels was simulated by changing channel parameter values to mimic saturating concentrations of a β -adrenergic agonist.

The authors discovered that β -adrenergic stimulation, when combined with CACNA1C mutation, increases the occurrence of alternans, delayed after-depolarizations and early after-depolarizations (all triggers for arrhythmia). These predictions help validate the use of β -blockers as treatment for Timothy syndrome patients. Further simulations identified reduction of the L-type calcium current as the most effective target for reducing β -adrenergic-stimulated arrhythmia. The authors also identified reduction of SERCA-mediated Ca uptake as another potential target.

Several signaling pathways have been implicated in pathological hypertrophy, the abnormal growth that often leads to heart failure¹⁴⁵, including the inositol-4-5-biphosphate (IP₃)-calcineurin pathway¹⁴⁶. IP₃ is produced in response to the activation of members of the G_q family of G-protein coupled receptors including the α -adrenergic, endothelin and angiotensin receptors. Activation of these receptors results in liberation of G_{q α} which activates phospholipase C. Phospholipase C causes hydrolysis of phosphatidyl inositol-4-5-biphosphate to form the second messenger IP₃. IP₃ is thought to contribute to activation of the phosphatase calcineurin, which causes changes in cardiac gene expression through its effect on the transcription factor NFAT¹⁴⁷. In order to understand the control mechanisms underlying pathway activation, a computational model of the IP₃ pathway described above was developed by Cooling et al.¹⁴⁸. Model parameters were fit to match the relatively fast kinetics of IP₃ in response to endothelin-1 seen experimentally. Then, by changing only the parameters for receptor activation, the model was able to predict the experimentally-observed slower kinetics in response to angiotensin. Global sensitivity analysis suggested that the most sensitive parameter controlling the IP₃ transient was the rate constant for phosphorylation of the active

receptor. Despite both agonists stimulating IP₃ production via an identical signal transduction pathway, the IP₃ responses are remarkably distinct. From their simulation results, an effective strategy at combating pathological hypertrophy influenced by IP₃ can be achieved by targeting the receptors for endothelin-1 and angiotensin II. This could be more successful than attempts at attenuating hypertrophy with calcineurin inhibitors¹⁴⁹, especially since G-protein coupled receptors are among the most druggable protein targets¹⁵⁰. Indeed, angiotensin converting enzyme (ACE) inhibitors and angiotensin receptor blockers are widely used for heart failure.

2.5 Future directions

The rate of attrition in drug discovery represents one of the most serious challenges to the pharmaceutical industry⁴⁸. A main reason is the difficulty in extrapolating pre-clinical data to predict clinical efficacy⁴⁸. Computational modeling can help bridge this gap at various stages in the drug discovery pipeline¹⁵¹. Species-specific models of the cellular cardiac action potential allows the quantification of properties of potential drugs in various species and, with the help of human models, gain further insight into how the drugs might function in a clinical setting⁷². In addition, the further integration of electrophysiology, signaling and metabolic models will allow the accurate simulation of complex diseases like heart failure with multiple etiologies.

Improvement of current signaling and metabolic models and the development of disease-specific models will require the integration of data made available by the recent emergence of cardiac specific proteomic¹⁵² and metabolic¹⁵³ data sets. For example, data

on expression levels of calcium handling proteins in heart failure myocytes was used by Winslow et al.^{154,155} to develop a heart failure ventricular cell model. By changing the expression levels of four proteins, namely SERCA, sodium-calcium exchanger, inward rectifying potassium channel and the calcium independent transient outward potassium channel, they were able to simulate the observed changes in calcium transients and action potential duration seen in failing cardiac cells¹⁵⁶. These approaches will need to be extended further, because for example in dilated cardiomyopathy, one of the leading causes of heart failure, over 100 proteins are differentially expressed in humans¹⁵⁷.

Unraveling the complexity of disease states will require development of new systems modeling approaches that leverage the breadth of available ‘omics data⁵⁴. For example, Berger et al.¹⁵⁸ combined protein-protein interaction and drug databases to identify a signaling network consisting of 1629 gene products that regulates ion channels involved in LQTS. Comprehensive cardiac models such as these may help predict off-target effects and unexpected connections. Simulation of multi-target treatment can also be achieved (as opposed to the identification of a single “silver bullet”), to overcome disease network properties like redundancy, crosstalk and robustness¹⁵⁹. This has led to the development of successful drug therapies for complex diseases affecting other organ systems including cancer and depression¹⁶⁰.

Cardiac phenomena like arrhythmias depend on changes at the molecular and cellular level but they are fatal because of their effect on whole organ function¹⁶¹. In addition to 1D fiber, 2D sheet and 3D ventricular wedge models, whole heart models have been developed to examine the role of heart anatomy on arrhythmia⁴²). Multiscale electromechanical models of the heart have also been developed¹⁶² and, if coupled with

molecularly-detailed ion channel and signaling models, present a unique opportunity to explore drug intervention for conditions associated with structural remodeling such as myocardial infarction and hypertrophy. A limiting feature of multiscale models is the high computational requirements, with the simulation of one cardiac cycle in a human whole-heart model developed by Potse et al.¹⁶³ requiring approximately 2 days on 32 processors. Future advances in CPU performance and the use of alternative tools including GPU-aided simulations¹⁶⁴ will make multi-scale computer models more commonplace, presenting an opportunity to merge tissue modeling with physiologically based pharmacokinetic models¹⁶⁵. Pharmacokinetics, which determines how rapidly and for how long a drug is available at a particular organ¹⁶⁶, is crucial for predicting clinical efficacy¹⁶⁷. Integrating multi-scale models with pharmacokinetic models will result in a modeling platform that is as close to clinical trials as possible. A recent example of the utility of this strategy is provided by Wu et al.¹⁶⁸ who use a multi-scale tissue model to investigate soluble VEGF receptor's potential as an anti-angiogenic therapeutic.

Cellular computational modeling has already informed the development of several drugs including ranolazine and ivabradine⁴⁹. Such modeling approaches have until recently been primarily used in academia. For the goals of FDA's Critical Path Initiative to be realized, it will require increased collaboration between academia and industry to harness the potential of cardiac computational modeling for drug discovery and development. The rewards of this collaboration should help reduce the clinical burden of cardiovascular disease.

The text of Chapter 2, in part, is a partial reprint of material as it appears in Amanfu, R. K. & Saucerman, J. J. Cardiac models in drug discovery and development: a review. *Crit Rev Biomed Eng* **39**, 379–395 (2011).

3. Automated image analysis of cardiac myocyte Ca^{2+} signaling

3.1 Introduction

Ca^{2+} is a ubiquitous second messenger and is important in many cellular processes. During every heartbeat, electrical activity induces an oscillation in cytosolic Ca^{2+} called a Ca^{2+} transient, which activates the myofilaments and allows contraction. This coupling of electrical and mechanical activity is termed excitation-contraction coupling¹⁶⁹. The advent of fluorescent organic dyes sensitive to changes in Ca^{2+} concentration has permitted extensive studies of how Ca^{2+} dynamics modulates excitation-contraction coupling in cardiac myocytes. These fluorescent dyes enabled substantial new insights including the role of Ca^{2+} sparks as elementary units of Ca^{2+} -induced Ca^{2+} release¹⁷⁰, cellular mechanisms underlying the heart's force-frequency relationships¹⁷¹, and identification of spontaneous Ca^{2+} release as a trigger for cardiac arrhythmia¹⁷².

Ca^{2+} transients can be experimentally observed by loading cells with a dye that fluoresces upon binding of released Ca^{2+} from specialized stores into the cytosol¹⁷³. The most common method of recording the resultant fluorescent signal is to couple a photomultiplier tube (PMT) to an epifluorescence microscope¹⁷⁴. The advantages of PMT's are their high sensitivity and temporal resolution. However, these advantages come at the cost of spatial resolution as fluorescence is only recorded from a single position. This limits recording to a single cell and does not allow simultaneous analysis of potentially interesting spatial features including cell size and shape or subcellular

heterogeneity. Recent advances in the temporal resolution and sensitivity of charge-coupled device (CCD) cameras and raster-scanning confocal microscopes provide the opportunity to simultaneously image Ca^{2+} transients from multiple cardiac myocytes, which would greatly increase experimental throughput and enable assessment of cell-cell variability. Confocal imaging is already used to examine subcellular Ca^{2+} dynamics such as Ca^{2+} sparks and Ca^{2+} waves¹⁷⁵. Imaging approaches are also used to image electrical and Ca^{2+} activity in monolayers of cultured neonatal myocytes¹⁷⁶. In this study, we optimized a system for CCD-based imaging of Ca^{2+} transients in multiple adult ventricular myocytes, which increases experimental throughput ~10-fold. Accurate extraction and analysis of Ca^{2+} signals from such large data sets becomes a new bottleneck. To address this, an automated cell segmentation and shape analysis pipeline was developed. This provides rapid and objective quantification of Ca^{2+} dynamics in cell populations and the comparison of Ca^{2+} dynamics with cell shape characteristics. An overview of this approach is provided in Figure 3.1.

3.2 Materials and methods

3.2.1 Data acquisition

Single adult rat ventricular myocytes were isolated similar to¹⁷⁷ from 4 adult male (250 g) Sprague-Dawley rats. All procedures were performed in accordance with the *Guide for the Care and Use of Laboratory Animals* published by the US National Institutes of Health and approved by the University of Virginia Institutional Animal Care and Use Committee. Collagenase used for tissue digestion was obtained from Cellutron Life Technologies (Baltimore, MD).

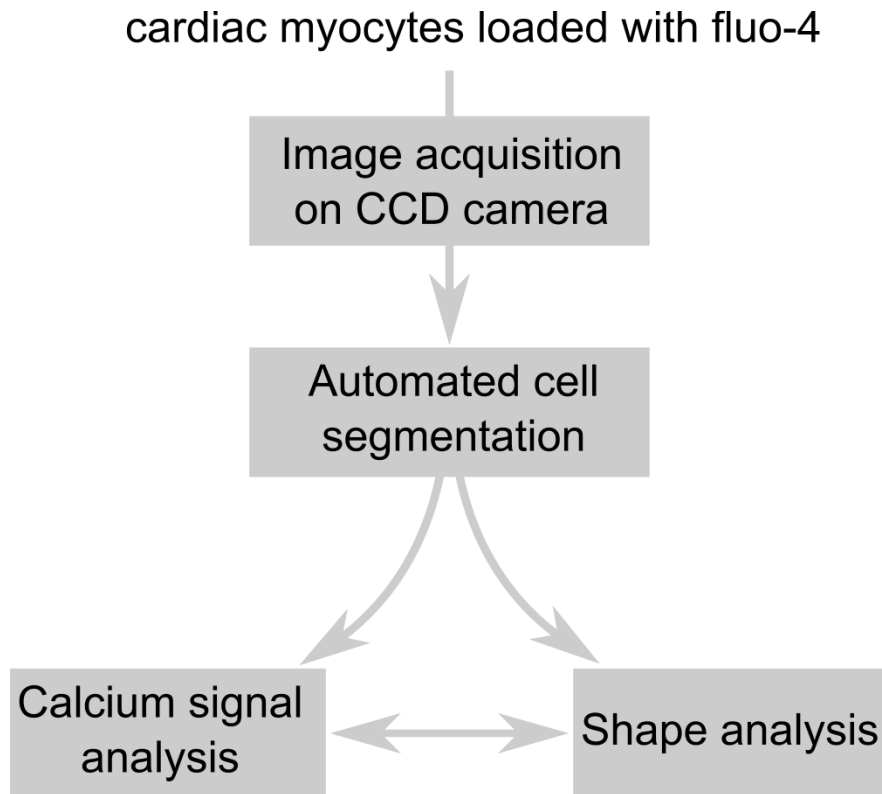


Figure. 3.1: **Flow diagram for the proposed method**

Isolated ventricular myocytes were plated on 35 mm glass coverslips treated with 40 $\mu\text{g/ml}$ laminin at a density of $\sim 3 \times 10^6$ cells per ml. Unattached cells were removed after 1 hour by removing and replenishing media. Cells were loaded with 1 μM fluo-4 acetoxymethyl¹⁷³ (Invitrogen, Carlsbad, CA) for 30 minutes at room temperature in a solution of MEM containing (in mM) NaHCO_3 4.7, pyruvic acid 2, Na-HEPES 10, HEPES 10 and (in units/ml) insulin 0.4, and penicillin-streptomycin 50 (pH 7.35). The non-ratiometric Ca^{2+} dye fluo-4 was selected over commonly used ratiometric dyes (indo-1 and fura-2) due to its high signal-to-noise ratio and simplified imaging requirements¹⁷⁵. Cells were incubated in MEM for another 30 minutes to allow for dye de-esterification. Next, they were placed in a slotted bath chamber with platinum electrical field electrodes (Warner Instruments, Hamden, CT). Cells were imaged on an IX-81 microscope (Olympus, Center Valley, PA) with 10X (either 0.3 or 0.4 numerical aperture) objectives for CCD imaging and 40X 0.6 numerical aperture objective for PMT recording. All experiments were performed at room temperature (21-24 $^\circ\text{C}$).

Ca^{2+} transients were detected with either a PMT400 system (Ionoptix, Milton, MA) or a Hamamatsu C9300 CCD camera (Bridgewater, NJ) at 8X8 binning and 15 ms exposure time. Sampling frequency was 1000 Hz and 67 Hz for the PMT and CCD camera respectively. The camera was set in stream acquisition mode using Metamorph imaging software (Molecular Devices, Sunnyvale, CA). This setting enables image acquisition at an interval approximately equal to the exposure time. Excitation light was generated using a Lambda DG4 300 watt xenon lamp (Sutter, Novato, CA), filtered through a 5% neutral density filter and 480/40 nm bandpass excitation filter. Fluorescence emission was detected using a 505 nm dichroic and 535/50 nm bandpass emission filter (Chroma,

Bellows Falls, VT). The cell chamber was constantly perfused with Tyrodes solution containing (in mM) NaCl 140, KCl 4, MgCl₂ 1, and HEPES 10 (pH 7.4). Cells were paced with an electrical stimulator (Ionoptix, Milton, MA) at a frequency of 0.5-1 Hz with a bipolar pulse of duration 4 ms at a voltage of 10 V.

3.2.2 *Automated cell segmentation*

As shown in Figure 3.2 A, individual frames of an image stack contained considerable noise, particularly at diastole when Ca²⁺ is low. The low signal-to-noise makes cell segmentation particularly difficult. To overcome this difficulty, we automatically identified and then averaged image frames of maximum Ca²⁺ intensity (coinciding with the stimulation frequency of the electrical pacer) to increase the signal-to-noise ratio used for cell segmentation (Figure 3.2 B). Images were then segmented using Otsu's method for threshold selection¹⁷⁸, which works by identifying the optimum threshold in an image's intensity histogram that minimizes the variance between pixels in the background and foreground (Figure 3.2 C). Using this threshold, a mask image was created with identified regions of interest (ROIs). An example of the resulting segmented ventricular myocytes is shown in Figure 3.2 D.

3.2.3 *Ca²⁺ signal analysis*

The resulting regions of interests (ROIs) were used to extract each cell's fluorescence intensity at each time point (or acquired image). Background signal at each timepoint was quantified by taking the average intensity of all regions below the segmentation threshold.

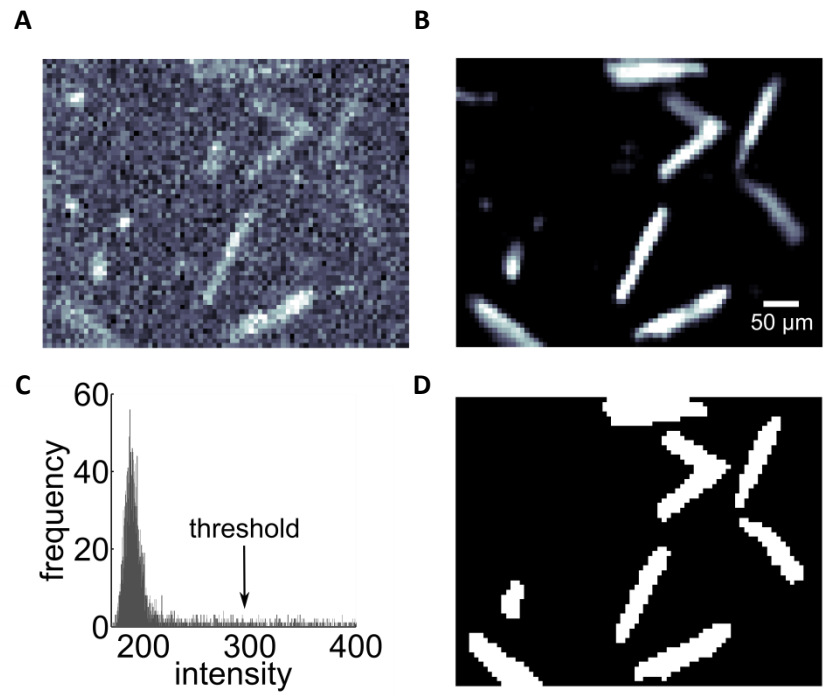


Figure 3.2: **Automated image segmentation.** **A**, Single image frame during diastole (low Ca^{2+}). **B**, Averaged image from frames during systole (high Ca^{2+}). **C**, Histogram of intensity values of the averaged image. The threshold is identified using Otsu's method. **D**, Segmented image

Raw fluorescence values were background-subtracted and then normalized to diastolic Ca^{2+} intensity F_0 as $(F-F_0)/F_0$, or $\Delta F/F_0$. Averaged Ca^{2+} transients were calculated by averaging 5 consecutive transients. Diastolic and systolic values are estimated by finding the minimum and maximum intensities of the averaged transient. An estimate of the relaxation time (signal decay) was obtained by identifying the time at which normalized fluorescence intensity is 50% of the max amplitude. All segmentation and feature extraction was implemented in MATLAB (The Mathworks, Natick MA). MATLAB code for these analyses and example movies are freely available at <http://bme.virginia.edu/saucerman>.

3.3 Results

3.3.1 CCD-based imaging of Ca^{2+} transients

To determine the image acquisition rate necessary to adequately sample Ca^{2+} transient signals, Ca^{2+} transients were measured at 1000 Hz using the PMT system and then downsampled to simulate various CCD camera sampling frequencies (Figure 3.3 A). During CCD-based image acquisition each pixel well integrates the photons hitting the detector during the exposure time, essentially averaging the signal. To simulate these effects of photon integration during CCD acquisition at various sampling frequencies, a moving average filter with width corresponding to the exposure time was used (for example a 10 Hz sampling rate corresponds to 100 ms exposure time on a CCD camera). Spectral analysis of the 1000 Hz PMT signal indicates that the Ca^{2+} signal bandwidth is ~ 14.4 Hz (Figure 3.3 B), corresponding to a Nyquist sampling rate of 28.8 Hz. Thus an image acquisition frequency of 67 Hz is sufficient to minimize aliasing artifact.

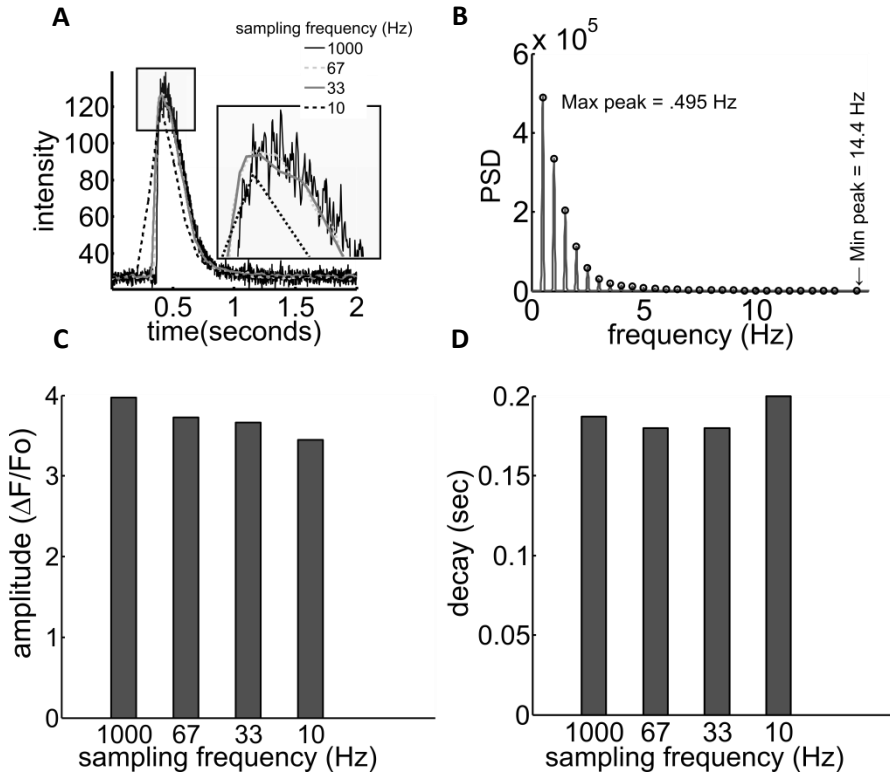


Figure 3.3: **Analysis of the effects of down-sampling PMT data.** **A**, Averaged transients of down-sampled PMT data. **B**, Power spectral density (PSD) of original PMT data. The peak corresponds with the pacing frequency, and the signal has a bandwidth of ~ 14.4 Hz. **C**, Effect of sampling frequency on amplitude of averaged Ca^{2+} transients. **D**, Effect of sampling on decay time t_{50} of averaged Ca^{2+} transients.

Qualitatively, aliasing is evident at lower sampling frequencies of Figure 3.3 A, especially 10 Hz. Quantification of Ca^{2+} transient parameters amplitude and decay rate t_{50} is shown in Figure 3.3 C-D. While these graphs alone suggests that even 67 Hz down-sampling rates underestimates those parameters, inspection of the inset in Figure 3.3 A demonstrates that the larger Ca^{2+} transient amplitude seen with 1000 Hz sampling is largely an artifact of larger signal noise. Thus photon integration occurring on the CCD camera acts as a low-pass filter.

We then used the CCD camera system to record Ca^{2+} transients from adult ventricular myocytes at 67 Hz sampling and image exposure time of 15 ms. As described in Methods and Materials, automated cell segmentation was performed to identify individual myocytes and Ca^{2+} signals were normalized to obtain signals as shown in Figure 3.4. This demonstrates that Ca^{2+} transients can be simultaneously measured from multiple cardiac myocytes with reasonably high signal-to-noise. We found that using this approach, ~7% photobleaching occurs in 60 sec of continuous imaging. Restricting imaging to 10 sec intervals every 1 minute enabled longer-term observation of Ca^{2+} signals.

3.3.2 *Ventricular myocyte shape analysis*

Using the Image Processing Toolbox in MATLAB, morphologic parameters were quantified automatically from 176 myocytes including cell area, major and minor axis lengths (fitted to an ellipse). As shown in Figure 3.5 A, myocytes had a median cell area of $1.36 \times 10^3 \mu\text{m}^2$ but, the distribution of cells exhibits substantial variability and a long tail with several much larger myocytes.

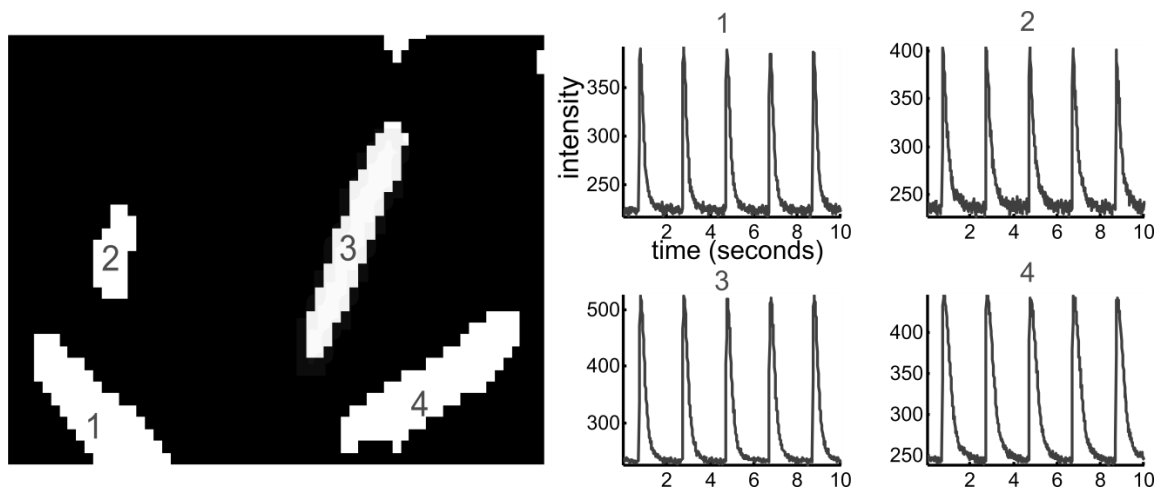


Figure 3.4: **Raw fluorescent intensity values for Ca^{2+} transients obtained from 4 ventricular myocyte ROIs**

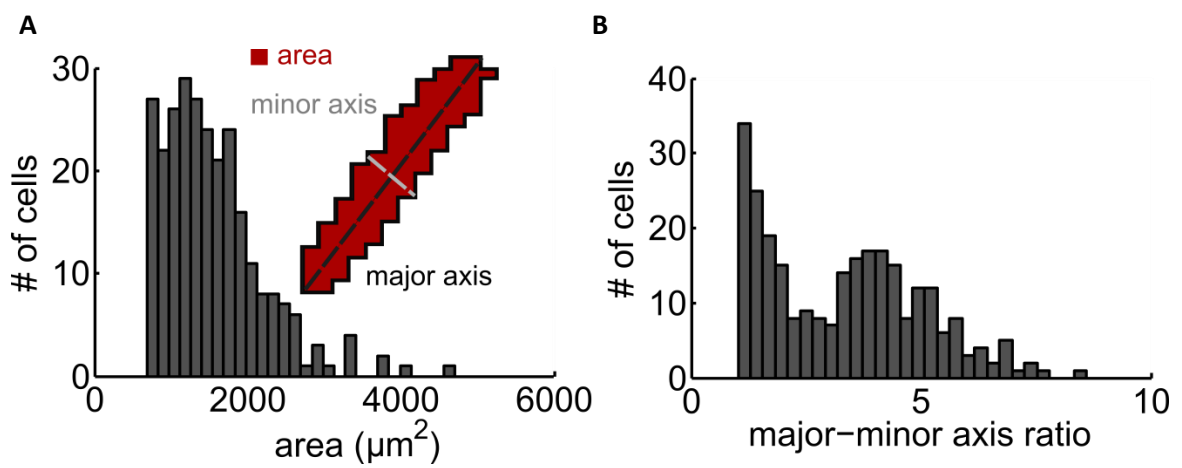


Figure 3.5: **Histogram of cell size and shape features calculated from automated segmentation of 176 myocytes. A**, Histogram of cell area. **B**, Histogram of major-minor axis length ratio.

Note that overlapping myocytes erroneously segmented as a single cell (as in the upper-center of Figure 3.2 D) were manually excluded from this analysis, but could be identified automatically in the future.

The ratio of major to minor axis lengths is a simple measure of cell shape. The distribution of major-minor axis length ratios shows two distinct populations of cells corresponding to rod-shaped and hypercontracted cells (for example cell 2 in Figure 3.4), with the former more commonly described as being healthy, normal myocytes¹⁷⁹. Isolated ventricular myocytes can become hypercontracted when overloaded by Ca^{2+} , typically no longer exhibiting normal Ca^{2+} dynamics.

Combining the information provided by Ca^{2+} signals and cell morphology may provide new insights into myocyte function. Comparison of Ca^{2+} dynamics and major-minor axis ratio may enable identification of unhealthy cells that should be excluded from subsequent analysis. Further, there may be relationships between cell size, shape and Ca^{2+} signaling within the rod-shaped myocyte population. For example, myocytes isolated from failing hearts are hypertrophied (enlarged), and swelling of cardiac myocytes is a known aspect of ischemia-reperfusion¹⁸⁰. Both of these conditions are typically associated with decreased Ca^{2+} transient magnitude.

The relationships between Ca^{2+} transient amplitude, myocyte area, and major-minor axis ratio were examined in normal ventricular myocytes. As shown in Figure 3.6 A, Ca^{2+} transient amplitudes varied considerably from cell to cell, even when in the same experiment and field of view. However, Ca^{2+} transient amplitude was not correlated with cell area (Pearson correlation coefficient $r = -0.15$), indicating that cell size is not a substantial determinant of Ca^{2+} transients within this myocyte population.

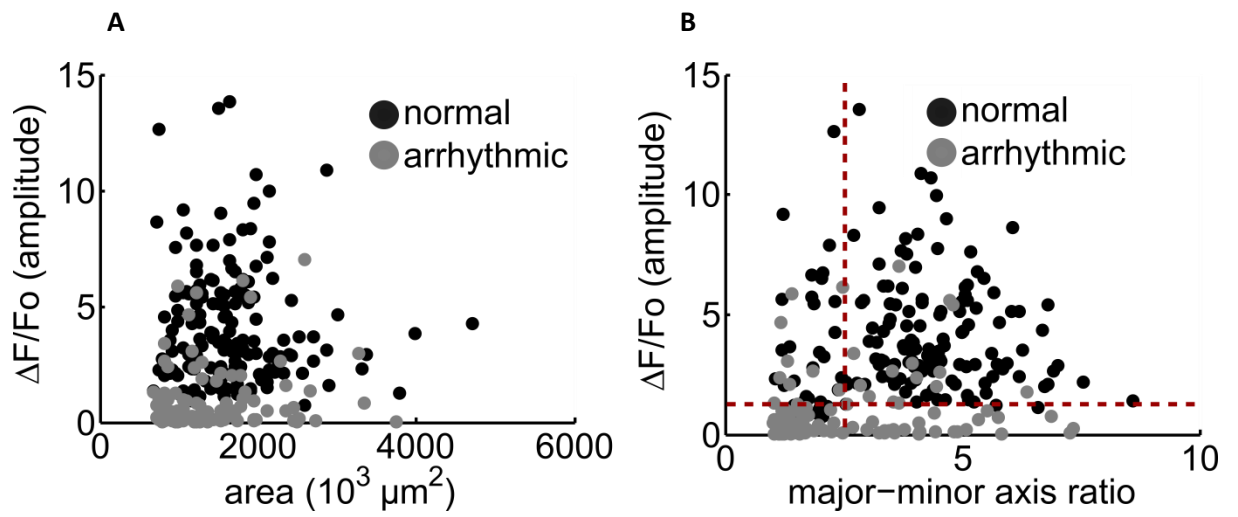


Figure 3.6: **Correlation plots.** **A**, Amplitude vs. area. **B**, Amplitude vs. major-minor axis ratio.

Given previous data on the effects of cell swelling on Ca^{2+} transients¹⁸⁰, this could indicate that myocytes regulate ion channel expression to maintain normal Ca^{2+} transients. Figure 3.6 B shows the relationship between major-minor axis ratio and Ca^{2+} transient amplitude in normal myocytes. Rounded or hypercontracted myocytes typically had very small or no Ca^{2+} transients and were typically arrhythmic (i.e. displaying abnormal calcium transients). More rod-shaped myocytes exhibited larger Ca^{2+} transients as expected of healthy myocytes. However, even when excluding hypercontracted cells with axis ratios less than 2, rod-shaped myocytes exhibited considerable variation in Ca^{2+} transients not accounted for by major-minor axis ratio alone ($r = -0.22$).

3.4 Discussion

Here we have developed a method for simultaneous imaging of Ca^{2+} transients in multiple adult ventricular myocytes with sufficient temporal and spatial resolution for quantitative analysis. Automated cell segmentation and Ca^{2+} signal analysis substantially increases the throughput, sensitivity, and objectivity of the approach. The improved spatial resolution also provides an opportunity to examine relationships between Ca^{2+} signaling and cell morphology.

While we did not observe appreciable correlation between cell morphology and Ca^{2+} transients in normal rod-shaped myocytes, cell shape was able to identify rounded myocytes with dysfunctional Ca^{2+} regulation. This demonstrates proof-of-principle that this approach may be subsequently extended to pathological conditions such as heart failure or ischemia where coordinated changes in cell size, shape, and Ca^{2+} signaling have been noted. More advanced measures of cell shape including eccentricity could be

analyzed as well. Extensions of this approach may allow automated analysis of arrhythmic Ca^{2+} waves where Ca^{2+} signals are not uniform within the cell.

The text of Chapter 3 is a reprint of material as it appears in Amanfu, R. K., Muller, J. B. & Saucerman, J. J. Automated image analysis of cardiac myocyte Ca^{2+} dynamics. in 2011 Annual International Conference of the IEEE Engineering in Medicine and Biology Society, EMBC 4661–4664 (IEEE, 2011).

4. Modeling the effect of β_1 -adrenergic receptor blockers and polymorphisms on cardiac myocyte calcium handling

4.1 Introduction

Heart failure, the inability of the heart to provide adequate blood flow to meet the body's demand, is one of the leading causes of hospitalization and mortality in the United States^{1,2}. β -adrenergic receptor blockers (β -blockers) are commonly used to treat this condition. However the biological mechanism governing their success is poorly understood^{3,21,22}. The β_1 -adrenergic receptor pathway has a dominant role in the regulation of heart contractility⁵. Elevated catecholamine release, a hallmark of heart failure, has been shown to desensitize the β -adrenergic pathway¹⁷ causing an inability to increase contractility and cardiac output in response to acute stress. Two conflicting theories commonly postulated are that β -blockers are effective by either inhibiting the harmful consequences of sustained stimulation or maintaining the beneficial aspects of β_1 -adrenergic receptor pathway activation²³. The inhibition hypothesis is supported by clinical and experimental evidence that β -blockers help prevent or reverse the cardiac remodeling that leads to heart failure²⁴. Conversely, the maintenance hypothesis is given credence by clinical evidence that β -blockers increase β_1 -adrenergic receptor levels²⁵ and exercise tolerance²⁶.

The adoption of β -blockers as standard treatment for heart failure faced early resistance due to a belief it was contraindicated. Studies began to slowly confirm that blockade of the β -adrenergic receptor could increase cardiac function in heart failure

leading to the eventual acceptance of β -blockers²⁰. First generation β -blockers like propranolol are non-selective for the different β -adrenergic isoforms. They were replaced with second generation compounds; examples include metoprolol, which selectively target the β_1 -adrenergic receptor¹⁹. This was done to reduce the contraindication of non-selective blockers in asthmatics and to target the more abundant β_1 -adrenergic receptor. Third generation β -blockers were developed with ancillary properties like vasodilation (achieved through antagonism of the α -adrenergic receptors) to additionally treat hypertension¹⁹. Carvedilol, a third generation compound, is however more selective for the β_1 -adrenergic receptor at moderate doses²⁷. The ability of different β -blockers to either inhibit or maintain signaling is varied causing controversy on which β -blocker is more effective in heart failure³². There is a greater diversity of effect on receptor states among the 17 FDA approved β -blockers beyond just receptor specificity³¹. This diversity complicates attempts to determine which β -blockers are efficacious in the treatment of heart failure. One important property is the ability of β -blockers to behave as inverse agonists³², i.e. reduce the basal level of signaling following receptor binding³³. The importance of inverse agonism in determining clinical patient outcome during β -blocker treatment is unclear.

Genetic differences among patients also impacts β -blocker efficacy³⁵. A common polymorphism of the β_1 -adrenergic receptor is the glycine for arginine substitution at amino acid 389³⁶. *In vitro* experiments in cell expression systems show that the β_1 -Arg389 variant has a higher fold increase in adenylyl cyclase after receptor stimulation but is desensitized the most^{36,37}. Carvedilol and metoprolol have equal affinity for both receptor variants³⁸ *in vitro* but carvedilol has a larger effect on receptor conformation of

the β_1 -Arg389 variant³⁹ suggesting compound-specific phenotypes for the β_1 -adrenergic receptor polymorphisms⁷.

The complexity of the β -adrenergic receptor pathway coupled with the influence of receptor polymorphisms makes it difficult to intuit the effect of β -blockers on observed cardiac physiology. Recent studies from our group have used computational models to gain insight into the β_1 -adrenergic receptor pathway's influence on excitation contraction coupling^{135,137,181–183}. Here we use a systems pharmacology approach¹⁸⁴ to investigate the mechanisms responsible for the efficacy of β -blockers in treating heart failure. We tested the hypothesis that both proposed mechanisms for β -blocker efficacy can occur concurrently. To do this, a published computational model of the β_1 -adrenergic receptor pathway developed in our group was extended to include detailed receptor interactions. Model predictions, validated with Ca^{2+} and FRET imaging of isolated rat cardiac myocytes, surprisingly suggest that β -blockers can both inhibit and maintain signaling depending on the magnitude of receptor stimulation. In additions, these responses are modulated by receptor polymorphisms.

4.2 Methods and materials

4.2.1 Computational modeling of β -blockers

A computational model was previously developed that integrates β_1 -adrenergic receptor signaling with excitation contraction coupling in rat cardiac myocytes and is based on mass action kinetics¹⁸⁵. The receptor module was described by a ternary complex model¹⁸⁶. To better model the inverse agonism of some β -blockers seen in *in vitro* experiments¹⁸⁷, the receptor module of our original β_1 -adrenergic receptor signaling

model was replaced with the extended ternary complex model (ETCM)¹⁸⁸. The ETCM (Figure 4.1) proposes two receptor states i.e. active and inactive and appropriately describes the constitutive activity of β -adrenergic receptors. The existence of these receptor states has been recently confirmed by determination of the crystal structure of the β_2 -adrenergic receptor¹⁸⁹. Parameters for ETCM and fitting procedures are listed in the Appendix. The expanded model has 49 algebraic and differential equations and is constrained by 102 parameters. Computational model and fitting procedures were performed in MATLAB (The Mathworks, Natick MA).

4.2.2 *Isolation and culture of rat cardiac myocytes*

All procedures were performed in accordance with the *Guide for the Care and Use of Laboratory Animals* published by the US National Institutes of Health and approved by the University of Virginia Institutional Animal Care and Use Committee. Adult rat ventricular myocytes were isolated similar to Bers et al.¹⁷⁷ from adult male (250 g) Sprague-Dawley rats. Briefly, rats were anesthetized with ketamine/xylazine and hearts quickly excised before being Langendorff-perfused with collagenase (Cellutron Life Technologies, Baltimore, MD). Ventricular tissue was removed, mechanically dispersed, filtered, and myocyte suspensions rinsed and plated on 35 mm glass coverslips treated with 40 $\mu\text{g/ml}$ laminin (Invitrogen, Carlsbad, CA) at a density of $\sim 3 \times 10^6$ cells per ml. Unattached myocytes were removed after 1 hour by replenishing media. Cells were then loaded with 1 μM fluo-4 acetoxymethyl¹⁷³ (Invitrogen, Carlsbad, CA) or infected with AKAR3 adenovirus (Vector Biolabs, Philadelphia, PA) following manufacturer's

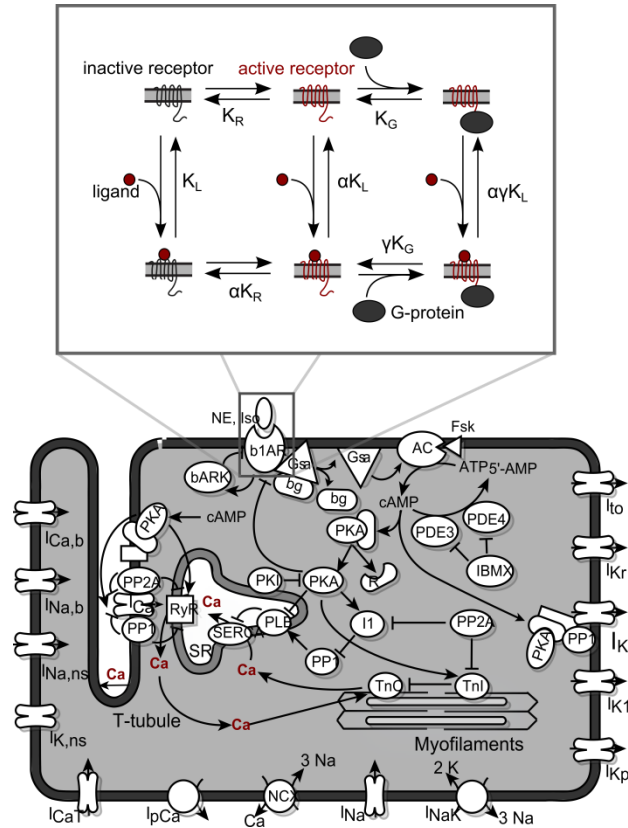


Figure 4.1: **Model of β_1 -adrenergic signaling and EC coupling with extended ternary complex model (ETCM).** Extended ternary complex model is embedded in EC coupling and signaling model. K_L , equilibrium dissociation constant of the agonist receptor complex; K_R , propensity for switching between active and inactive receptor states; K_G , binding affinity of G-protein to the receptor; α , differential affinity of the ligand for the active receptor; γ , differential affinity of the ligand-receptor complex for G-protein.

instructions in a solution of MEM containing (in mM) NaHCO_3 4.7, pyruvic acid 2, Na-HEPES 10, HEPES 10 and (in units/ml) insulin 0.4, and penicillin-streptomycin 50 (pH 7.35). Myocytes were then placed in a RC-21BRFS slotted bath chamber (Warner Instruments, Hamden, CT). The chamber was constantly perfused with Tyrodes solution containing (in mM) NaCl 140, KCl 4, MgCl_2 1, and HEPES 10 (pH 7.4) before cells were stimulated with isoproterenol (ISO; Tocris, Minneapolis, MN) and various β -blockers (propranolol, PRO; metoprolol, MET; carvedilol, CAR; Tocris, Minneapolis, MN). The flow rate of the perfusate was approximately 1-1.5 ml/min. Myocytes were field paced with the Myopacer (Ionoptix, Milton, MA) at a frequency of 1 Hz with bipolar pulse duration of 4 ms at a voltage of 10 V. All measurements were performed at room temperature.

4.2.3 Camera-based Ca^{2+} imaging of myocytes

Ca^{2+} was measured using fluo-4 with a method described previously¹⁹⁰. Myocytes were imaged on an Olympus IX-81 inverted microscope (Olympus, Center Valley, PA) with a Hamamatsu C9300 CCD camera (Bridgewater, NJ) and automated stage (Prior Scientific, Rockland, MA) at a sampling frequency of 67 Hz using Metamorph (Molecular Devices, Sunnyvale, CA). To minimize photobleaching and phototoxicity, cells were imaged intermittently for 10 seconds after every minute. Automated cell segmentation using Otsu's method identified regions of interest from which Ca^{2+} transients for each cell were extracted at each time point. Raw fluorescence values were background-subtracted and normalized to yield fold change in Ca^{2+} intensity:

$$Ca^{2+} \text{ fold change} = \frac{\left(\frac{\Delta F}{F_o}\right)_t}{\left(\frac{\Delta F}{F_o}\right)_{t=0}}$$

Average Ca^{2+} fold change was calculated by averaging 5-7 consecutive transients at specific time points. All segmentation and feature extraction was implemented in MATLAB. Code for these analyses and example movies are freely available at <http://bme.virginia.edu/saucerman>.

4.2.4 FRET imaging of cardiac myocytes

Adenovirus was constructed from plasmid DNA of AKAR3 protein kinase-A reporter¹⁹¹. Myocytes were infected with adenovirus immediately following isolation in serum MEM media for 1 hour. Cells were then cultured for 24 hours in serum free MEM media. Myocytes were pre-incubated in solutions of 0.1 μ M isoproterenol with and without 0.1 μ M propranolol. Cells were placed in a slotted bath with Tyrodes perfusate and paced at 10 Hz. Expressing myocytes were imaged on an Olympus IX-81 inverted microscope with a Hamamatsu C9300 CCD camera. A cocktail of 10 μ M forskolin (FSK; Tocris, Minneapolis, MN) and 100 μ M 3-isobutyl-1-methylxanthine (Sigma-Aldrich, St. Louis, MO) was used as positive control at the end of each experiment. Automated cell segmentation and FRET computation (using PFRET algorithm¹⁹²) were performed in MATLAB. FRET response was normalized to positive control.

4.3 Results

4.3.1 *Validation of β_1 -adrenergic model with extended ternary complex receptor model*

To investigate the mechanisms responsible for the efficacy of β -blockers in treating heart failure, a computational model of the β_1 -adrenergic receptor pathway was developed that includes detailed receptor interactions in the form of the extended ternary complex model (Figure 4.1). The integrated model describes stimulation of the β_1 -adrenergic receptor, activation of receptor intermediates, production of cAMP, activation of PKA, phosphorylation of downstream PKA targets and its effect on Ca^{2+} . Receptor desensitization by both the β -adrenergic receptor kinase and PKA is also included. The model was validated with experimental data from literature (Figure 4.2). The shift in agonist binding to the receptor in the presence of GPP³⁶ was reproduced (Figure 4.2 A). The model replicates cAMP production in response to isoproterenol stimulation¹⁹³ (Figure 4.2 B, C). Phosphorylation of phospholamban by PKA¹⁹⁴ is also accurately represented (Figure 4.2 D). Simulations show consistent relationship between isoproterenol concentration and the Ca^{2+} response (Figure 4.2 E). These results indicate that the updated model is consistent at various levels of the β_1 -adrenergic receptor cascade, providing confidence in the utility of the model for testing hypotheses on β -blocker efficacy.

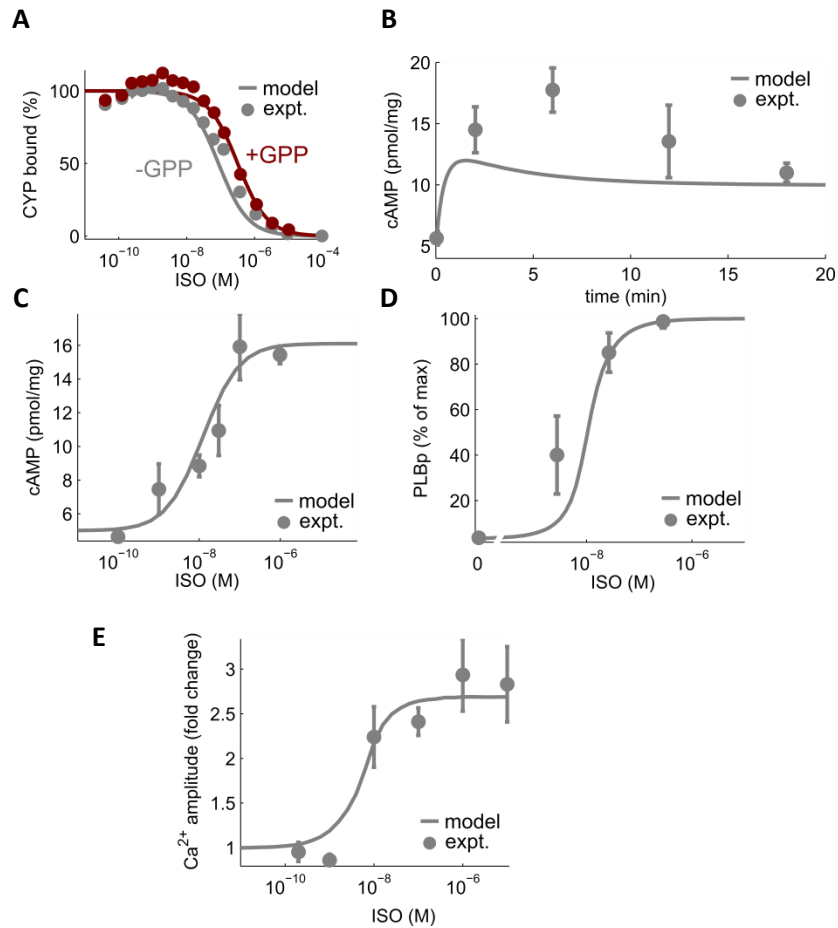


Figure 4.2: **Experimental validation of coupled β_1 -adrenergic signaling and EC coupling model.** **A**, Model reproduces shift in agonist binding affinity in the presence of GPP, which displaces G_s from the receptor. **B**, Kinetics of [cAMP] in response to 10 nM isoproterenol (ISO) stimulation. **C**, cAMP dose response to ISO. **D**, Phospholamban phosphorylation in response to ISO. **E**, Ca^{2+} dose response to ISO. Results in A-D show direct comparison with published experimental data (Mason et al., 1999),(Vila Petroff et al., 2001),(Vittone et al., 1998), whereas data in E was acquired in the current study.

4.3.2 *Propranolol inhibits and maintains the β -adrenergic response depending on the magnitude of receptor stimulation*

In-silico simulations involved the application of low (0.1 μ M) and high (10 μ M) levels of isoproterenol in the absence and presence of the first generation β -blocker propranolol. Low and high doses of isoproterenol are analogous to chronically elevated levels of catecholamines in HF and acutely elevated levels in exercise, respectively. In the absence of propranolol, the model predicts that low receptor stimulation increases Ca^{2+} amplitude (Figure 4.3A). However, the β_1 -adrenergic receptor pathway is not further sensitive to subsequent high levels of isoproterenol (Figure 4.3B). In the presence of propranolol, response to low receptor stimulation is blocked but the pathway maintains sensitivity to high isoproterenol, maintaining the Ca^{2+} response (Figure 4.3 C). Ca^{2+} experiments with isolated rat cardiac myocytes are consistent with model predictions (Figures 4.3 D, E, and F). These simulations and experiments indicate that the apparently conflicting roles of the β -blocker propranolol to inhibit signaling and maintain responsiveness are in fact compatible.

To investigate the effect of propranolol during *chronic* receptor stimulation, cells were pre-treated with a low dose of isoproterenol for 24 hours before subsequent stimulation with high isoproterenol (Figure 4.4). In the absence of propranolol, the Ca^{2+} response in pre-treated cells was not sensitive (Figure 4.4 C) to further stimulation with high isoproterenol (however Ca^{2+} levels were still elevated). In contrast, the Ca^{2+} response in pre-treated cells was sensitive to high dose of isoproterenol in the presence of propranolol (similar to model predictions).

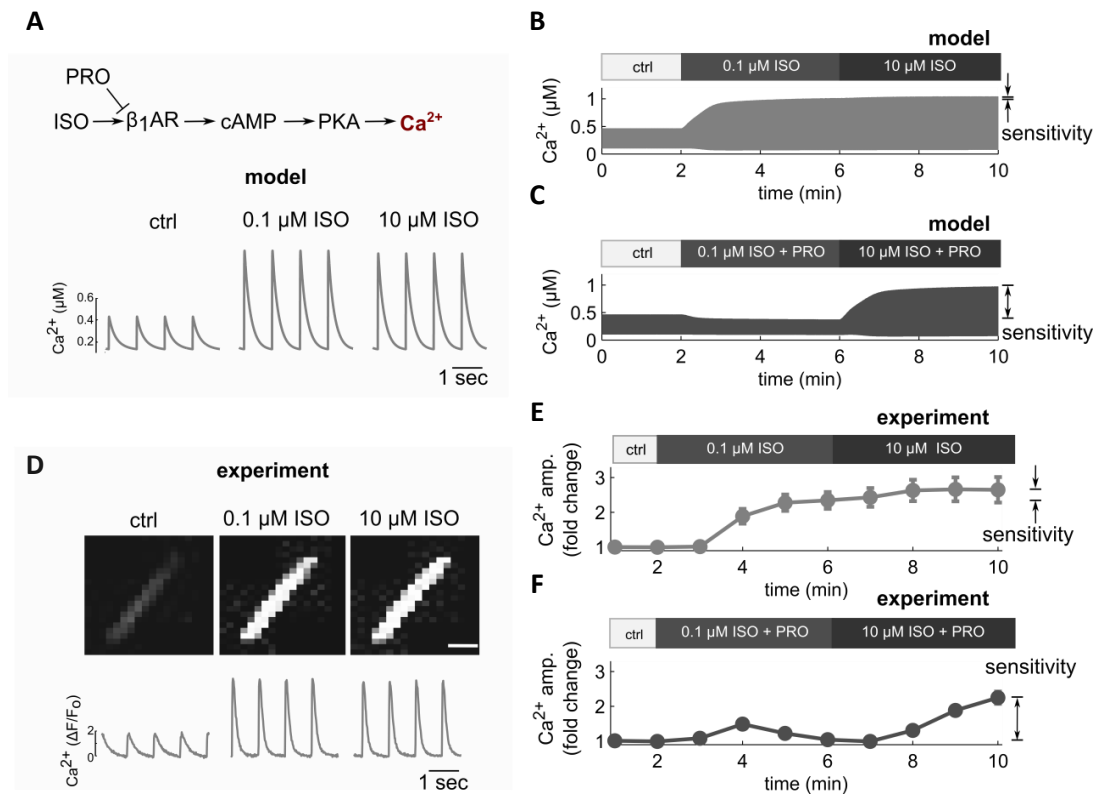


Figure 4.3: Propranolol both inhibits and maintains β_1 -adrenergic-mediated regulation of Ca^{2+} transients. **A**, Model-predicted individual Ca^{2+} transients in response to increasing [ISO]. **B**, Ca^{2+} concentration increased in response to 0.1 μM ISO, with no further response to subsequent stimulation with 10 μM ISO. **C**, The model predicted that propranolol (PRO) inhibits response to 0.1 μM ISO, but the responsiveness to 10 μM ISO is maintained (large sensitivity). **D**, Individual Ca^{2+} transients from rat ventricular myocytes exposed to increasing [ISO]; scale bar 20 μm . **E**, Similar to model predictions, myocytes were not responsive to further stimulation with 10 μM ISO. **F**, PRO inhibited response to 0.1 μM ISO, but myocytes were responsive to further stimulation with 10 μM ISO ($n \geq 13$). Sensitivity was quantified as the increase in Ca^{2+} transient magnitude when increasing from 0.1 μM ISO (analogous to chronically elevated catecholamines in heart failure) to 10 μM ISO (analogous to exercise).

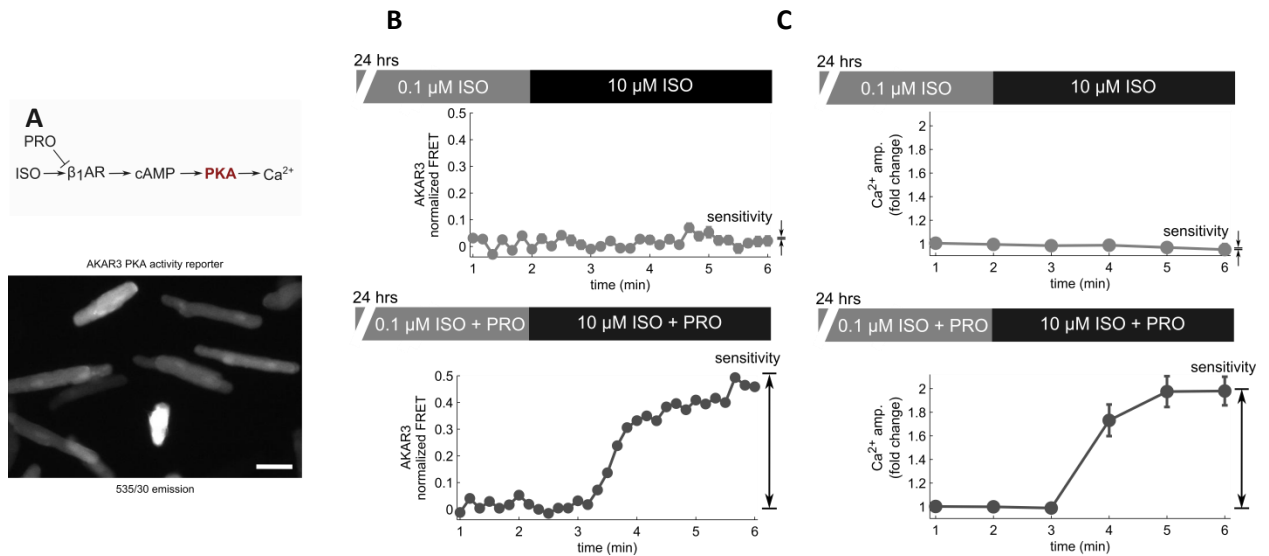


Figure 4.4: **Propranolol both inhibits and maintains the β_1 -adrenergic-mediated Ca^{2+} and PKA response following 24 hour ISO pre-treatment.** **A.** Expression and cytosolic distribution of PKA activity biosensor AKAR3 in rat adult cardiac myocytes (YFP emission); scale bar 40 μM . Following 24 hour pre-treatment with both 0.1 μM ISO and 0.1 μM PRO, both **B)** PKA activity measured by AKAR3 AND **C)** Ca^{2+} transients were still sensitive to subsequent increase to 10 μM ISO ($n \geq 9$).

These effects on Ca^{2+} are mirrored upstream of the β_1 -adrenergic receptor pathway with FRET measurements of PKA activity showing similar sensitivity to high isoproterenol in the presence of propranolol (Figure 4.4 B).

4.3.3 *β -blockers differ in their ability to inhibit and maintain β -adrenergic responsiveness*

To investigate whether the dual role of propranolol in inhibiting and maintaining β -adrenergic responsiveness is universal to β -blockers, an in-silico screen of various β -adrenergic ligands was performed (Figure 4.5). Two key ligand specific properties, binding affinity ($K_{L,A}$) and inverse agonism ($\alpha_{L,A}$), were estimated using data from Hoffmann et al¹⁹⁵. The authors determined receptor binding and adenylyl cyclase activity for 21 β -adrenergic ligand in Chinese hamster ovary cells expressing human β -adrenergic subtypes. Similar to earlier simulations, low and high isoproterenol were both simulated in the presence and absence of the indicated ligand at a concentration of 1 μM . The model predicted substantial diversity in the ability of ligands to maintain cAMP sensitivity to subsequent high dose isoproterenol (Figure 4.5 A). Ligand binding affinity influences cAMP sensitivity and there is an optimal binding affinity (for example metoprolol where sensitivity is highest). There is a mild positive correlation between α and cAMP sensitivity suggesting that ligands with high α (indicating a high degree of inverse agonism) preferentially increase cAMP sensitivity. This is due to such ligands keeping the receptor in an inactive state, preventing receptor desensitization (Figures 4.6-4.8).

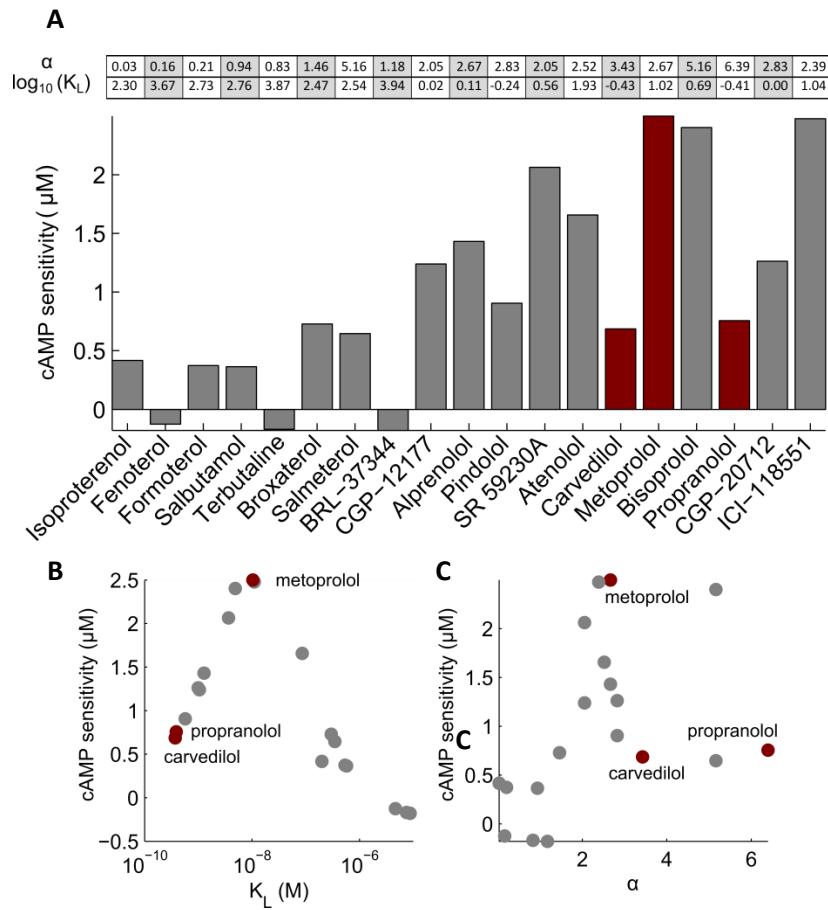


Figure 4.5: **Ligand binding affinity and inverse agonism both predicted to influence ligand cAMP sensitivity.** **A**, In-silico screen of 19 β_1 -adrenergic ligands predicts differential cAMP sensitivity. **B**, Effect of ligand dissociation constant (K_L) on predicted cAMP sensitivity. **C**, Effect of ligand inverse agonism (α) on predicted cAMP sensitivity. PRO, metoprolol and carvedilol (highlighted in red) were predicted to have distinct effects on cAMP sensitivity with varying combinations of ligand dissociation constant and inverse agonism.

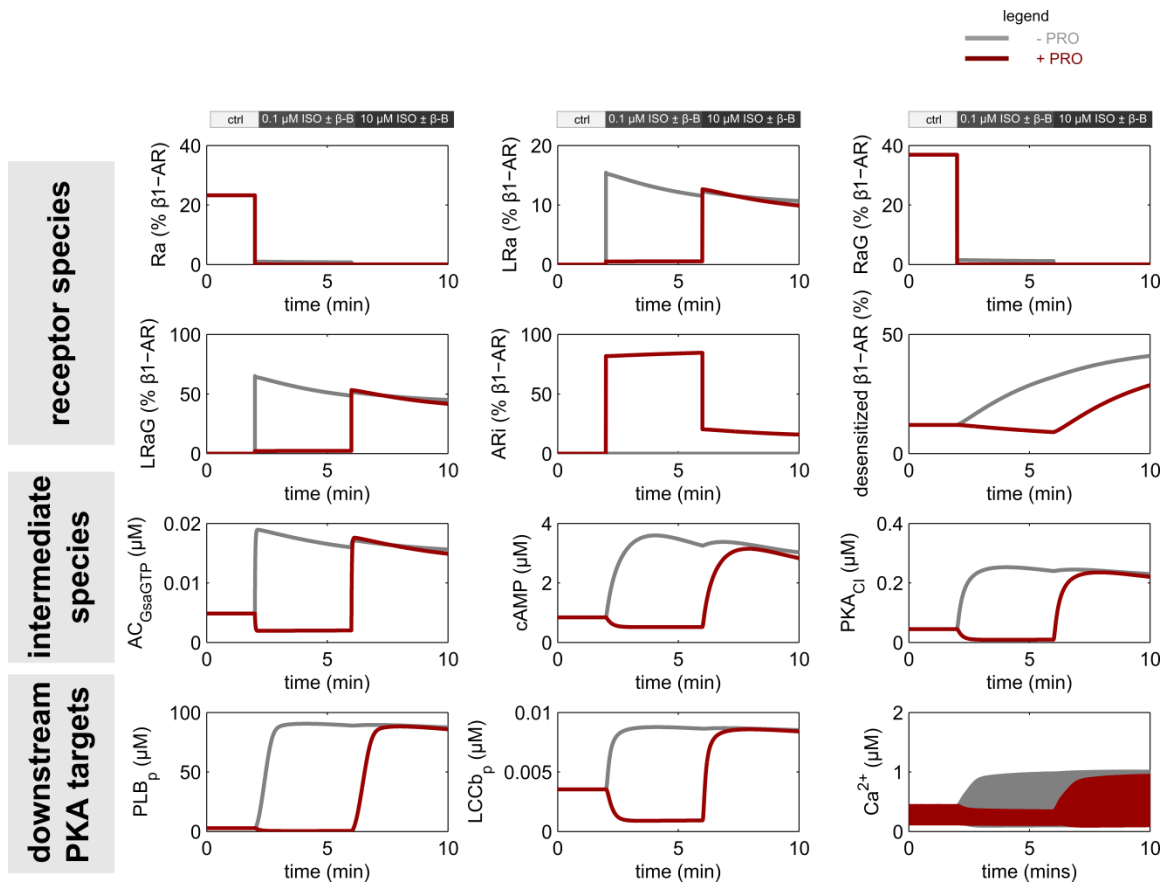


Figure 4.6: **Predicted effect of propranolol on kinetics of selected model state variables.**

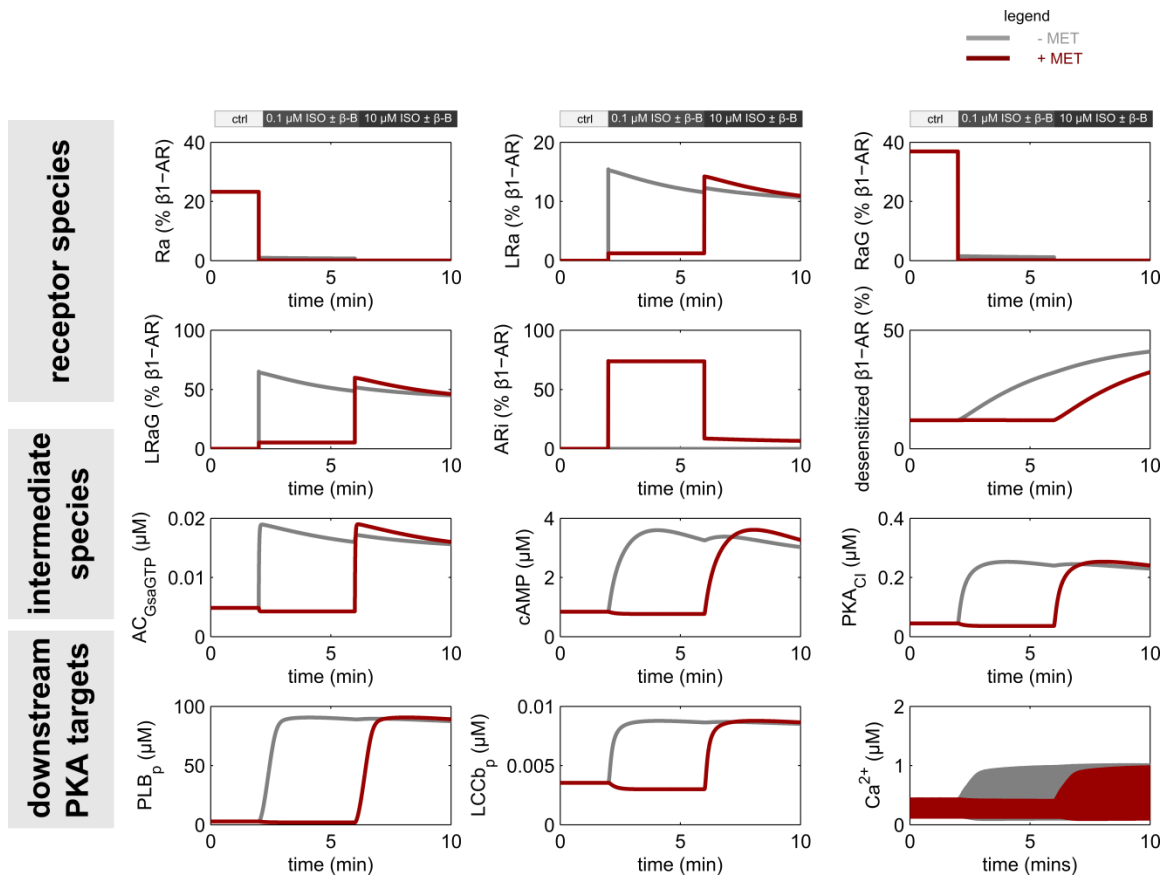


Figure 4.7: Predicted effect of metoprolol on kinetics of selected model state variables.

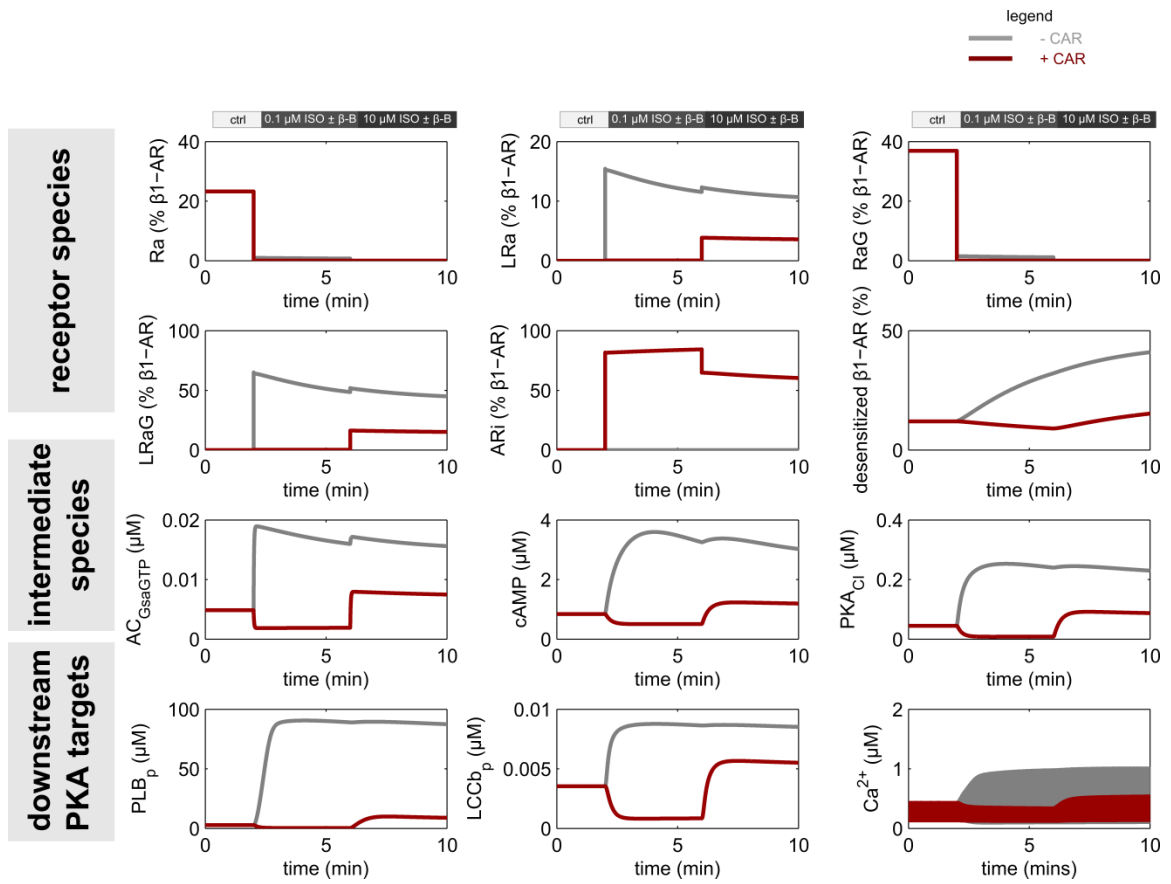
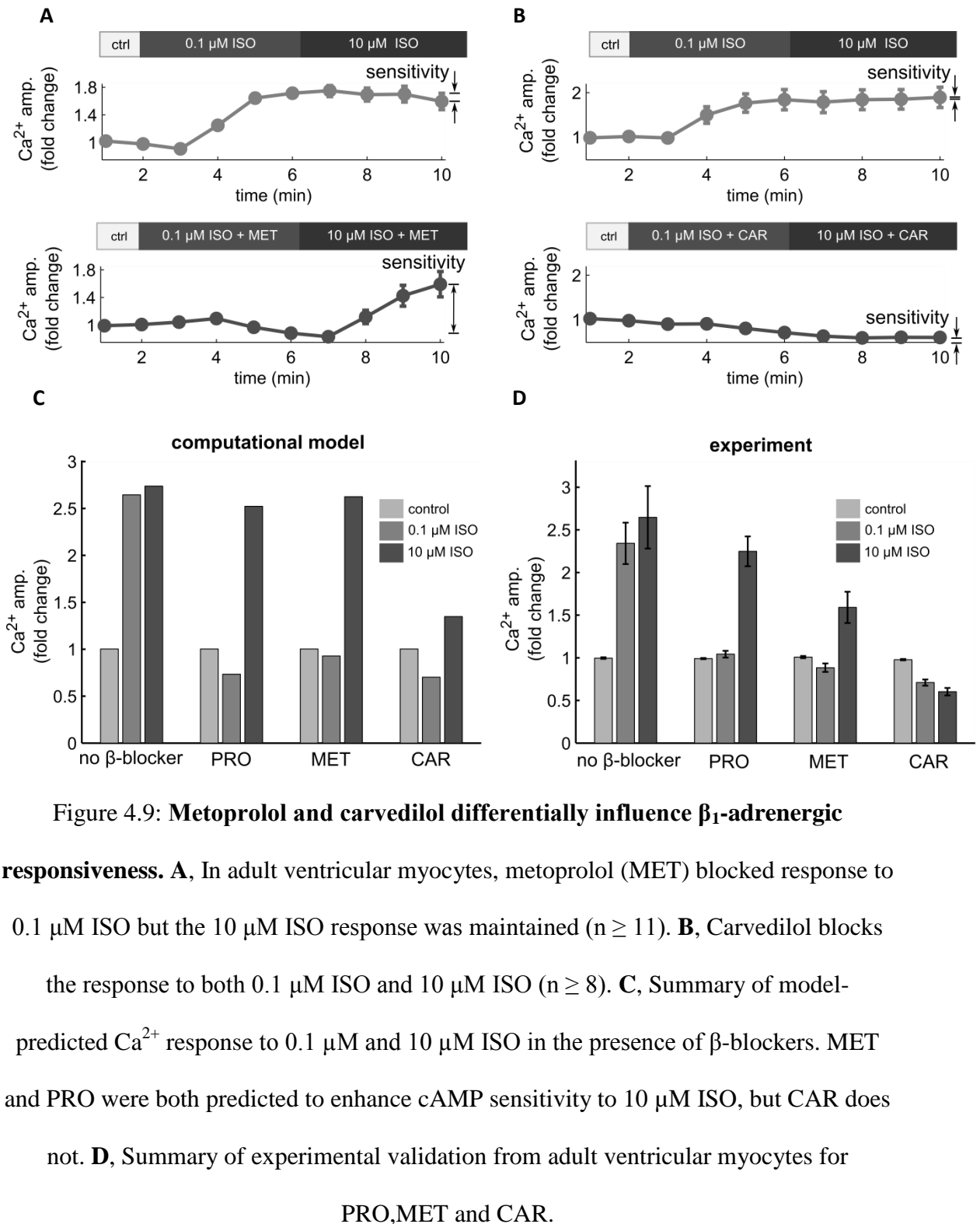


Figure 4.8: Predicted effect of carvedilol on kinetics of selected model state variables.

However, neither ligand binding affinity nor inverse agonism is sufficient to predict cAMP sensitivity. In order for the initial binding event to occur, a β -blocker needs to have a low enough binding affinity to compete out the receptor agonist. Thus the ability of β -blockers like metoprolol to maintain cAMP sensitivity is due to both inverse agonism and binding affinity.

4.3.4 Metoprolol and carvedilol differ in their ability to maintain β -adrenergic responsiveness

An interesting prediction of the in-silico screen is that the two clinically prescribed β -blockers carvedilol and metoprolol differ in their ability to enhance cAMP sensitivity. This discrepancy indicates that the two drugs might be beneficial through distinct mechanisms (inhibition or maintenance of the β_1 -adrenergic response). Evidence for why this might be important clinically can be seen in a double blind study comparing the efficacy of the two compounds in patients with heart failure¹⁹⁶. Although carvedilol had a greater overall anti-adrenergic effect, patients treated with metoprolol had increased exercise tolerance²⁶ implying increased sensitization to high receptor stimulation. To experimentally validate model predictions for carvedilol and metoprolol, Ca^{2+} imaging experiments of cardiac myocytes were performed. Consistent with our model predictions (Figure 4.9 C, D), sensitivity to high isoproterenol was maintained in cardiac myocytes treated with 1 μM metoprolol (Figure 4.9 A). In contrast, 1 μM carvedilol did not maintain β -adrenergic responsiveness to high isoproterenol stimulation (Figure 4.9 B).



4.3.5 *Receptor polymorphisms are differentially modulated by diverse β -blockers*

Genetic differences among patients also impacts β -blocker efficacy¹⁹⁷. Patients with the β_1 -Arg389 variant have a better prognosis following β -blocker administration compared with patients with the β_1 -Gly389 polymorphism. Increased G-protein binding is observed experimentally for the β_1 -Arg389 variant causing higher constitutive activity. This behavior was modeled by altering K_G , the ETCM model parameter that affects G-protein binding. The β_1 -Arg389 model is able to replicate the shift in agonist binding in the presence of GPP (Figure 4.10 A). In addition, the model is able to replicate the higher constitutive activity of the Arg389 variant (Figure 4.10 B). The polymorphisms had varying responses to PRO. Propranolol had more of an effect inhibiting the low isoproterenol cAMP and Ca^{2+} response in the Arg389 variant (Figure 7C) but also enhanced sensitivity to high isoproterenol. The 19 ligands have varying effect on cAMP sensitivity (Figure 7 D), similar to the β_1 -Gly389 variant (Figure 4.5 A). However, there are differences in the response to particular ligands between the receptor polymorphisms. (Figure 7 E). For example, atenolol produces a smaller cAMP response to further stimulation with high isoproterenol for the β_1 -Arg389 variant. This suggests that atenolol may not be suitable for individuals possessing the β_1 -Arg389 variant if maintaining β -adrenergic responsiveness to high stimulation is desired. This diversity of responses may help guide the selection of optimal β -blockers that elicit the desired clinical outcome in patient populations.

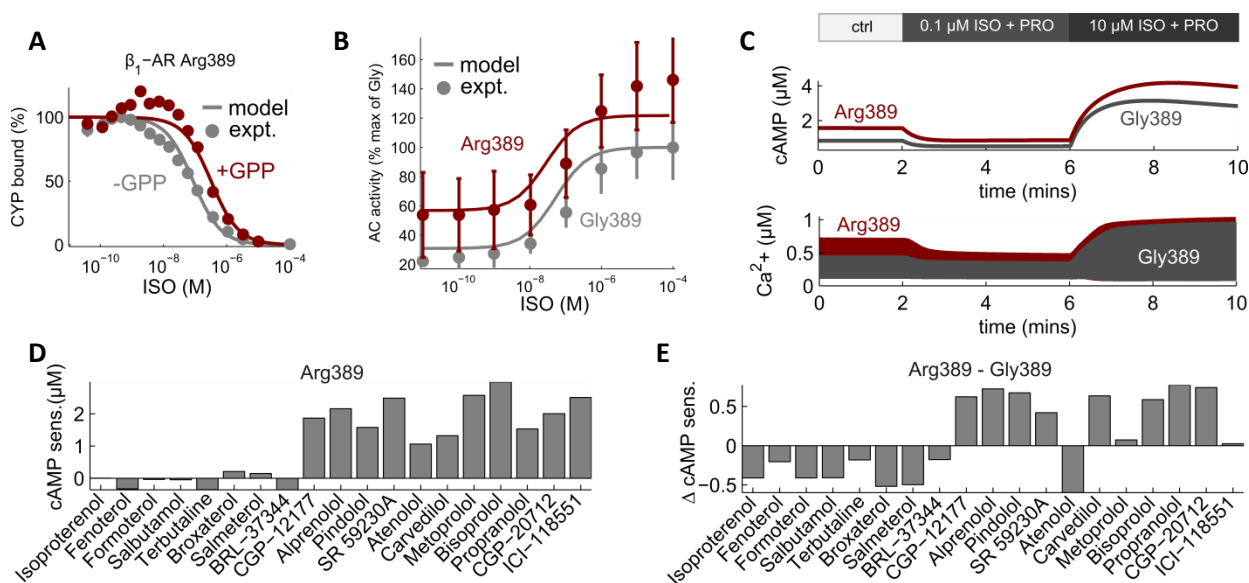


Figure 4.10: β_1 AR-Arg389 polymorphism responds differently to β -blockers. **A**, Model reproduces shift in agonist binding affinity in the presence of GPP for Arg389. **B**, Concentration dependence of adenylyl cyclase (AC) activity to isoproterenol for Gly389 and Arg389. **C**, Arg389 is predicted to have higher cAMP sensitivity and Ca^{2+} response versus Gly389. **D**, In-silico screen of 19 β_1 -adrenergic ligands against Arg389. **E**, Differential cAMP sensitivity between Arg389 and Gly389 for different β_1 -adrenergic ligands. Experimental data in panels A and B from (Mason et al., 1999; Rathz et al., 2003).

4.4 Discussion

4.4.1 Mechanisms of β -blocker efficacy in heart failure

A key feature of heart failure (HF) is the modest chronic elevation of circulating catecholamines (e.g. epinephrine) which desensitizes the β -adrenergic receptor signaling pathway, rendering patients incapable of increasing cardiac output in response to intense acute stress (e.g. exercise). Crucial alterations to the signaling pathway in this chronically activated state include reduced β_1 -adrenergic receptor density¹⁵ and Ca^{2+} ¹⁹⁸ in response to adrenergic stimulation. Sustained stimulation has detrimental long term consequences including apoptosis and hypertrophy^{9,10}. Maintenance of signaling in cardiomyopathy by adenylyl cyclase overexpression¹⁹⁹ or G-protein receptor kinase 2 inhibition²⁰⁰ has improved cardiac function in *in vitro* murine models. Previous studies of mechanisms governing β -blocker efficacy have focused exclusively on one of two mechanisms i.e. the inhibition²⁴ or maintenance of β_1 -adrenergic receptor signaling^{25,26}. With evidence supporting both theories, it is unclear how these two contradictory mechanisms can explain the same biological phenomena or the appropriate context where one mechanism dominates. We propose that both mechanisms can occur concurrently dependent on the magnitude of receptor stimulation.

Complexities at the receptor level and the influence of receptor polymorphisms complicate attempts to infer these mechanisms. Computational modeling is highly suited for this task by allowing the unbiased comparison of clinically available β -blockers. Previous computational models of the β_1 -adrenergic receptor pathway have used simplified receptor kinetic models^{185,201,202}. Although sufficient to describe the activation of the signaling pathway by agonists, these pathway models do not have the mechanistic

detail of receptor kinetics needed to adequately model the inverse agonism of β -blockers. Detailed receptor models have been developed but these models have been evaluated in isolation from downstream signaling pathways¹⁸⁸. To model β -blockers, detailed models of receptor kinetics were linked to the cardiac β_1 -adrenergic receptor pathway and excitation contraction coupling. Computational model simulations indicate that both inhibition and maintenance of signaling are compatible, dependent on the magnitude of receptor stimulation. Propranolol, a first generation β -blocker, inhibited low dose isoproterenol (analogous to chronic levels of catecholamine seen in heart failure) but enabled sensitivity to high dose isoproterenol (analogous to acute catecholamine levels during exercise). Ca^{2+} and FRET imaging of isolated cardiac myocytes confirmed this prediction.

4.4.2 Metoprolol and carvedilol have distinct mechanisms of action

Separate clinical trials of the two β -blockers commonly used to treat heart failure show reduction in mortality. Results of the COMET trial, which aimed to compare both treatments, concluded that carvedilol had a larger effect on mortality²⁰³. Significant controversy surrounds this result with questions raised on the appropriate dose of each compound that merits fair comparison²⁰⁴. Another important clinical measure of heart failure treatment effectiveness is exercise tolerance. Studies have shown that metoprolol has a larger effect on exercise tolerance versus carvedilol¹⁹⁶. Our computer simulations and Ca^{2+} imaging experiments confirm that metoprolol maintains β -adrenergic signaling due to its moderate binding affinity and high inverse agonism. Carvedilol, although also

an inverse agonist, did not maintain isoproterenol sensitivity due to its tight binding to the β_1 -adrenergic receptor. In vivo, carvedilol persistently blocks the β -adrenergic receptors 44 hours after drug withdrawal²⁰⁵. Despite its tight binding, carvedilol might offer longer term benefits because of its potential to reduce elevated signaling in patients whose receptors are already desensitized. In addition, the ancillary properties of carvedilol (e.g. blocking of α -adrenergic receptors), offers additional benefits over metoprolol.

4.4.3 *Pharmacogenomic targeted treatment with β -blockers*

Another factor complicating treatment of heart failure patients is the presence of β -adrenergic receptor polymorphisms. β_1 -Gly389 has been shown to couple less effectively to G-protein in expression cell systems but the β_1 -Arg389 variant provides higher risk to heart failure and differential response to β -blockers²⁰⁶. A recent study has shown that carvedilol exhibits enhanced inverse agonism with the β_1 -Arg389 variant³⁹, an example of the potential for personalized medicine. Understanding how genotype affects therapeutic response is expected to open a new era of pharmacogenomics and personalized medicine. One obstacle is that existing knowledge of β_1 -adrenergic receptor polymorphisms comes from cell lines and they may function differently in healthy or failing myocytes. We modeled β_1 -adrenergic receptor polymorphisms in the background of a cardiac myocyte. The model identified differences between the receptor polymorphisms cAMP sensitivity to high isoproterenol in the presence of particular ligands. For example, atenolol produces a smaller cAMP response to further stimulation

with high isoproterenol for the β_1 -Arg389 variant and might be less suited for patients with this particular polymorphism in maintaining β -adrenergic responsiveness.

4.4.4 *Limitations and Considerations*

A critical decision in developing computational models is specifying its scope. Uncertainty in parameters, and henceforth the ensuing predictions, becomes overwhelming as model scope increases. We have restricted our model to the β_1 -adrenergic receptor pathway because it is most abundant and largely responsible for mediating the contractile cell response following β -adrenergic stimulation. However, an alternative hypothesis is that ancillary properties of β -blockers i.e. blocking of other adrenergic receptors and pharmacokinetic properties e.g. half-life and lipid solubility may play a larger role than blockade of the β_1 -adrenergic receptors. Our current computational model is not able to explore this hypothesis. Future work could couple pharmacokinetic models to the β_1 -adrenergic signaling model with the inclusion of other adrenergic receptors including the β_2 -adrenergic receptor which has been shown to couple to other signaling pathways and could be a node for extensive signaling crosstalk²⁰⁷.

For this work, low (0.1 μ M) and high (10 μ M) ISO are intended to be analogous to chronically elevated levels of catecholamines in HF and acutely elevated levels in exercise respectively. Measurements of catecholamine levels in the bloodstream of heart failure patients indicate that the concentration ranges from 5-10 nM²⁰⁸. During exercise, cardiac catecholamine spillover into blood circulation increases 13 fold in healthy subjects and 5 fold in heart failure patients. While plasma levels of catecholamines are

indicative of the severity of the disease at rest²⁰⁹ and during exercise, they do not accurately reflect concentrations in the synaptic cleft (where concentrations could be significantly higher²¹⁰).

4.4.5 *Conclusions*

Previous studies have suggested two seemingly conflicting mechanisms (inhibition or maintenance of the β -adrenergic receptor signaling pathway) to explain β -blocker efficacy. Here we show that the β -blockers propranolol and metoprolol (but not carvedilol) not only block response to low isoproterenol (analogous to chronic stimulation in HF) but maintain the β -adrenergic receptor response to subsequent high isoproterenol (analogous to acute stimulation in exercise). Thus both inhibition and maintenance of signaling can occur concurrently dependent on the magnitude of receptor stimulation. Computational simulations indicate that these responses are modulated by particular receptor polymorphisms. Evaluating the mechanisms for these differences, with the help of computational models, is an important step towards designing personalized β -blocker therapies.

5. Integration of human transcriptome and systems models to analyze adrenergic responsiveness in human heart failure

5.1 Introduction

Heart failure is a condition in which cardiac output is not sufficient to supply the body's tissues with enough blood¹. Approximately 5 million Americans have the disease and although death rates have declined, the burden of the disease remains high with an estimated 20% of all hospital admissions of persons older than 65 due to heart failure². The disease is a clinical syndrome that represents the final pathway of a myriad of diseases that affect the heart² including myocardial infarction, coronary artery disease (ischemic cardiomyopathy) and genetic factors (hypertrophic cardiomyopathy). In addition there are a considerable number of patients where the cause is not apparent (idiopathic cardiomyopathy). Despite the varying etiologies and progression of the disease, key clinically observed symptoms include fatigue, breathlessness and exercise intolerance¹. One unifying clinical observation is the elevated levels of catecholamines in heart failure patients which remodels various signaling pathways²¹¹. This includes the β_1 -adrenergic receptor pathway which regulates cardiac contractility. Chronic exposure to catecholamines desensitizes the β_1 -adrenergic receptor pathway causing a loss of adrenergic responsiveness and an inability to increase cardiac output¹⁷. Alterations in protein levels of signaling components in the β_1 -adrenergic receptor pathway have been observed, most prominently the β_1 -adrenergic receptor which is downregulated 50% in heart failure patients¹⁵. Other altered pathway components include sarcoplasmic

reticulum Ca^{2+} ATPase (SERCA)²¹², G-protein receptor kinase (GRK2)²¹³ and phospholamban²¹⁴. Determining which of the observed changes are most influential in causing the heart failure phenotype has proved challenging²¹⁵. Studies investigating altered gene expression and protein remodeling in heart failure have either focused on a limited number of perturbations in the signaling pathway or studied them in isolation. Comprehensive investigation of how changes to the pathway contribute to the heart failure phenotype is required to understand or design therapies that restore adrenergic responsiveness. Examples of current therapies where adrenergic responsiveness is restored in heart failure include treatment with certain β -blockers²⁶ and implantation of a left ventricular assist device (LVAD)²¹⁶.

Computational modeling of the heart has been influential in understanding heart physiology and pathology²¹⁷ and such models have been identified as an appropriate system for understanding genotype-phenotype relationships in human populations²¹⁸. Britton et al. studied human variability in electrophysiological activity by constructing population computational models through randomly altering model parameters²¹⁹. Walmsey et al. developed population models of normal and failing cardiac myocytes by altering parameter values associated with significantly altered genes in heart failure²²⁰. Both studies, however, used parameter values sampled from idealized probability distributions rather than experimentally measured gene expression levels. Recently, our group has developed an EC coupling model of the Gq-overexpression mouse model of heart failure using both RNAseq and microarray data. Here we extend this approach to include both β_1 -adrenergic signaling and EC coupling and constrain model parameters based on human patient transcriptional profiles from the cardioGenomics consortium²²¹.

In spite of limited information on patient specific post-transcriptional and post-translation regulation, we hypothesized that the integration of mRNA expression alone would be sufficient to predict key aspects of the heart failure phenotype for different etiologies. Alterations in heart failure was studied comprehensively by mapping differential gene expression in idiopathic, ischemic and hypertrophic cardiomyopathy heart failure patients onto the protein species present in a previously developed β_1 -adrenergic signaling and EC coupling model¹³⁵. Sensitivity analysis predicted genes that contribute and compensate against the loss of adrenergic responsiveness in human heart failure. In addition, diverse patient transcriptional profiles resulted in distinct patient model responses that were correlated with clinical measures.

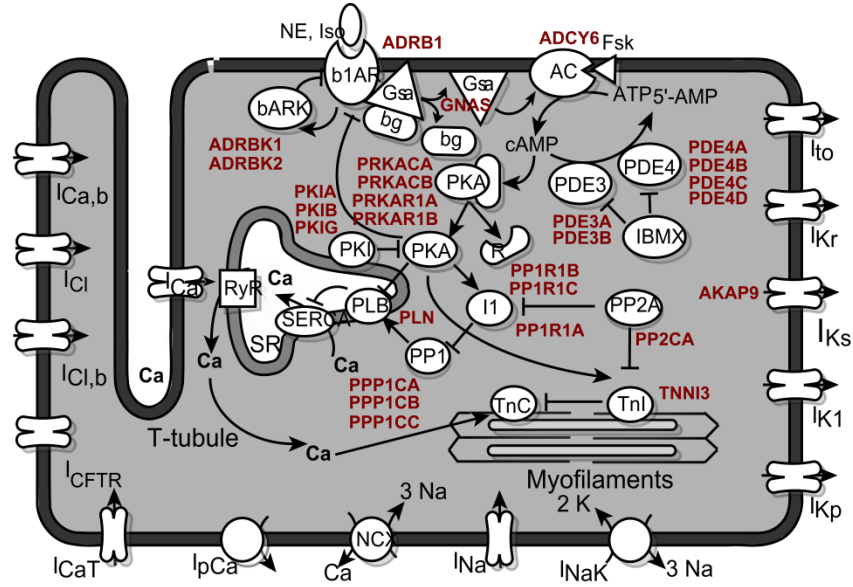
5.2 Materials and methods

5.2.1 Computational model of β_1 -adrenergic signaling and EC coupling in rabbit mouse ventricular myocytes

Experimentally determined mRNA expression profiles were integrated with a previously developed model of the rabbit ventricular myocyte that includes EC coupling, CaMKII and PKA signaling¹³⁵ (Figure 5.1). Computational modeling was performed in MATLAB (The Mathworks, Natick MA).

A

gene-protein-parameter mapping: signaling module



B

gene-protein-parameter mapping: excitation-contraction coupling module

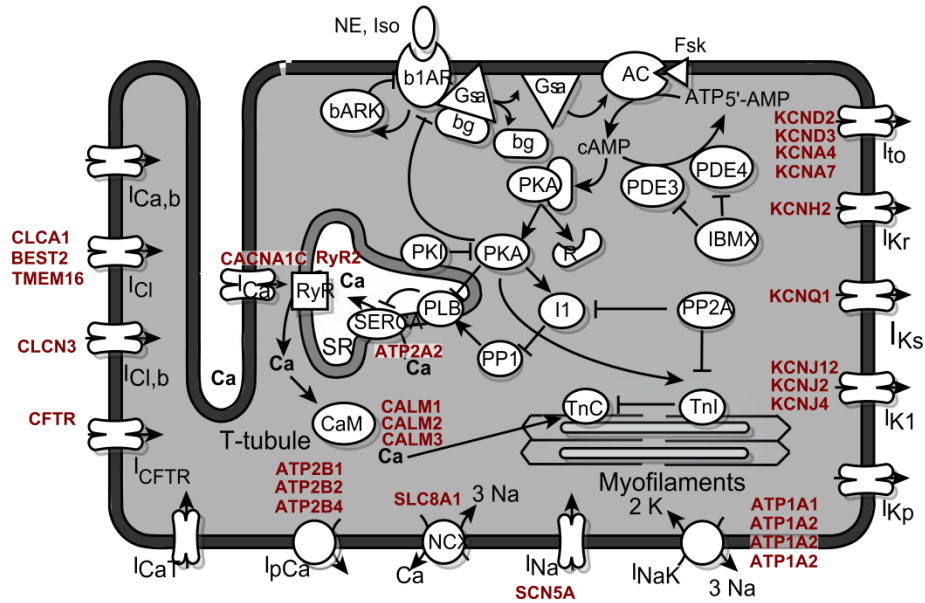


Figure 5.1: **Model schematic.** **A**, Signaling module. **B**, Excitation-contraction (EC)

coupling module. Mapped genes shown in red

5.2.2 Gene-protein parameter mapping

Gene-protein-parameter mapping of 59 genes associated with 30 proteins was mapped to 30 parameters in the model (Table 5.1 & 5. 2). Specific parameter/gene/gene/symbol assignments were made using NCBI gene (<http://www.ncbi.nlm.nih.gov/gene>) supplemented by literature references for chloride channels²²². Changes in ion channel gene expression were mapped by altering corresponding ion channel conductance parameters. Activity of the β -adrenergic kinase was altered by modifying the phosphorylation rate. Other gene expression levels were mapped to total protein concentration parameters. When a single gene's expression (G) is mapped to a parameter, fold change is determined as:

$$FC_{\text{HF condition}} = \frac{G_{\text{HF condition}}}{G_{\text{normal}}}$$

When multiple genes are mapped to a given parameter, fold change is determined as:

$$FC_{\text{HF condition}} = \frac{G_{1\text{HF condition}} + G_{2\text{HF condition}} + \dots + G_{n\text{HF condition}}}{G_{1\text{normal}} + G_{2\text{normal}} + \dots + G_{n\text{normal}}}$$

Parameters were modified by multiplying the normal parameters by the fold change. For the mRNA models, this assumes a linear relationship between mRNA expression level, protein abundance and the corresponding parameter value.

Table 5.1: **Gene-protein-parameter mapping: signaling module**

gene names	proteins	parameters
ADRB1	β_1 -adrenergic receptor	sumb1AR
GNAS	Gs protein	$G_{s_{tot}}$
ADCY5	adenylate cyclase	AC_{tot}
ADCY6		
PDE3A	phosphodiesterase 3	$PDE3_{tot}$
PDE3B		
PDE4A	phosphodiesterase 4	$PDE4_{tot}$
PDE4B		
PDE4C		
PDE4D		
PRKACA	protein kinase A type I	$PKAI_{tot}$
PRKACB		
PRKAR1A		
PRKACA	protein kinase A type II	$PKAII_{tot}$
PRKACB		
PRKAR2A		
PKIA	protein kinase inhibitor	PKI_{tot}
PKIB		
PKIG		
PLN	phospholamban	PLB_{tot}
PPP1CA	protein phosphatase I	$PP1_{tot}$
PPP1CB		
PPP1CC		
PPP1R1A	protein phosphatase inhibitor 1	$Inhib1_{tot}$
PPP1R1B		
PPP1R1C		
TNNI3	troponin I	TnI_{tot}
AKAP9	yotiao	$Yotiao_{tot}$
ADRBK1	β -adrenergic receptor kinase	$k_{f_{BARK}}$
ADRBK2		

Table 5. 2: **Gene-protein-parameter mapping: EC coupling module**

gene names	proteins	parameters
CACNA1C	L-type Ca channel, $\alpha 1c$ subunit	LCC_{tot}
RYR2	ryanodine receptor	RyR_{tot}
KCNQ1	slow potassium current	$I_{ks_{tot}}$
SLC8A1	Na/Ca exchanger	$I_{bar_{NCX}}$
CALM1	calmodulin	CaM_{tot}
CALM2		
CALM3		
SCN5A	sodium channel, voltage-gated, type V, alpha subunit	G_{Na}
KCND2	potassium voltage-gated channel, Shal-related subfamily	G_{toFast}
KCND3		
KCNH2	potassium voltage-gated channel subunit h	G_{Kr}
KCNJ2	potassium inwardly-rectifying channel	G_{K1}
KCNJ12		
KCNJ4		
ATP1A1	alpha subunit of Na ⁺ /K ⁺ -ATPases	$I_{bar_{NaK}}$
ATP1A2		
ATP1A3		
ATP1A4		
ATP2B1	Ca ²⁺ -pumping ATPase Sarcolemnal Ca Pump	$I_{bar_{SLCaP}}$
ATP2B2		
ATP2B4		
ATP2A2	one of the sarcoplasmic reticulum Calcium ATPase	$Vmax_{SRCaP}$
CLCN3	background chloride channel	G_{ClB}
CLCA1	calcium activated chloride channel	G_{Cl}
BEST2		
TMEM16		
KCNA4	potassium voltage-gated channel, shaker-related subfamily	G_{toSlow}
KCNA7		
CFTR	cystic fibrosis transmembrane conductance regulator	$CFTR_{tot}$

5.2.3 *Gene expression data*

Gene expression data was obtained from the cardioGenomics consortium (<http://cardiogenomics.med.harvard.edu/home>)²²¹. The database contains gene expression profiles of myocardial samples from patients undergoing cardiac transplantation with heart failure arising from different etiologies i.e. idiopathic dilated (27 patients), ischemic (31 patients) and hypertrophic (5 patients) cardiomyopathies. In addition, the database includes profiles of “normal” (14 patients) organ donors whose hearts were deemed unsuitable for transplantation. Gene expression data was analyzed using MATLAB’s Bioinformatics Toolbox.

5.2.4 *Simulation conditions*

All simulations were first run to steady state for 30 seconds and Ca^{2+} current and action potential were simulated. 6 functional readouts were quantified: diastolic Ca^{2+} transient level (Ca_{min}), Ca^{2+} transient amplitude (Ca_{amp}), time for 80% decay of Ca^{2+} transient (CaT_{80}), resting membrane potential (RMP), action potential duration at 50% repolarization (APD_{50}), and action potential duration at 70% repolarization (APD_{70}). Ca^{2+} transients and action potential were simulated at 1 Hz pacing. For patient simulations, fold change for each patient (normal, idiopathic, ischemic and hypertrophic) was calculated with reference to the normal population mean. Each patient model was run to steady state for 30 seconds. For simulations with isoproterenol (ISO), a dose of 1 μM was used.

5.2.5 Sensitivity analysis

Sensitivity analysis was performing by perturbing a single model parameter with corresponding fold change in mRNA expression. The effect of a single-gene perturbation of the i_{th} gene on a functional readout (FR) is quantified (similar to Feilun et al.; in preparation) by:

$$Z_{FR_i} = \frac{FR_i - FR_{normal}}{FR_{HF\ condition} - FR_{normal}}$$

5.2.6 Statistical analysis

Pearson correlation matrix was determined by finding correlation between each model output and clinical measures. Coefficient was considered significant for $p < 0.1$ without corrections for multiple comparisons.

5.3 Results

5.3.1 Validating computational models of human heart failure

Despite limited correlation between protein and mRNA expression, we hypothesized that mRNA expression measured by microarrays would be sufficient to predict the loss of adrenergic responsiveness seen in heart failure. To test this, transcriptional profiles of heart failure patients with different etiologies was integrated with a previously developed EC coupling and β_1 -adrenergic signaling model (Tables 5.1 & 5.2). The models of idiopathic, hypertrophic and ischemic cardiomyopathies was able to capture essential qualitative features of altered Ca^{2+} signaling in heart failure including reduced adrenergic responsiveness seen in heart failure (Figure 5.2 A).

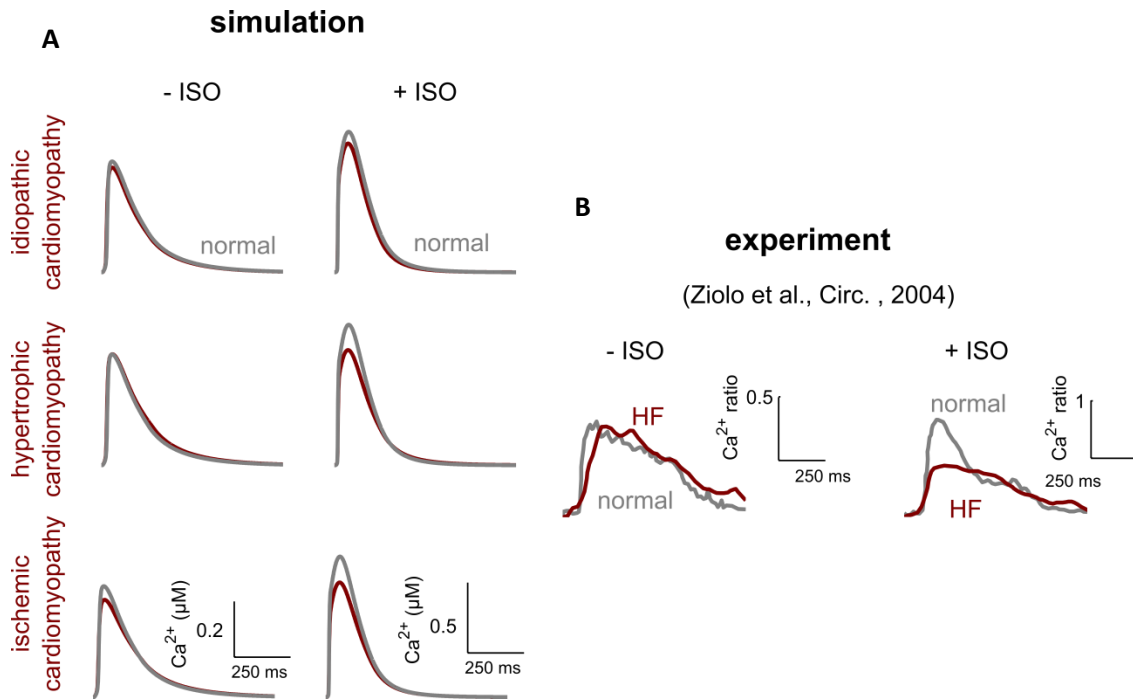


Figure 5.2: **Etiology-specific computational models capture altered features of Ca^{2+} signaling in failing human myocytes.** **A**, Simulation of Ca^{2+} transients from the idiopathic, hypertrophic and ischemic population models in the presence/absence of 1 μM ISO. **B**, Experimental recording of Ca^{2+} transients from isolated myocytes obtained from normal and failing human hearts (in the presence and absence of 1 μM ISO).

Experimentally, this manifests as lowered Ca^{2+} amplitude in heart failure patients compared to normal patients (Figure 5.2 B). Although model simulations differ quantitatively from the experimental measurement, Ziolo et al.²²³ measured Ca^{2+} transients from a single failing human heart while our model includes information from a large patient population. Thus the quantitative differences could be due to patient transcriptional profile diversity. The dearth and variability of single cell Ca^{2+} measurements of isolated human ventricular myocytes makes it difficult to verify this prediction.

5.3.2 Single gene-protein-parameter perturbations identify therapeutic targets for restoring adrenergic responsiveness

Single gene-protein-parameter perturbations were performed to examine the contribution of individual genes to the overall changes in the 6 functional readouts. For each simulation, only one parameter was altered from normal. When parameter mapping was based on average gene profiles of idiopathic patients, the Na-Ca exchanger (SLC8A1), which is upregulated in this condition, had the largest effect on both Ca^{2+} transient and action potential readouts with and without ISO stimulations (Figure 5.3 A,C). Inclusion of this parameter reduced Ca^{2+} amplitude and increased APD_{50} , consistent with observed changes seen in heart failure. The model however captures compensatory mechanisms that restore adrenergic responsiveness including ryanodine receptor (RYR2) and adenylyl cyclase (ADCY) which are both upregulated (Figure 5.3 B, D).

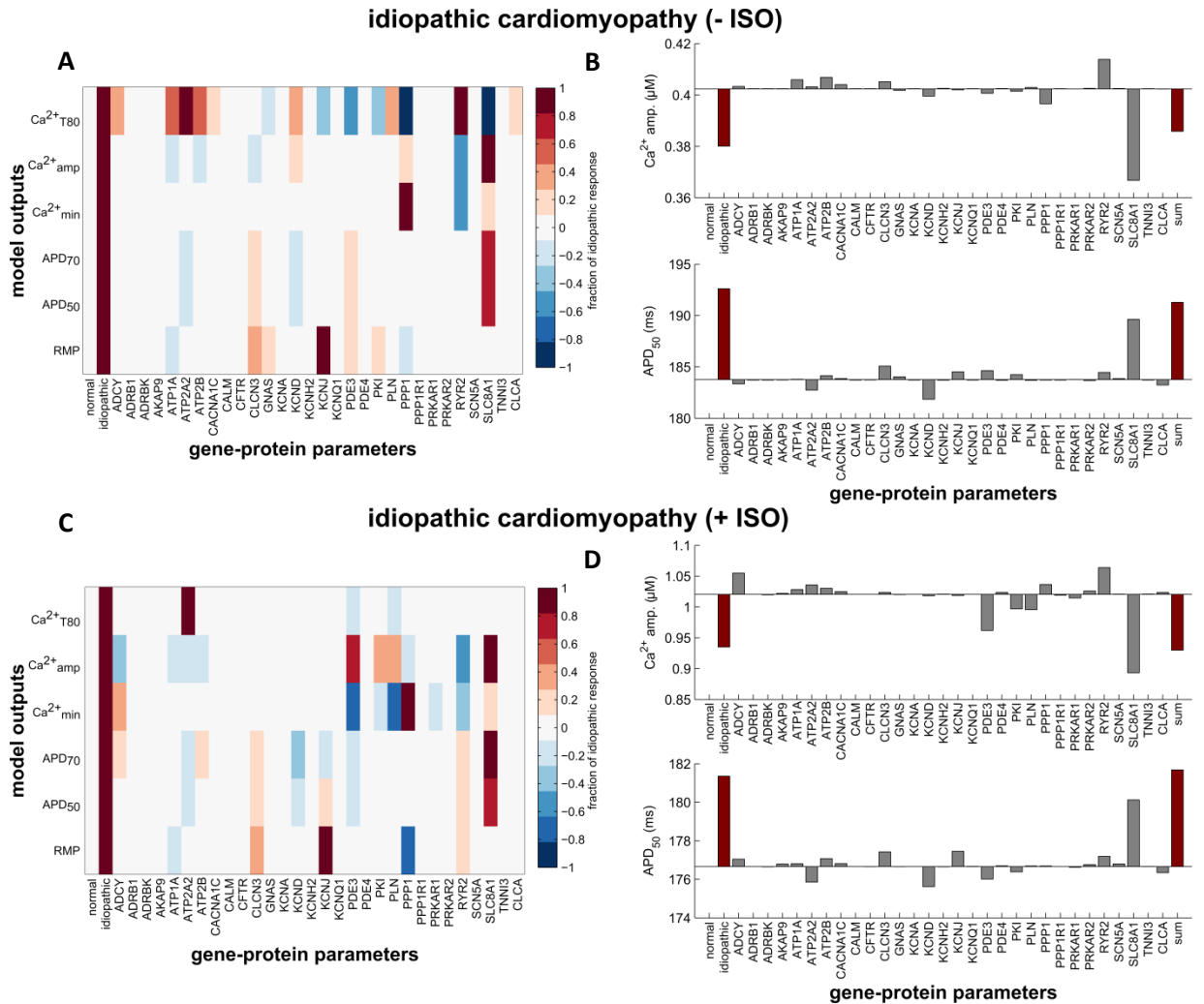


Figure 5.3: Single gene-protein-parameter perturbations of computational model based on idiopathic cardiomyopathy patient gene profiles. A, Fractional change in the idiopathic cardiomyopathy model response following single gene-protein-parameter perturbations in the absence of ISO. **B,** Ca^{2+} amplitude and action potential duration in the absence of ISO (full idiopathic cardiomyopathy model and sum of single gene-protein-parameter perturbations shown in red). **C,** Fractional change in the idiopathic cardiomyopathy model response following single gene-protein-parameter perturbations in the presence of ISO (1 μM). **D,** Ca^{2+} amplitude and action potential duration in the presence of ISO.

A similar trend is seen in model simulations with parameters altered using expression profiles of patients with hypertrophic cardiomyopathy (Figure 5.4). The Na-Ca exchanger still has the largest effect but different compensatory changes, which enhance adrenergic responsiveness, are present in this condition. This includes PKA type II (PRKAR2, upregulated) and the inward rectifying potassium channel (KCNH2, downregulated). For model simulations with parameters altered using gene profiles for ischemic cardiomyopathy patients, deleterious changes include the slow transient outward potassium channel (KCNA, upregulated). However, similar to the other two cardiomyopathies, Na-Ca exchanger expression is the major driver of altered Ca^{2+} transients and electrophysiology (Figure 5.5).

5.3.3 Model outputs predict patient clinical measures

Clustering of mapped genes for normal, idiopathic and ischemic patients was done to better understand the influence of individual patient gene profiles on adrenergic responsiveness (Figure 5.6 A). Clustering identified idiopathic patients with reduced expression of various signaling components including protein phosphatase I (PPP1), calmodulin (CALM) and the A-kinase anchoring protein yotiao (AKAP9). There was significant patient variability in other parameters, including the Na-Ca exchanger (SLC8A1), the major driver in the population averaged gene profiles. Clustering of individual patient profiles without ISO stimulation suggests that idiopathic patients have significant altered electrophysiology with prolonged action potential duration.

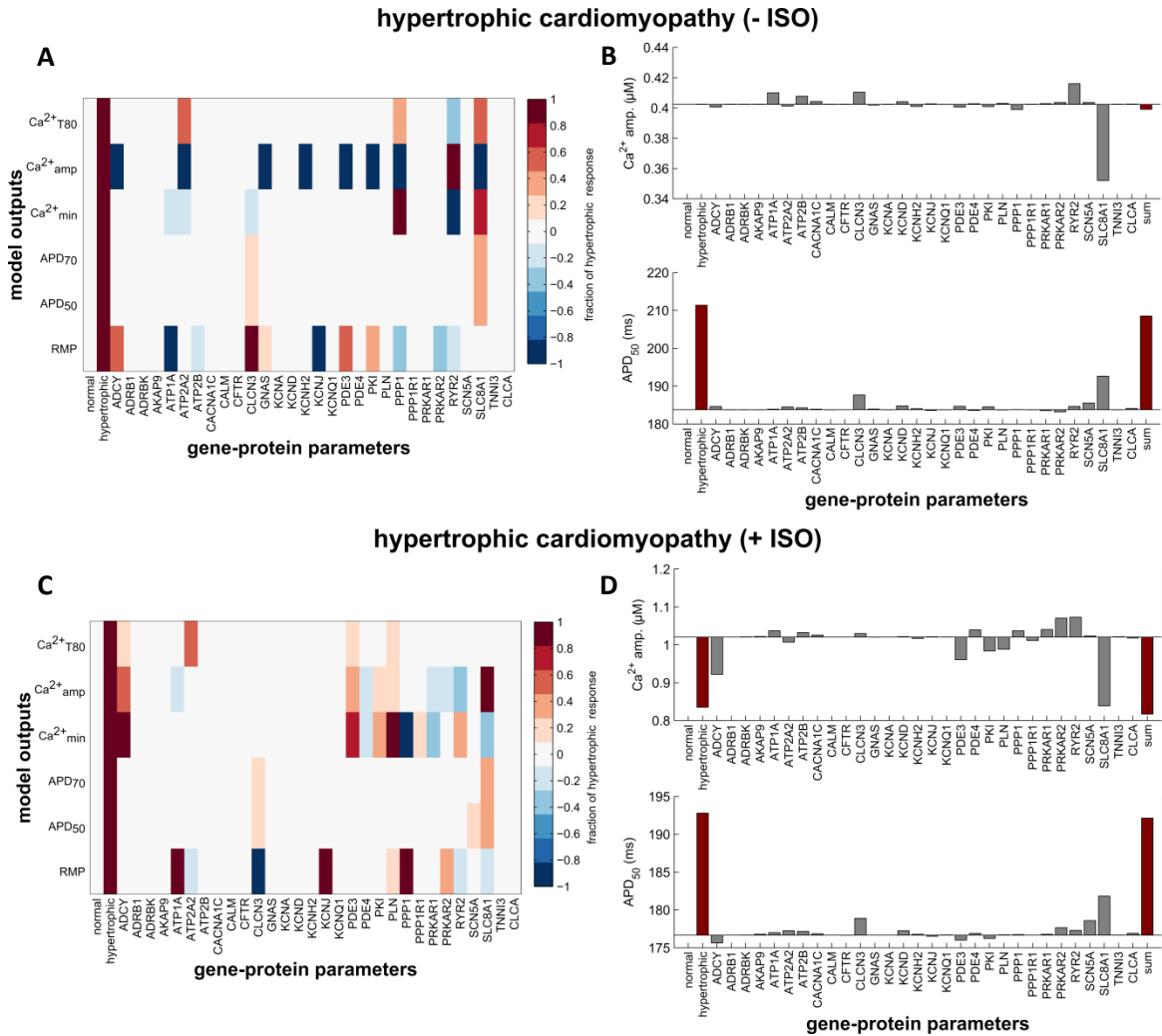


Figure 5.4: Single gene-protein-parameter perturbations of computational model based on hypertrophic cardiomyopathy patient gene profiles. A, Fractional change in the hypertrophic cardiomyopathy model response following single gene-protein-parameter perturbations in the absence of ISO. **B,** Ca^{2+} amplitude and action potential duration in the absence of ISO (full hypertrophic cardiomyopathy model and sum of single gene-protein-parameter perturbations shown in red). **C,** Fractional change in the hypertrophic cardiomyopathy model response following single gene-protein-parameter perturbations in the presence of ISO (1 μM). **D,** Ca^{2+} amplitude and action potential duration in the presence of ISO.

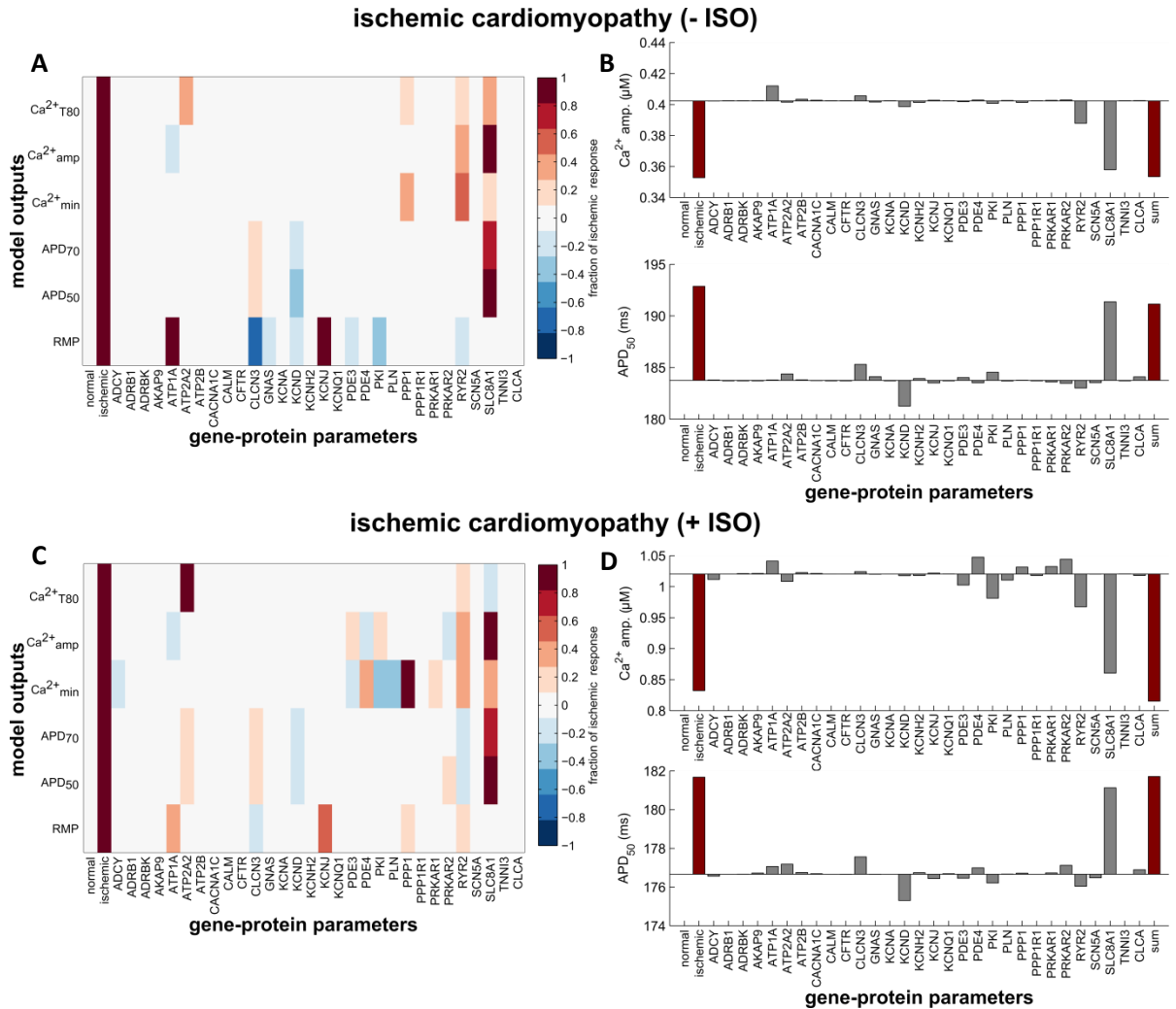


Figure 5.5: Single gene-protein-parameter perturbations of computational model based on ischemic cardiomyopathy patient gene profiles. **A**, Fractional change in the ischemic cardiomyopathy model response following single gene-protein-parameter perturbations in the absence of ISO. **B**, Ca^{2+} amplitude and action potential duration in the absence of ISO (full ischemic cardiomyopathy model and sum of single gene-protein-parameter perturbations shown in red). **C**, Fractional change in the ischemic cardiomyopathy model response following single gene-protein-parameter perturbations in the presence of ISO (1 μM). **D**, Ca^{2+} amplitude and action potential duration in the presence of ISO.

Following ISO stimulation, idiopathic and ischemic cardiomyopathy patients predominantly have reduced adrenergic responsiveness although there is variability in diastolic Ca^{2+} levels ($\text{Ca}^{2+}_{\text{min}}$). This highlights the diversity present in heart failure gene profiles and presents a significant challenge in developing appropriate therapeutic interventions. Model driven drug discovery can be useful in this endeavor especially if model outputs are predictive of clinical measures. Regression analysis was performed to determine which patient clinical measures are adequately predicted by the model's functional readouts (Figure 5.7 A, G). Ca^{2+} amplitude without ISO stimulation was positively correlated with cardiac output ($p = 0.09$). Model outputs are thus mildly predictive of particular clinical measures.

5.4 Discussion

In this study, high-throughput measurement of human mRNA expression was integrated into a mechanistic model of cardiac myocyte electrophysiology and β_1 -adrenergic signaling. Model predictions on Ca^{2+} dynamics in failing human hearts was validated against an independent experiment²²³ and sensitivity analysis identified the Na-Ca exchanger (NCX) as a major contributor to altered Ca^{2+} transient and action potential duration in all the heart failure etiologies tested. Simulations with individual patient transcriptional profiles resulted in distinct patient model Ca^{2+} responses that were correlated with cardiac output.

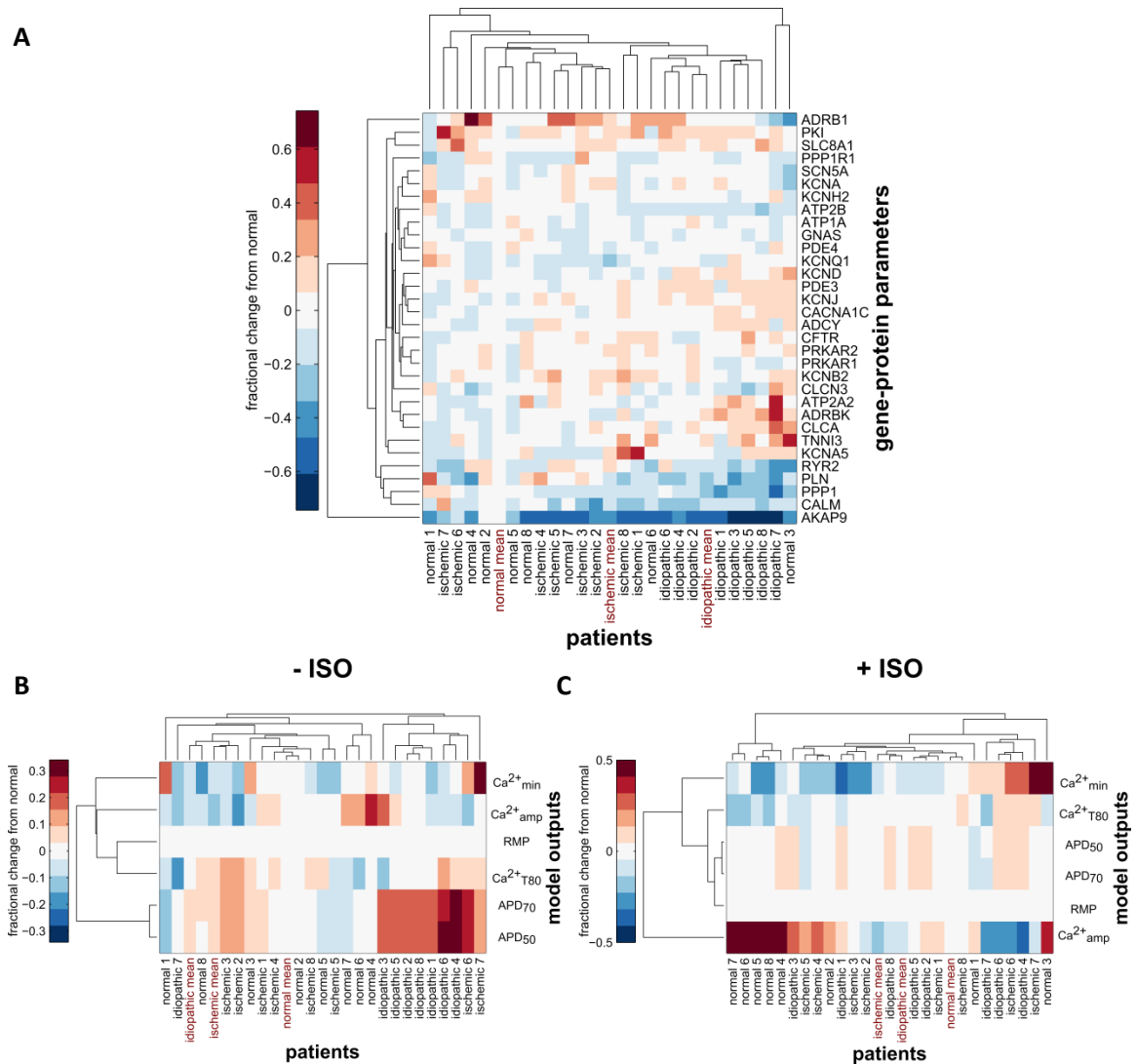


Figure 5.6: **Gene expression-based models model predict patient-specific adrenergic responsiveness.** **A**, Cluster map of fractional change in expression of mapped genes for normal, idiopathic and ischemic patients ($n = 24$). **B**, Fractional change in model outputs for single patient simulations ($n = 24$) in the presence and **C**, absence of ISO ($1 \mu\text{M}$).

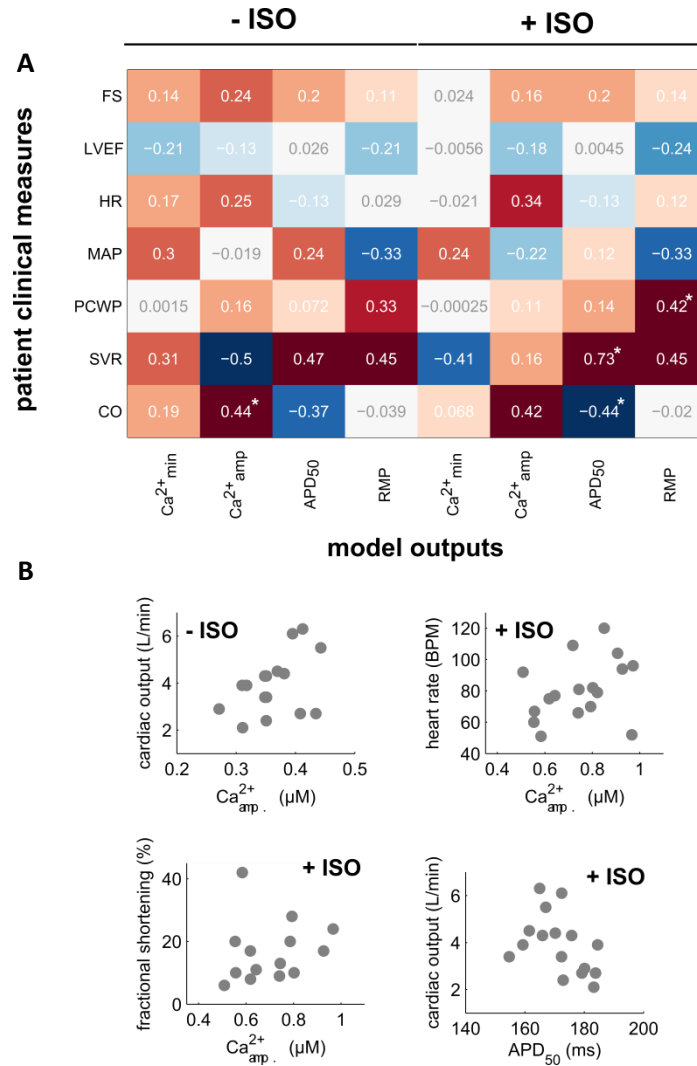


Figure 5. 7: **Gene-expression based models predict patient clinical measures. A,** Correlation matrix of model outputs versus patient clinical outcomes (* $p < 0.1$). **B,** Scatter plot of model outputs versus patient clinical measures. FS, fractional shortening; LVEF, left ventricular ejection fraction; HR, heart rate; MAP, mean arterial pressure; PCWP, pulmonary wedge pressure; SVR, systemic vascular resistance; CO, cardiac output.

5.4.1 *Genes contributing to altered β_1 -adrenergic signaling and EC coupling*

Patients with heart failure have depressed ventricular contractility²²⁴, also seen in ventricular myocytes isolated from heart failure patients²²⁵. These contractile deficits are associated with altered Ca^{2+} transient and action potentials, consistent with our model simulations²²⁶. Yet experimental data investigating the molecular mechanisms underlying these deficits are limited and inconsistent. For example, experimental measurement of protein levels of SERCA show disagreement in the literature. SERCA, a Ca^{2+} ATPase that resides in the sarcoplasmic reticulum, is responsible for Ca^{2+} removal from the cytosol. SERCA down regulation is thought to underlie the slow decay rate of Ca^{2+} transient in the failing heart²²⁷. However, some direct protein measurements have shown no change in SERCA expression^{228,229}. This suggests that the altered features of Ca^{2+} handling in the failing heart are not always caused by reduction in SERCA²³⁰.

Sensitivity analysis provided a number of interesting etiology-specific readouts that might help elucidate the roles of other individual genes in determining the cardiac phenotype. The NCX, which aids SERCA to remove cytosolic Ca^{2+} , predominantly reduced adrenergic responsiveness and prolonged action potential duration for all three etiologies. NCX is increased in heart failure²³¹ and is upregulated in all 3 cardiomyopathies included in our study. Interestingly, NCX protein levels are reduced in heart failure patients under LVAD treatment²³². This implicates increase in NCX protein abundance as a potential reason for the improvement in Ca^{2+} handling seen during LVAD treatment. Compensatory changes to increase adrenergic responsiveness were also detected, though the mechanisms differed across cardiomyopathies, including the ryanodine receptor (idiopathic and ischemic cardiomyopathies) adenylyl cyclase

(idiopathic cardiomyopathy) and PKA type II (hypertrophic and ischemic cardiomyopathies). This diversity in patient model responses is driven by etiology specific transcriptional profiles. Model outputs can thus serve as a tool in the classification of heart failure patients especially when linked with traditional statistical approaches.

5.4.2 Computational models can relate patient transcriptional profiles to clinical measures

Previous studies have used mechanistic models of cardiac myocytes to understand the genotype-phenotype gap in heart pathology. Several models have incorporated gene mutation or changes in protein expression, predicting mechanistic links to pathology^{71,137}. Regression analysis and global sensitivity of model parameters has also guided studies in phenotypic variation^{219,233}. While those studies simultaneously varied all parameters, results of our sensitivity analysis suggest that the heart failure phenotype can be explained by a combination of single gene interactions. This potentially reduces the search space for novel therapeutic targets. While a recent study has mapped genes to parameters in a cardiac computational model, parameter values were obtained from idealized probability distributions instead of directly incorporating measured changes in mRNA expression²²⁰. Also, our approach allows direct extension to other patient populations where transcriptional profiles have been measured including heart failure patients undergoing treatment with LVAD and β -blockers

Computational models that account for human genetic variability have the potential to significantly contribute to our understanding of human biological processes.

Understanding population variation is crucial in developing patient specific diagnoses of heart failure (which arises from multiple etiologies) and developing personalized therapies.

5.4.3 Limitations and Considerations

There are several limitations to the overall approach developed here. This includes the use of mRNA expression which is only partially correlated with protein expression. Comparison of the mouse cardiac proteome by mass spectrometry with Affymetrix microarray showed lower correlation between the transcriptome and proteome²³⁴. While proteomic information might be preferred for integration into mechanistic computational models, the dearth of such data leaves mRNA profiles as the best available alternative. In addition, the limited number of studies measuring Ca^{2+} and electrophysiology of isolated human myocytes made exhaustive model validation difficult. Despite these issues, this current study indicates that mRNA profiles may be sufficient to predict patient phenotypes.

A hypothesis suggested by our studies is that adrenergic responsiveness can be restored via therapeutic targeting of particular proteins. This could be tested by applying the same approach used here to datasets from patients undergoing treatment with LVAD and β -blockers. These treatments have been shown to restore adrenergic responsiveness and could confirm the targets suggested in this work. In addition, alterations in other

signaling pathways besides the β_1 -adrenergic pathway could be studied to identify other potential therapeutic targets.

Here we integrated transcriptional profiles with a rabbit computational model which shares many features of human excitation-contraction coupling²³⁵. Although no conflict arose between mappings of human genotypes to proteins in a rabbit computational model, this could be a potential issue as more comprehensive “omic” datasets are made available. In the future, our approach can be extended with the use of recently developed human ventricular myocyte models.

5.4.4 *Conclusions*

Integration of “omic” data into mechanistic models complements standard bioinformatics approaches that search for significantly correlated genes. Such an approach can provide a predictive and mechanistic linkage between genotype and phenotype in human populations. In this study, human transcriptional profiles were integrated with mechanistic computational models of β_1 -adrenergic signaling and EC coupling. Integration of mRNA expression alone was sufficient to predict key aspects of the heart failure phenotype for different etiologies.

6. Summary and Conclusions

The focus of this dissertation was to quantitatively examine how cardiac β -adrenergic signaling is modulated by β -blockers, receptor polymorphisms and altered expression of pathway components. This was achieved through the use of mechanistic computational models and live-cell imaging of isolated adult rat ventricular cardiac myocytes. While the focus was on β -adrenergic signaling and β -blockers, this work required the development of new computational and experimental approaches that could prove valuable for systems level analysis of therapeutics on other signaling networks.

6.1 Contribution to understanding of the mechanisms of β -blocker efficacy in heart failure

Previous studies of mechanisms governing β -blocker efficacy have focused exclusively on one of two mechanisms i.e. the inhibition²⁴ or sensitization of the β_1 -adrenergic receptor pathway^{25,26}. With evidence supporting both theories, it is unclear how these two contradictory mechanisms can explain the same biological phenomena or the appropriate context where one mechanism dominates. We proposed the novel concept that both mechanisms can occur concurrently dependent on the magnitude of receptor stimulation. This hypothesis was investigated using both computational and experimental approaches. Computational modeling allowed perturbation and observation of pathway components in a manner that is impossible with current experimental approaches. Ca^{2+} imaging experiments in adult rat ventricular cardiac myocytes was used to test model

predictions. This interplay between computational modeling and experimental validation allowed comprehensive study of the potential mechanisms governing β -blocker efficacy.

Previous models of the β_1 -adrenergic receptor pathway have used simplified receptor kinetic models^{185,201,202}. Although sufficient to describe the activation of the signaling pathway by agonists, these pathway models do not have the mechanistic detail of receptor kinetics needed to adequately model β -blockers or receptor polymorphisms. Detailed receptor models have been developed but these models have been evaluated in isolation from downstream signaling pathways¹⁸⁸. To model β -blockers, detailed models of receptor kinetics was linked to the cardiac β_1 -adrenergic receptor pathway and excitation contraction coupling.

The study of β -blocker inverse agonism *in vivo* is hampered by the ubiquitous presence of endogenous ligands. This limits experimental studies primarily to cell expression systems. We integrated these experiments to create a quantitative framework to study the mechanisms of β -blocker efficacy in cardiac myocytes. Complexities at the receptor level and the influence of receptor polymorphisms complicate attempts to infer these mechanisms. We discovered that computational modeling is highly suited for this task by allowing the unbiased comparison of clinically available β -blockers.

6.2 Contributions to understanding how altered expression of β_1 -adrenergic pathway components causes the heart failure phenotype

Previous studies have used mechanistic models of cardiac myocytes to understand the genotype-phenotype gap in heart pathology. Several models have incorporated gene mutation or changes in protein expression, predicting mechanistic links to pathology^{71,137}.

Regression analysis and global sensitivity of model parameters has also guided studies in phenotypic variation^{219,233}. While those studies simultaneously varied all parameters, results of our sensitivity analysis suggest that the heart failure phenotype can be explained by a combination of single gene interactions. This potentially reduces the search space for novel therapeutic targets. While a recently study has mapped genes to parameters in a cardiac computational model, parameter values were obtained from idealized probability distributions instead of directly incorporating measured changes in mRNA expression²²⁰. By incorporating patient transcriptional profiles into a cardiac computational model, we discovered that the compensatory changes that occur in heart failure are etiology-specific suggesting personalized therapeutics for certain heart failure patients.

6.3 Contributions to live-cell imaging of signaling networks in cardiac myocytes

Ca²⁺ imaging of isolated adult rat cardiac ventricular myocytes was used to validate our model predictions. The most common method of recording the fluorescent Ca²⁺ dye used in this model system is a photomultiplier tube (PMT) coupled to an epifluorescence microscope¹⁷⁴. The advantages of PMT's are their high sensitivity and temporal resolution. However, these advantages come at the cost of spatial resolution as fluorescence is only recorded from a single position. This limits recording to a single cell and does not allow simultaneous analysis of potentially interesting spatial features including cell size and shape. To address this issue, we developed a CCD based Ca²⁺ imaging platform¹⁹⁰. This method increased experimental throughput 10-fold reducing the number of animals required for this study. In addition, the increase in spatial

resolution achieved allows the future study of hypertrophy (caused by sustained β_1 -adrenergic signaling) through cell shape analysis.

6.4 Limitations

It is important not to underestimate the challenges involved in developing computational models. A key step in model development is identifying scope and the appropriate level of mechanistic detail. For example, the model developed in Chapter 4 was restricted to the β_1 -adrenergic receptor pathway because it is most abundant and largely responsible for mediating the contractile cell response following β -adrenergic stimulation. Most models are carefully optimized to address a particular set of biological questions or applications, often employing Albert Einstein's advice to "make everything as simple as possible, but not simpler." But when repurposing a model for drug discovery or integrating models with "omic" data, one must carefully re-evaluate the underlying model assumptions and revalidate for the new experimental system.

Parameter selection is particularly difficult when integrating multiple models, as most models are based on data from a range of experimental systems and animal species^{49,168}. And as modeling efforts are generally data-limited, the majority of models described in Chapter 4 and 5 were validated under a limited set of available experimental conditions. While fully comprehensive model validation is not feasible, a key challenge is to identify the extent of validation that builds sufficient confidence in new model predictions to guide the next experimental or clinical phase. Systematic efforts to validate fundamental aspects of myocyte physiology across a range of models are likely to help in this regard²³⁶.

6.5 Future directions

An alternative hypothesis suggested by our work in Chapter 4 is that ancillary properties i.e. pharmacokinetic properties e.g. half-life and lipid solubility play a larger role than blockade of the β -adrenergic receptors. While the development of the pharmacokinetic models was outside the scope of this thesis, future work could couple such models to the developed β_1 -adrenergic signaling model.

The increased efficacy of carvedilol, a non-selective β -blocker, compared to β_1 -specific blockers in clinical trials^{237,238} suggest that other isoforms of the β -adrenergic pathway, specifically the β_2 -adrenergic receptor (the second most abundant isoform), might be equally important. The β_2 -adrenergic receptor pathway plays a similar role in modulating contractility but is coupled to non-classical β -adrenergic pathways that reduce contractility and are anti-apoptotic²³⁹. Others have proposed, in contrast with non-selective β -blockade, that β_1 -specific blockers be combined with β_2 -specific agonists²⁴⁰. A complete understanding of the mechanisms of efficacy of β -blockers in heart failure might require the integration of the β_2 -adrenergic receptor pathway to current paradigms that focus on the β_1 -adrenergic receptor pathway.

As illustrated in Chapter 5, transcriptional profiles integrated with computational models can be useful in understanding human genotypes. In our study, we used transcriptional profiles of heart failure patients undergoing heart transplantation. An alternative approach is to focus on the mechanisms of therapeutic efficacy using microarray datasets of patients undergoing treatment with β -blockers and LVAD. A recently concluded clinical trial measured differential gene expression between patients undergoing treatment with the β -blockers carvedilol and metoprolol

(<http://clinicaltrials.gov/show/NCT01798992>). Iterations of the computational model could utilize this dataset and data from other similar future studies.

A hypothesis suggested by our studies is that adrenergic responsiveness is restored by reversal of the deleterious changes in the signaling pathway. An interesting alternative hypothesis is that adrenergic responsiveness is restored via changes to other signaling components. This could lead to the identification of novel therapeutic targets for heart failure.

The text of Chapter 6, in part, is a reprint of material as it appears in Amanfu, R. K. & Saucerman, J. J. Cardiac models in drug discovery and development: a review. *Crit Rev Biomed Eng* **39**, 379–395 (2011).

Appendix

Supplementary Methods

We previously developed a kinetic model that integrates β_1 -adrenergic receptor signaling with excitation contraction coupling in rat cardiac myocytes^{131,137}. The receptor module of this model is described by the ternary complex model (TCM) first developed by De Lean et al.¹⁸⁶. Later work by Samama et al.¹⁸⁸ suggested that the TCM could not adequately capture the constitutive activity of β -adrenergic receptors seen experimentally²⁴¹. An extended ternary complex model (ETCM) was then developed which proposes two receptor states i.e. an active and inactive. The existence of these states has been confirmed by recent determination of the crystal structure of the β_2 -adrenergic receptor¹⁸⁹. An agonist would then preferentially keep the receptor in an active state while; conversely, an inverse agonist would keep the receptor in the inactive conformation. There has been increasing evidence that β blockers function as inverse agonists²⁴². To better model β -blockers, we replaced the receptor module of the Saucerman-McCulloch β_1 -adrenergic model¹³¹ with the ETCM. We developed models of 9 agonists and 10 β -blockers of the receptor. This was done by determining the relevant receptor module parameters (K_R , K_L , K_A , K_G , α_L , α_A , γ_L , γ_A) using the following steps (Figure 1).

1. ETCM parameters were set equal to Samama et al¹⁸⁸.
2. K_G was altered (rate constant governing G protein binding to the active receptor) to achieve appropriate adenylyl cyclase constitutive activity following isoproterenol stimulation similar to *in vitro* cell membrane assays performed by Vila Petroff et al.¹⁹³ (Fig).
3. γ was altered for ISO to achieve max adenylyl cyclase activation in response to isoproterenol similar to Vila Petroff et al¹⁹³.

4. Non-linear least squares fit was performed to find α (the differential affinity of a ligand for the active receptor) for ligands that results in adenylyl cyclase activity measured by Hoffmann et al.¹⁹⁵. The influence of binding affinity was nullified by using a uniformly saturating concentration of ligand.
5. K_L (binding affinity of agonist) and K_A (binding affinity of antagonist) was calculated from binding affinity data in Hoffmann et al.¹⁹⁵. and the α 's fitted using the following relationship:

$$K_L = \frac{K_i K_R}{(K_R + 1)}$$

For experiments in cardiac myocytes, binding affinity was scaled to match the Ca^{2+} -isoproterenol dose response in cardiac myocytes.

6. Polymorphisms were modeled by altering K_G , rate constant governing G-protein binding to the active receptor, to match the difference in adenylyl cyclase activity seen in receptor variants (Figure 4.1).

In instances where mass balance of the receptor was violated due to numerical errors, the particular time steps and corresponding state variable values were removed (less than 0.1% of all time steps).

Model Equations and Parameters

β_1 -Adrenergic Signaling

Receptor/Gs module

Parameter	Description	Value	Units	Source
Ltot	agonist concentration (when used)	variable	μM	
b1ARtot	total β_1 -adrenergic receptors	0.0132	μM	

Gstot	total Gs protein	3.83	μM
K _R	propensity for switching between active and inactive receptor states	10	μM
K _L	equilibrium dissociation constant of the agonist receptor complex	variable	μM
K _A	equilibrium dissociation constant of the antagonist receptor complex	variable	μM
KG	ligand bound β1-AR associating with G-protein	variable	μM
α _L	differential affinity of the agonist for the active receptor	1	
α _A	differential affinity of the antagonist for the active receptor	variable	
γ _L	differential affinity of the agonist-receptor complex for G-protein	0.3762	
γ _A	differential affinity of the antagonist-receptor complex for G-protein	1	
K _d AC:Gs	Binding affinity of G-protein to AC		

$$Ra = \frac{Ri}{K_R}$$

$$LRi = \frac{Ltot * Ri}{K_R}$$

$$LRa = \frac{Ltot * Ra}{\alpha_L * K_L}$$

$$RaG = \frac{Ra * G}{K_G}$$

$$LRaG = \frac{LRa * G}{\gamma_L * K_G}$$

$$ARi = \frac{Atot * Ri}{K_A}$$

$$ARa = \frac{Atot * Ra}{\alpha_A * K_A}$$

$$ARaG = \frac{ARa * G}{\gamma_A * K_G}$$

$$\beta 1ARact = b1ARtot - b1AR_{S464} - b1AR_{S301}$$

$$\frac{dRi}{dt} = \beta 1ARact - Ra - L Ri - L Ra - RaG - LRaG - ARi - ARaG - Ri$$

$$\frac{dG}{dt} = Gstot - LRaG - RaG - ARaG$$

CV

Robert Kwesi Amanfu

University of Virginia
PO Box 800759
Charlottesville, VA 22908
rka2p@virginia.edu

EDUCATION

- **Ph.D. Candidate, Biomedical Engineering** expected 2013
University of Virginia,
Charlottesville, VA Advisor:
Jeffrey J. Saucerman, Ph.D.
Thesis topic: *Systems analysis of β -blockers and β -adrenergic responsiveness in cardiac myocytes*
- **B.S., Biomedical Engineering** 2007
University of Virginia,
Charlottesville, VA
Advisor: Edward A. Botchwey,
Ph.D.
Thesis topic: *Tissue engineering applications of sphingosine 1 phosphate.*

TEACHING

- BME 3080: Integrative Design and Experimental Analysis Lab I (TA, BME., UVA) Fall 2008
- BME 2101: Physiology for Engineers I (TA, BME., UVA) Fall 2009

PEER REVIEWED PUBLICATIONS (* denotes equal contribution)

- **Amanfu RK**, Saucerman JJ. *Integration of human transcriptome and systems models to analyze adrenergic responsiveness in human heart failure. (in preparation)*
- **Amanfu RK**, Meredith S, Connolly R, Saucerman JJ. *Modeling β 1-adrenergic receptor blockers and polymorphisms in cardiac myocytes. (submitted)*
- **Amanfu RK**, Saucerman JJ. *Cardiac models in drug discovery and development: a review. Crit Rev Biomed Eng **39**, 379–395 (2011).*
- **Amanfu RK**, Muller, J, Saucerman JJ. *Automated image analysis of cardiac myocyte Ca^{2+} dynamics. Conf Proc IEEE Eng Med Biol Soc 2011.*
- Benedict KF, Mac Gabhann F*, **Amanfu RK***, Chavali AK*, Gianchandani EP*, Glaw LS*, Oberhardt MA*, Thorne BC*, Yang JH*, Papin JA, Peirce SM, Saucerman JJ, Skalak TC. *Systems analysis of bounded signaling modules generates experimental roadmap for eight major diseases. Ann Biomed Eng. 2011; 39(2):621-35.*

PLATFORM PRESENTATIONS (presenter italicized)

Regional / National / International Meetings

- **Amanfu RK**, Saucerman JJ. *β -blockers simultaneously inhibit and enhance receptor sensitivity in silico and in vitro. 2012 Annual Fall Meeting of the Biomedical Engineering Society. 2012.*
- **Amanfu RK**, Saucerman JJ. *Automated image analysis of cardiac myocyte Ca^{2+} dynamics. 33rd Annual International Conference of the IEEE Engineering in Medicine and Biology Society, 2011.*
- **Amanfu RK**, Meredith S, Connolly R, Saucerman JJ. *β -blockers can enhance short term receptor sensitivity in silico and in vitro. 2009 Annual Fall Meeting of the Biomedical Engineering Society. 2009.*
- Benedict KF, Mac Gabhann F*, **Amanfu RK***, Chavali AK*, Gianchandani EP*, Glaw LS*, Oberhardt MA*, Yang JH*, Thorne BC, Papin JA, Peirce SM, Saucerman JJ, Skalak TC. *Systems Analysis of Bounded Signaling Modules Generates Novel Insight into Eight Major Diseases. 2009 Annual Fall Meeting of the Biomedical Engineering Society. 2009.*
- Saucerman JJ, **Amanfu RK**, Meredith S, Connolly R. *Modeling β 1-adrenergic receptor blockers and polymorphisms in cardiac myocytes. The Cardiac Physiome Project. 2009.*

- Saucerman JJ, **Amanfu RK**, Meredith S, Connoly R. *Modeling β 1-adrenergic receptor blockers and polymorphisms in cardiac myocytes*. 2008 Annual Fall Meeting of the Biomedical Engineering Society. 2008.

University of Virginia

- **Amanfu RK**, Saucerman JJ. *Understanding the mechanisms of β -blocker efficacy through automated analysis of cardiac myocyte Ca^{2+} dynamics*. 2013 Robert J. Huskey Graduate Research Exhibition. 2013.
- **Amanfu RK**, Saucerman JJ. *How do β -blockers work in heart failure?* GBS4 Graduate Biosciences Society Student Seminar Series. 2012.
- **Amanfu RK**, Saucerman JJ. *Automated image analysis of calcium myocyte calcium imaging*. UVA BMES Annual Graduate Student Symposium. 2011.

POSTER PRESENTATIONS

(presenter italicized)

Regional / National / International Meetings

- **Amanfu RK**, Saucerman JJ. *β -blockers can simultaneously enhance short term receptor sensitivity in silico and in vitro*. 2011 American Heart Association Basic Cardiovascular Sciences. 2011.
- **Amanfu RK**, Saucerman JJ. *Negative feedback regulation of Toll like receptor $\frac{1}{2}$ signaling in malaria*. 2009 Annual Fall Meeting of the Biomedical Engineering Society. 2009.
- Benedict K, MacGabhann F*, **Amanfu R***, Chavali A*, Gianchandani E*, Glaw L*, Oberhardt M*, Thorne B*, Yang J*, Papin J, Peirce S, Saucerman J, Skalak T. *Systems Analysis of Bounded Signaling Modules Generates Novel Insights into Eight Major Diseases*. 10th International Conference on Systems Biology. 2009.

University of Virginia

- **Amanfu RK**, Saucerman JJ. *Automated image analysis of cardiac myocyte Ca^{2+} imaging*. University of Virginia Engineering Research Symposium. 2013.
- **Amanfu RK**, Saucerman JJ. *β -blockers can simultaneously enhance short term receptor sensitivity in silico and in vitro*. 2012 Robert J. Huskey Graduate Research Exhibition. 2012.
- **Amanfu RK**, Saucerman JJ. *β -blockers can simultaneously enhance short term receptor sensitivity in silico and in vitro*. UVA BMES Annual Graduate Student Symposium. 2011.
- **Amanfu RK**, Botchwey EA. *Tissue engineering applications of sphingosine-1-phosphate*. UVA BME Capstone Symposium. 2007.

GRANTS / FELLOWSHIPS

- University of Virginia, Biomedical Engineering Department Year End Fellowship (\$6,115; Summer 2012)

AWARDS / HONORS

- Finalist, 2013 University of Virginia Engineering Research Symposium (\$100; 2013)
- 3rd Place, 2012 Robert J. Huskey Graduate Research Exhibition (\$100; 2012)
- Dean's List (University of Virginia; 2003-2007)
- Tau Beta Pi
- Longevity of Excellence Award
- Intermediate Honors

LEADERSHIP / SERVICE

- Co-founder, Vice-President, Graduate Student Consulting and Beyond Club at UVA (2012 -)
- Biomedical Engineering representative, Graduate School Arts and Sciences Council (2011- 2013)
- Member, Huskey Research Committee Planning Committee (2013)
- Member, Graduate Days Planning Committee (2012)
- Consultant, Student Entrepreneurs for Economic Development (2012)
- Member, Black Graduate Professional Students Association Economic Empowerment Committee (2011- 2012)

- Invited Speaker, JMU Virginia Biotechnology Association Graduate Bioscience Symposium (2011)
- Volunteer Tutor, Center for Diversity in Engineering (2010)
- Leader, University of Virginia Center for Systems Bioengineering Journal Club (2008 – 2009)

AFFILIATIONS

- American Association for the Advancement of Science (2007 – 2009)
- American Heart Association (2011 – Present)
- Biomedical Engineering Society (2003 – 2007)
- National Society of Black Engineers (2003 – 2007)

ADVISING / MENTORSHIP

Undergraduate Students (Years; Post-Graduate Activities)

- Selase Torkonoo, UVA (2012)
- James Muller, UVA (2010 – 2011)
- Brooks Taylor, UVA (2007 – 2009; Bioengineering Ph.D. Student, UC San Diego)

References

1. Mudd, J. O. & Kass, D. A. Tackling heart failure in the twenty-first century. *Nature* **451**, 919–928 (2008).
2. Jessup, M. & Brozena, S. Heart Failure. *N Engl J Med* **348**, 2007–2018 (2003).
3. El-Armouche, A. & Eschenhagen, T. {beta}-Adrenergic stimulation and myocardial function in the failing heart. *Heart Failure Reviews* doi:10.1007/s10741-008-9132-8
4. Wallukat, G. The β -Adrenergic Receptors. *Herz* **27**, 683–690 (2002).
5. Saucerman, J. J. & McCulloch, A. D. Cardiac β -Adrenergic Signaling: From Subcellular Microdomains to Heart Failure. *Annals of the New York Academy of Sciences* **1080**, 348–361 (2006).
6. Bers, D. M. Cardiac excitation–contraction coupling. *Nature* **415**, 198–205 (2002).
7. Dorn, G. W. & Liggett, S. B. Mechanisms of Pharmacogenomic Effects of Genetic Variation within the Cardiac Adrenergic Network in Heart Failure. *Molecular Pharmacology* **76**, 466–480 (2009).
8. Thomas, J. A. & Marks, B. H. Plasma norepinephrine in congestive heart failure. *The American Journal of Cardiology* **41**, 233–243 (1978).
9. Taimor, G., Schlüter, K.-D. & Piper, H. M. Hypertrophy-associated Gene Induction after β - Adrenergic Stimulation in Adult Cardiomyocytes. *Journal of Molecular and Cellular Cardiology* **33**, 503–511 (2001).
10. Communal, C., Singh, K., Pimentel, D. R. & Colucci, W. S. Norepinephrine Stimulates Apoptosis in Adult Rat Ventricular Myocytes by Activation of the β -Adrenergic Pathway. *Circulation* **98**, 1329–1334 (1998).
11. Bünemann, M., Lee, K. B., Pals-Rylaarsdam, R., Roseberry, A. G. & Hosey, M. M. Desensitization of G-Protein–coupled Receptors in the Cardiovascular System. *Annual Review of Physiology* **61**, 169–192 (1999).
12. Omori, K. & Kotera, J. Overview of PDEs and Their Regulation. *Circ Res* **100**, 309–327 (2007).
13. Carr, A. N. *et al.* Type 1 Phosphatase, a Negative Regulator of Cardiac Function. *Mol Cell Biol* **22**, 4124–4135 (2002).
14. Lefkowitz, R. J. G Protein-coupled Receptors III. NEW ROLES FOR RECEPTOR KINASES AND β -ARRESTINS IN RECEPTOR SIGNALING AND DESENSITIZATION. *J. Biol. Chem.* **273**, 18677–18680 (1998).
15. Bristow, M. *et al.* Decreased catecholamine sensitivity and β -adrenergic receptor density in failing human hearts. *N Engl J Med* **307**, 205–211 (1982).
16. Zarain-Herzberg, A., Afzal, N., Elimban, V. & Dhalla, N. S. Decreased expression of cardiac sarcoplasmic reticulum Ca(2+)-pump ATPase in congestive heart failure due to myocardial infarction. *Mol. Cell. Biochem.* **163-164**, 285–290 (1996).
17. Ungerer, M. *et al.* Expression of beta-arrestins and beta-adrenergic receptor kinases in the failing human heart. *Circ Res* **74**, 206–213 (1994).
18. Neumann, J. Altered phosphatase activity in heart failure, influence on Ca²⁺ movement. *Basic Res. Cardiol.* **97 Suppl 1**, I91–95 (2002).
19. Bristow, M. R. β -Adrenergic Receptor Blockade in Chronic Heart Failure. *Circulation* **101**, 558–569 (2000).
20. Waagstein, F., Hjalmarson, A., Varnauskas, E. & Wallentin, I. Effect of chronic beta-adrenergic receptor blockade in congestive cardiomyopathy. *Br Heart J* **37**, 1022–1036 (1975).
21. Krum, H. Beta-blockers in chronic heart failure: what have we learned? What do we still need to know? *Curr Opin Pharmacol* **3**, 168–174 (2003).

22. Tilley, D. G. & Rockman, H. A. Role of beta-adrenergic receptor signaling and desensitization in heart failure: new concepts and prospects for treatment. *Expert Rev Cardiovasc Ther* **4**, 417–432 (2006).
23. Lohse, M. J., Engelhardt, S. & Eschenhagen, T. What Is the Role of {beta}-Adrenergic Signaling in Heart Failure? *Circ Res* **93**, 896–906 (2003).
24. Lowes, B. D. *et al.* Effects of carvedilol on left ventricular mass, chamber geometry, and mitral regurgitation in chronic heart failure. *Am. J. Cardiol.* **83**, 1201–1205 (1999).
25. Michel, M. C. *et al.* Selective regulation of beta 1- and beta 2-adrenoceptors in the human heart by chronic beta-adrenoceptor antagonist treatment. *Br. J. Pharmacol.* **94**, 685–692 (1988).
26. Engelmeier, R. S. *et al.* Improvement in symptoms and exercise tolerance by metoprolol in patients with dilated cardiomyopathy: a double-blind, randomized, placebo-controlled trial. *Circulation* **72**, 536–546 (1985).
27. Yoshikawa, T. *et al.* Cardiac adrenergic receptor effects of carvedilol. *Eur. Heart J.* **17 Suppl B**, 8–16 (1996).
28. The Cardiac Insufficiency Bisoprolol Study II (CIBIS-II): a randomised trial. *The Lancet* **353**, 9–13 (1999).
29. Effect of metoprolol CR/XL in chronic heart failure: Metoprolol CR/XL Randomised Intervention Trial in Congestive Heart Failure (MERIT-HF). *Lancet* **353**, 2001–2007 (1999).
30. Packer, M. *et al.* Effect of carvedilol on survival in severe chronic heart failure. *N. Engl. J. Med.* **344**, 1651–1658 (2001).
31. Mason, R. P., Giles, T. D. & Sowers, J. R. Evolving Mechanisms of Action of Beta Blockers: Focus on Nebivolol. *Journal of Cardiovascular Pharmacology* **54**, 123–128 (2009).
32. Metra, M., Cas, L. D. & Cleland, J. G. F. Pharmacokinetic and Pharmacodynamic Characteristics of [beta]-Blockers: When Differences May Matter. *Journal of Cardiac Failure* **12**, 177–181 (2006).
33. Parra, S. & Bond, R. A. Inverse agonism: from curiosity to accepted dogma, but is it clinically relevant? *Current Opinion in Pharmacology* **7**, 146–150 (2007).
34. Baker, J. G. The selectivity of beta-adrenoceptor antagonists at the human beta1, beta2 and beta3 adrenoceptors. *Br. J. Pharmacol.* **144**, 317–322 (2005).
35. Krum, H. Beta-blockers in chronic heart failure: What have we learned? What do we still need to know? *Current Opinion in Pharmacology* **3**, 168–174 (2003).
36. Mason, D. A., Moore, J. D., Green, S. A. & Liggett, S. B. A Gain-of-function Polymorphism in a G-protein Coupling Domain of the Human β 1-Adrenergic Receptor. *J. Biol. Chem.* **274**, 12670–12674 (1999).
37. Rathz, D. A., Gregory, K. N., Fang, Y., Brown, K. M. & Liggett, S. B. Hierarchy of Polymorphic Variation and Desensitization Permutations Relative to B1- and B2-Adrenergic Receptor Signaling. *J. Biol. Chem.* **278**, 10784–10789 (2003).
38. Joseph, S. S., Lynham, J. A., Grace, A. A., Colledge, W. H. & Kaumann, A. J. Markedly reduced effects of (–)-isoprenaline but not of (–)-CGP12177 and unchanged affinity of β -blockers at Gly389- β 1-adrenoceptors compared to Arg389- β 1-adrenoceptors. *Br J Pharmacol* **142**, 51–56 (2004).
39. Rochais, F. *et al.* Real-time optical recording of β 1-adrenergic receptor activation reveals supersensitivity of the Arg389 variant to carvedilol. *J Clin Invest* **117**, 229–235 (2007).
40. Noble, D. Cardiac Action and Pacemaker Potentials based on the Hodgkin-Huxley Equations. *Nature* **188**, 495–497 (1960).
41. Fink, M. & Noble, D. Pharmacodynamic Effects in the Cardiovascular System: The Modeller’s View. *Basic & Clinical Pharmacology & Toxicology* **106**, 243–249 (2010).
42. Reumann, M. [1], Gurev, V. & Rice, J. J. Computational modeling of cardiac disease: potential for personalized medicine. *Personalized Medicine* **6**, 45–66 (2009).

43. Lloyd-Jones, D. *et al.* Heart Disease and Stroke Statistics--2010 Update. A Report From the American Heart Association. *Circulation* CIRCULATIONAHA.109.192667 (2009). doi:10.1161/CIRCULATIONAHA.109.192667
44. Echt, D. S. *et al.* Mortality and morbidity in patients receiving encainide, flecainide, or placebo. The Cardiac Arrhythmia Suppression Trial. *N. Engl. J. Med* **324**, 781–788 (1991).
45. Foody, J. M., Farrell, M. H. & Krumholz, H. M. {beta}-Blocker Therapy in Heart Failure: Scientific Review. *JAMA* **287**, 883–889 (2002).
46. Roden, D. M. Drug-induced prolongation of the QT interval. *N. Engl. J. Med* **350**, 1013–1022 (2004).
47. DiMasi, J. A., Hansen, R. W. & Grabowski, H. G. The price of innovation: new estimates of drug development costs. *Journal of Health Economics* **22**, 151–185 (2003).
48. Kola, I. & Landis, J. Can the pharmaceutical industry reduce attrition rates? *Nat Rev Drug Discov* **3**, 711–716 (2004).
49. Rodriguez, B. *et al.* The Systems Biology Approach to Drug Development: Application to Toxicity Assessment of Cardiac Drugs. *Clin Pharmacol Ther* **88**, 130–134 (2010).
50. Woodcock, J. & Woosley, R. The FDA critical path initiative and its influence on new drug development. *Annu. Rev. Med* **59**, 1–12 (2008).
51. Critical Path Initiative. at <http://www.fda.gov/ScienceResearch/SpecialTopics/CriticalPathInitiative/default.htm>
52. Lesko, L. J. Paving the Critical Path: How can Clinical Pharmacology Help Achieve the Vision? *Clin Pharmacol Ther* **81**, 170–177
53. Hunter, P. J. & Viceconti, M. The VPH-Physiome Project: Standards and Tools for Multiscale Modeling in Clinical Applications. *Biomedical Engineering, IEEE Reviews in* **2**, 40–53 (2009).
54. Cho, C. R., Labow, M., Reinhardt, M., van Oostrum, J. & Peitsch, M. C. The application of systems biology to drug discovery. *Curr Opin Chem Biol* **10**, 294–302 (2006).
55. Bers, D. M. Cardiac excitation-contraction coupling. *Nature* **415**, 198–205 (2002).
56. Modell, S. M. & Lehmann, M. H. The long QT syndrome family of cardiac ion channelopathies: A HuGE review*. *Genetics in Medicine* **8**, 143–155 (2006).
57. Priori, S. G. *et al.* Risk Stratification in the Long-QT Syndrome. *N Engl J Med* **348**, 1866–1874 (2003).
58. Jordan, P. N. & Christini, D. J. Therapies for ventricular cardiac arrhythmias. *Crit Rev Biomed Eng* **33**, 557–604 (2005).
59. Beeler, G. W. & Reuter, H. Reconstruction of the action potential of ventricular myocardial fibres. *J Physiol* **268**, 177–210 (1977).
60. Luo, C. & Rudy, Y. A model of the ventricular cardiac action potential. Depolarization, repolarization, and their interaction. *Circ Res* **68**, 1501–1526 (1991).
61. Luo, C. & Rudy, Y. A dynamic model of the cardiac ventricular action potential. I. Simulations of ionic currents and concentration changes. *Circ Res* **74**, 1071–1096 (1994).
62. Jafri, M. S., Rice, J. J. & Winslow, R. L. Cardiac Ca²⁺ dynamics: the roles of ryanodine receptor adaptation and sarcoplasmic reticulum load. *Biophys. J* **74**, 1149–1168 (1998).
63. Williams, G. S. B., Smith, G. D., Sobie, E. A. & Jafri, M. S. Models of cardiac excitation-contraction coupling in ventricular myocytes. *Math Biosci* **226**, 1–15 (2010).
64. Gadsby, D. C. Ion channels versus ion pumps: the principal difference, in principle. *Nat Rev Mol Cell Biol* **10**, 344–352 (2009).
65. Rudy, Y. & Silva, J. R. Computational Biology in the Study of Cardiac Ion Channels and Cell Electrophysiology. *Quarterly Reviews of Biophysics* **39**, 57–116 (2006).
66. Fink, M. & Noble, D. Markov models for ion channels: versatility versus identifiability and speed. *Philosophical Transactions of the Royal Society A: Mathematical, Physical and Engineering Sciences* **367**, 2161–2179 (2009).

67. Pugsley, M. K. Antiarrhythmic drug development: Historical review and future perspective. *Drug Development Research* **55**, 3–16 (2002).
68. Zareba, W. *et al.* Modulating effects of age and gender on the clinical course of long QT syndrome by genotype. *J. Am. Coll. Cardiol* **42**, 103–109 (2003).
69. Bennett, P. B., Yazawa, K., Makita, N. & George, A. L. Molecular mechanism for an inherited cardiac arrhythmia. *Nature* **376**, 683–685 (1995).
70. Clancy, C. E., Zhu, Z. I. & Rudy, Y. Pharmacogenetics and anti-arrhythmic drug therapy: a theoretical investigation. *Am J Physiol Heart Circ Physiol* **292**, H66–75 (2007).
71. Clancy, C. E. & Rudy, Y. Na(+) channel mutation that causes both Brugada and long-QT syndrome phenotypes: a simulation study of mechanism. *Circulation* **105**, 1208–1213 (2002).
72. Moreno, J. D. & Clancy, C. E. Using computational modeling to predict arrhythmogenesis and antiarrhythmic therapy. *Drug Discovery Today: Disease Models* **6**, 71–84 (2009).
73. Priebe, L. & Beuckelmann, D. J. Simulation study of cellular electric properties in heart failure. *Circ. Res.* **82**, 1206–1223 (1998).
74. Ten Tusscher, K. H. W. J., Noble, D., Noble, P. J. & Panfilov, A. V. A model for human ventricular tissue. *Am J Physiol Heart Circ Physiol* **286**, H1573–1589 (2004).
75. Iyer, V., Mazhari, R. & Winslow, R. L. A computational model of the human left-ventricular epicardial myocyte. *Biophys. J.* **87**, 1507–1525 (2004).
76. Grandi, E., Pasqualini, F. S. & Bers, D. M. A novel computational model of the human ventricular action potential and Ca transient. *Journal of Molecular and Cellular Cardiology* **48**, 112–121 (2010).
77. Ten Tusscher, K. H. W. J., Bernus, O., Hren, R. & Panfilov, A. V. Comparison of electrophysiological models for human ventricular cells and tissues. *Prog. Biophys. Mol. Biol* **90**, 326–345 (2006).
78. Fredj, S., Sampson, K. J., Liu, H. & Kass, R. S. Molecular basis of ranolazine block of LQT-3 mutant sodium channels: evidence for site of action. *Br J Pharmacol* **148**, 16–24 (2006).
79. Curran, M. A molecular basis for cardiac arrhythmia: HERG mutations cause long QT syndrome. *Cell* **80**, 795–803 (1995).
80. Recanatini, M., Cavalli, A. & Masetti, M. Modeling HERG and its interactions with drugs: recent advances in light of current potassium channel simulations. *ChemMedChem* **3**, 523–535 (2008).
81. London, B. *et al.* Two isoforms of the mouse ether-a-go-go-related gene coassemble to form channels with properties similar to the rapidly activating component of the cardiac delayed rectifier K⁺ current. *Circ. Res* **81**, 870–878 (1997).
82. Sale, H. *et al.* Physiological Properties of hERG 1a/1b Heteromeric Currents and a hERG 1b-Specific Mutation Associated With Long-QT Syndrome. *Circ Res* **103**, e81–95 (2008).
83. Antzelevitch, C. Role of transmural dispersion of repolarization in the genesis of drug-induced torsades de pointes. *Heart Rhythm* **2**, S9–15 (2005).
84. Campbell, S. G., Flaim, S. N., Leem, C. H. & McCulloch, A. D. Mechanisms of transmurally varying myocyte electromechanics in an integrated computational model. *Philos Trans A Math Phys Eng Sci* **366**, 3361–3380 (2008).
85. Pereon, Y. *et al.* Differential expression of KvLQT1 isoforms across the human ventricular wall. *Am J Physiol Heart Circ Physiol* **278**, H1908–1915 (2000).
86. Antzelevitch, C. M Cells in the Human Heart. *Circulation Research* **106**, 815–817 (2010).
87. Brennan, T. P., Fink, M., Stokeley, D., Rodriguez, B. & Tarassenko, L. Modelling effects of sotalol on T-wave morphology. in *2007 Computers in Cardiology* 249–252 (2007). doi:10.1109/CIC.2007.4745468
88. Brennan, T., Fink, M., Rodriguez, B. & Tarassenko, L. T. in *11th Mediterranean Conference on Medical and Biomedical Engineering and Computing 2007* 50–53 (2007). at <http://dx.doi.org/10.1007/978-3-540-73044-6_14>

89. Peitersen, T. *et al.* Computational analysis of the effects of the hERG channel opener NS1643 in a human ventricular cell model. *Heart Rhythm* **5**, 734–741 (2008).
90. Hansen, R. S. *et al.* Activation of Human ether-a-go-go-Related Gene Potassium Channels by the Diphenylurea 1,3-Bis-(2-hydroxy-5-trifluoromethyl-phenyl)-urea (NS1643). *Molecular Pharmacology* **69**, 266–277 (2006).
91. Casis, O., Olesen, S.-P. & Sanguinetti, M. C. Mechanism of action of a novel human ether-a-go-go-related gene channel activator. *Mol. Pharmacol.* **69**, 658–665 (2006).
92. Mirams, G. R. *et al.* Simulation of multiple ion channel block provides improved early prediction of compounds' clinical torsadogenic risk. *Cardiovasc Res* **91**, 53–61 (2011).
93. Rodriguez, B., Trayanova, N. & Noble, D. Modeling Cardiac Ischemia. *Annals of the New York Academy of Sciences* **1080**, 395–414 (2006).
94. Ventura-Clapier, R., Garnier, A. & Veksler, V. Energy metabolism in heart failure. *J Physiol* **555**, 1–13 (2004).
95. Rubart, M. & Zipes, D. P. Mechanisms of sudden cardiac death. *J. Clin. Invest.* **115**, 2305–2315 (2005).
96. Carmeliet, E. Cardiac ionic currents and acute ischemia: from channels to arrhythmias. *Physiol. Rev.* **79**, 917–1017 (1999).
97. Doenst, T. *et al.* Three good reasons for heart surgeons to understand cardiac metabolism. *Eur J Cardiothorac Surg* **33**, 862–871 (2008).
98. Neubauer, S. The Failing Heart -- An Engine Out of Fuel. *N Engl J Med* **356**, 1140–1151 (2007).
99. Shaw, R. M. & Rudy, Y. Electrophysiologic effects of acute myocardial ischemia: a theoretical study of altered cell excitability and action potential duration. *Cardiovasc. Res* **35**, 256–272 (1997).
100. Cascio, W. E., Johnson, T. A. & Gettes, L. S. Electrophysiologic changes in ischemic ventricular myocardium: I. Influence of ionic, metabolic, and energetic changes. *J. Cardiovasc. Electrophysiol.* **6**, 1039–1062 (1995).
101. Noma, A. ATP-regulated K⁺ channels in cardiac muscle. *Nature* **305**, 147–148 (1983).
102. D'Alonzo, A. J. *et al.* Effect of potassium on the action of the KATP modulators cromakalim, pinacidil, or glibenclamide on arrhythmias in isolated perfused rat heart subjected to regional ischaemia. *Cardiovasc. Res.* **28**, 881–887 (1994).
103. D'Alonzo, A. J., Zhu, J. L., Darbenzio, R. B., Dorso, C. R. & Grover, G. J. Proarrhythmic effects of pinacidil are partially mediated through enhancement of catecholamine release in isolated perfused guinea-pig hearts. *J. Mol. Cell. Cardiol.* **30**, 415–423 (1998).
104. Trénor, B., Ferrero, J. M., Rodríguez, B. & Montilla, F. Effects of pinacidil on reentrant arrhythmias generated during acute regional ischemia: a simulation study. *Ann Biomed Eng* **33**, 897–906 (2005).
105. Ferrero, J. M., Saiz, J., Ferrero, J. M. & Thakor, N. V. Simulation of Action Potentials From Metabolically Impaired Cardiac Myocytes: Role of ATP-Sensitive K⁺ Current. *Circ Res* **79**, 208–221 (1996).
106. Ch'en, F. F., Vaughan-Jones, R. D., Clarke, K. & Noble, D. Modelling myocardial ischaemia and reperfusion. *Prog. Biophys. Mol. Biol* **69**, 515–538 (1998).
107. DiFrancesco, D. & Noble, D. A model of cardiac electrical activity incorporating ionic pumps and concentration changes. *Philos. Trans. R. Soc. Lond., B, Biol. Sci.* **307**, 353–398 (1985).
108. Noble, D. & Noble, P. J. Late sodium current in the pathophysiology of cardiovascular disease: consequences of sodium–calcium overload. *Heart* **92**, iv1–iv5 (2006).
109. Michailova, A. & McCulloch, A. Model study of ATP and ADP buffering, transport of Ca(2+) and Mg(2+), and regulation of ion pumps in ventricular myocyte. *Biophys J* **81**, 614–629 (2001).

110. Puglisi, J. L., Wang, F. & Bers, D. M. Modeling the isolated cardiac myocyte. *Prog. Biophys. Mol. Biol* **85**, 163–178 (2004).
111. Cortassa, S. *et al.* A computational model integrating electrophysiology, contraction, and mitochondrial bioenergetics in the ventricular myocyte. *Biophys. J* **91**, 1564–1589 (2006).
112. Cortassa, S., Aon, M. A., Marban, E., Winslow, R. L. & O'Rourke, B. An Integrated Model of Cardiac Mitochondrial Energy Metabolism and Calcium Dynamics. *Biophys J* **84**, 2734–2755 (2003).
113. Beard, D. A. Modeling of oxygen transport and cellular energetics explains observations on in vivo cardiac energy metabolism. *PLoS Comput. Biol* **2**, e107 (2006).
114. Wu, F., Zhang, J. & Beard, D. A. Experimentally observed phenomena on cardiac energetics in heart failure emerge from simulations of cardiac metabolism. *Proceedings of the National Academy of Sciences* **106**, 7143–7148 (2009).
115. Mudd, J. O. & Kass, D. A. Tackling heart failure in the twenty-first century. *Nature* **451**, 919–928 (2008).
116. Wallis, J. *et al.* Supranormal myocardial creatine and phosphocreatine concentrations lead to cardiac hypertrophy and heart failure: insights from creatine transporter-overexpressing transgenic mice. *Circulation* **112**, 3131–3139 (2005).
117. Salazar, N. C., Chen, J. & Rockman, H. A. Cardiac GPCRs: GPCR Signaling in Healthy and Failing Hearts. *Biochim Biophys Acta* **1768**, 1006–1018 (2007).
118. Schaub, M. C., Hefti, M. A. & Zaugg, M. Integration of calcium with the signaling network in cardiac myocytes. *Journal of Molecular and Cellular Cardiology* **41**, 183–214 (2006).
119. Bers, D. M. & Guo, T. Calcium signaling in cardiac ventricular myocytes. *Ann. N. Y. Acad. Sci.* **1047**, 86–98 (2005).
120. Maier, L. S. CaMKII δ overexpression in hypertrophy and heart failure: cellular consequences for excitation-contraction coupling. *Braz. J. Med. Biol. Res.* **38**, 1293–1302 (2005).
121. Bers, D. M. & Grandi, E. Calcium/calmodulin-dependent kinase II regulation of cardiac ion channels. *J. Cardiovasc. Pharmacol.* **54**, 180–187 (2009).
122. Livshitz, L. M. & Rudy, Y. Regulation of Ca²⁺ and electrical alternans in cardiac myocytes: role of CAMKII and repolarizing currents. *Am J Physiol Heart Circ Physiol* **292**, H2854–2866 (2007).
123. Hund, T. J. & Rudy, Y. Rate dependence and regulation of action potential and calcium transient in a canine cardiac ventricular cell model. *Circulation* **110**, 3168–3174 (2004).
124. Hund, T. J. & Rudy, Y. in *Basis and Treatment of Cardiac Arrhythmias* 201–220 (Springer Berlin Heidelberg, 2006). at <http://link.springer.com/chapter/10.1007/3-540-29715-4_7>
125. Erickson, J. R. *et al.* A dynamic pathway for calcium-independent activation of CaMKII by methionine oxidation. *Cell* **133**, 462–474 (2008).
126. Christensen, M. D. *et al.* Oxidized Calmodulin Kinase II Regulates Conduction Following Myocardial Infarction: A Computational Analysis. *PLoS Comput Biol* **5**, e1000583 (2009).
127. Ursell, P., Gardner, P., Albala, A., Fenoglio, J. & Wit, A. Structural and electrophysiological changes in the epicardial border zone of canine myocardial infarcts during infarct healing. *Circ Res* **56**, 436–451 (1985).
128. Veeraraghavan, R. & Poelzing, S. Mechanisms underlying increased right ventricular conduction sensitivity to flecainide challenge. *Cardiovasc. Res.* **77**, 749–756 (2008).
129. Anderson, M. E., Higgins, L. S. & Schulman, H. Disease mechanisms and emerging therapies: protein kinases and their inhibitors in myocardial disease. *Nat Clin Pract Cardiovasc Med* **3**, 437–445 (2006).

130. Saucerman, J. J. & McCulloch, A. D. Cardiac β -Adrenergic Signaling: From Subcellular Microdomains to Heart Failure. *Annals of the New York Academy of Sciences* **1080**, 348–361 (2006).
131. Saucerman, J. J., Brunton, L. L., Michailova, A. P. & McCulloch, A. D. Modeling β -Adrenergic Control of Cardiac Myocyte Contractility in Silico. *J. Biol. Chem.* **278**, 47997–48003 (2003).
132. Lohse, M. J., Engelhardt, S. & Eschenhagen, T. What Is the Role of β -Adrenergic Signaling in Heart Failure? *Circ Res* **93**, 896–906 (2003).
133. Hoch, B., Meyer, R., Hetzer, R., Krause, E. G. & Karczewski, P. Identification and expression of delta-isoforms of the multifunctional Ca^{2+} /calmodulin-dependent protein kinase in failing and nonfailing human myocardium. *Circ. Res.* **84**, 713–721 (1999).
134. Curran, J., Hinton, M. J., Rios, E., Bers, D. M. & Shannon, T. R. β -Adrenergic Enhancement of Sarcoplasmic Reticulum Calcium Leak in Cardiac Myocytes Is Mediated by Calcium/Calmodulin-Dependent Protein Kinase. *Circ Res* **100**, 391–398 (2007).
135. Soltis, A. R. & Saucerman, J. J. Synergy between CaMKII substrates and β -adrenergic signaling in regulation of cardiac myocyte Ca^{2+} handling. *Biophys. J.* **99**, 2038–2047 (2010).
136. Marx, S. O. *et al.* Requirement of a macromolecular signaling complex for beta adrenergic receptor modulation of the KCNQ1-KCNE1 potassium channel. *Science* **295**, 496–499 (2002).
137. Saucerman, J. J., Healy, S. N., Belik, M. E., Puglisi, J. L. & McCulloch, A. D. Proarrhythmic consequences of a KCNQ1 AKAP-binding domain mutation: computational models of whole cells and heterogeneous tissue. *Circ. Res* **95**, 1216–1224 (2004).
138. Darbar, D., Roden, D. M., Ali, M. F., Yang, T. & Wathen, M. S. Himalayan T Waves in the Congenital Long-QT Syndrome. *Circulation* **111**, e161–e161 (2005).
139. Shimizu, W. & Antzelevitch, C. Differential effects of beta-adrenergic agonists and antagonists in LQT1, LQT2 and LQT3 models of the long QT syndrome. *J Am Coll Cardiol* **35**, 778–786 (2000).
140. Ahrens-Nicklas, R. C., Clancy, C. E. & Christini, D. J. Re-evaluating the efficacy of beta-adrenergic agonists and antagonists in long QT-3 syndrome through computational modelling. *Cardiovasc. Res* **82**, 439–447 (2009).
141. Faber, G. M. & Rudy, Y. Action potential and contractility changes in $[\text{Na}^{+}]_i$ overloaded cardiac myocytes: a simulation study. *Biophys. J.* **78**, 2392–2404 (2000).
142. Splawski, I. *et al.* Severe arrhythmia disorder caused by cardiac L-type calcium channel mutations. *Proc. Natl. Acad. Sci. U.S.A.* **102**, 8089–8096; discussion 8086–8088 (2005).
143. Sung, R. J. *et al.* Beta-adrenergic modulation of arrhythmogenesis and identification of targeted sites of antiarrhythmic therapy in Timothy (LQT8) syndrome: a theoretical study. *Am. J. Physiol. Heart Circ. Physiol.* **298**, H33–44 (2010).
144. Faber, G. M., Silva, J., Livshitz, L. & Rudy, Y. Kinetic Properties of the Cardiac L-Type Ca^{2+} Channel and Its Role in Myocyte Electrophysiology: A Theoretical Investigation. *Biophysical Journal* **92**, 1522–1543 (2007).
145. Heineke, J. & Molkentin, J. D. Regulation of cardiac hypertrophy by intracellular signalling pathways. *Nat Rev Mol Cell Biol* **7**, 589–600 (2006).
146. Crabtree, G. R. & Olson, E. N. NFAT signaling: choreographing the social lives of cells. *Cell* **109 Suppl**, S67–79 (2002).
147. Molkentin, J. D. *et al.* A calcineurin-dependent transcriptional pathway for cardiac hypertrophy. *Cell* **93**, 215–228 (1998).
148. Cooling, M., Hunter, P. & Crampin, E. J. Modeling Hypertrophic IP_3 Transients in the Cardiac Myocyte. *Biophys J* **93**, 3421–3433 (2007).
149. Leinwand, L. A. Calcineurin inhibition and cardiac hypertrophy: A matter of balance. *Proc Natl Acad Sci U S A* **98**, 2947–2949 (2001).

150. Hopkins, A. L. & Groom, C. R. The druggable genome. *Nat Rev Drug Discov* **1**, 727–730 (2002).
151. Kumar, N., Hendriks, B. S., Janes, K. A., de Graaf, D. & Lauffenburger, D. A. Applying computational modeling to drug discovery and development. *Drug Discov. Today* **11**, 806–811 (2006).
152. McGregor, E. & Dunn, M. J. Proteomics of the Heart: Unraveling Disease. *Circ Res* **98**, 309–321 (2006).
153. Mervaala, E. *et al.* Metabolomics in angiotensin II-induced cardiac hypertrophy. *Hypertension* **55**, 508–515 (2010).
154. Winslow, R. L., Rice, J., Jafri, S., Marban, E. & O'Rourke, B. Mechanisms of Altered Excitation-Contraction Coupling in Canine Tachycardia-Induced Heart Failure, II : Model Studies. *Circ Res* **84**, 571–586 (1999).
155. Winslow, R. L., Cortassa, S. & Greenstein, J. L. Using models of the myocyte for functional interpretation of cardiac proteomic data. *J. Physiol. (Lond.)* **563**, 73–81 (2005).
156. O'Rourke, B. *et al.* Mechanisms of Altered Excitation-Contraction Coupling in Canine Tachycardia-Induced Heart Failure, I Experimental Studies. *Circulation Research* **84**, 562–570 (1999).
157. McGregor, E. & Dunn, M. J. Proteomics of heart disease. *Human Molecular Genetics* **12**, R135–R144 (2003).
158. Berger, S. I., Ma'ayan, A. & Iyengar, R. Systems Pharmacology of Arrhythmias. *Sci. Signal.* **3**, ra30 (2010).
159. Pujol, A., Mosca, R., Farrés, J. & Aloy, P. Unveiling the role of network and systems biology in drug discovery. *Trends Pharmacol. Sci* **31**, 115–123 (2010).
160. Ma, X. H. *et al.* In-Silico Approaches to Multi-target Drug Discovery. *Pharm Res* **27**, 739–749 (2010).
161. Noble, D. Modeling the heart. *Physiology (Bethesda)* **19**, 191–197 (2004).
162. Trayanova, N. A. Whole-Heart Modeling: Applications to Cardiac Electrophysiology and Electromechanics. *Circ Res* **108**, 113–128 (2011).
163. Potse, M., Dubé, B., Richer, J., Vinet, A. & Gulrajani, R. M. A comparison of monodomain and bidomain reaction-diffusion models for action potential propagation in the human heart. *IEEE Trans Biomed Eng* **53**, 2425–2435 (2006).
164. Sato, D. *et al.* Acceleration of cardiac tissue simulation with graphic processing units. *Med Biol Eng Comput* **47**, 1011–1015 (2009).
165. Vicini, P. Multiscale Modeling in Drug Discovery and Development: Future Opportunities and Present Challenges. *Clin Pharmacol Ther* **88**, 126–129 (2010).
166. Katzung, B. G., Masters, S. & Trevor, A. *Basic and Clinical Pharmacology 12/E*. (McGraw Hill Professional, 2011).
167. Michelson, S., Sehgal, A. & Friedrich, C. In silico prediction of clinical efficacy. *Curr. Opin. Biotechnol* **17**, 666–670 (2006).
168. Wu, F. T. H., Stefanini, M. O., Mac Gabhann, F. & Popel, A. S. A compartment model of VEGF distribution in humans in the presence of soluble VEGF receptor-1 acting as a ligand trap. *PLoS ONE* **4**, e5108 (2009).
169. Bers, D. M. Cardiac excitation-contraction coupling. *Nature* **415**, 198–205 (2002).
170. Cheng, H., Lederer, W. & Cannell, M. Calcium sparks: elementary events underlying excitation-contraction coupling in heart muscle. *Science* **262**, 740–744 (1993).
171. DeSantiago, J., Maier, L. S. & Bers, D. M. Frequency-dependent Acceleration of Relaxation in the Heart Depends on CaMKII, but not Phospholamban. *Journal of Molecular and Cellular Cardiology* **34**, 975–984 (2002).
172. Cheng, H., Lederer, M. R., Lederer, W. J. & Cannell, M. B. Calcium sparks and [Ca²⁺]_i waves in cardiac myocytes. *American Journal of Physiology - Cell Physiology* **270**, C148 – C159 (1996).

173. Gee, K. R. *et al.* Chemical and physiological characterization of fluo-4 Ca²⁺-indicator dyes. *Cell Calcium* **27**, 97–106 (2000).
174. Nickola, M. W. *et al.* Leptin Attenuates Cardiac Contraction in Rat Ventricular Myocytes : Role of NO. *Hypertension* **36**, 501–505 (2000).
175. Guatimosim, S., Guatimosim, C. & Song, L.-S. Imaging calcium sparks in cardiac myocytes. *Methods Mol. Biol* **689**, 205–214 (2011).
176. Darrow, B. J., Fast, V. G., Kleber, A. G., Beyer, E. C. & Saffitz, J. E. Functional and Structural Assessment of Intercellular Communication: Increased Conduction Velocity and Enhanced Connexin Expression in Dibutyryl cAMP- Treated Cultured Cardiac Myocytes. *Circ Res* **79**, 174–183 (1996).
177. Bers, D. M., Lederer, W. J. & Berlin, J. R. Intracellular Ca transients in rat cardiac myocytes: role of Na-Ca exchange in excitation-contraction coupling. *American Journal of Physiology - Cell Physiology* **258**, C944 –C954 (1990).
178. A Threshold Selection Method from Gray-Level Histograms. *Systems, Man and Cybernetics, IEEE Transactions on* **9**, 62–66 (1979).
179. Bishop, S. P. & Drummond, J. L. Surface morphology and cell size measurement of isolated rat cardiac myocytes. *Journal of Molecular and Cellular Cardiology* **11**, 423–430 (1979).
180. Li, G.-R. & Baumgarten, C. M. Modulation of cardiac Na⁺ current by gadolinium, a blocker of stretch-induced arrhythmias. *American Journal of Physiology - Heart and Circulatory Physiology* **280**, H272 –H279 (2001).
181. Saucerman, J. J., Brunton, L. L., Michailova, A. P. & McCulloch, A. D. Modeling {beta}-Adrenergic Control of Cardiac Myocyte Contractility in Silico. *J. Biol. Chem.* **278**, 47997–48003 (2003).
182. Saucerman, J. J. *et al.* Systems analysis of PKA-mediated phosphorylation gradients in live cardiac myocytes. *Proc. Natl. Acad. Sci. U.S.A.* **103**, 12923–12928 (2006).
183. Yang, J. H. & Saucerman, J. J. Phospholemman is a negative feed-forward regulator of Ca²⁺ in β -adrenergic signaling, accelerating β -adrenergic inotropy. *J. Mol. Cell. Cardiol.* **52**, 1048–1055 (2012).
184. Sorger, P. K. & Schoeberl, B. An expanding role for cell biologists in drug discovery and pharmacology. *Mol. Biol. Cell* **23**, 4162–4164 (2012).
185. Saucerman, J. J., Brunton, L. L., Michailova, A. P. & McCulloch, A. D. Modeling {beta}-Adrenergic Control of Cardiac Myocyte Contractility in Silico. *J. Biol. Chem.* **278**, 47997–48003 (2003).
186. De Lean, A., Stadel, J. M. & Lefkowitz, R. J. A ternary complex model explains the agonist-specific binding properties of the adenylate cyclase-coupled beta-adrenergic receptor. *Journal of Biological Chemistry* **255**, 7108 –7117 (1980).
187. Varma, D. R. *et al.* Inverse agonist activities of β -adrenoceptor antagonists in rat myocardium. *Br J Pharmacol* **127**, 895–902 (1999).
188. Samama, P., Cotecchia, S., Costa, T. & Lefkowitz, R. J. A mutation-induced activated state of the beta 2-adrenergic receptor. Extending the ternary complex model. *Journal of Biological Chemistry* **268**, 4625 –4636 (1993).
189. Rosenbaum, D. M. *et al.* Structure and function of an irreversible agonist-[bgr]2 adrenoceptor complex. *Nature* **469**, 236–240 (2011).
190. Amanfu, R. K., Muller, J. B. & Saucerman, J. J. Automated image analysis of cardiac myocyte Ca²⁺ dynamics. in *2011 Annual International Conference of the IEEE Engineering in Medicine and Biology Society, EMBC* 4661–4664 (IEEE, 2011). doi:10.1109/IEMBS.2011.6091154
191. Allen, M. D. & Zhang, J. Subcellular dynamics of protein kinase A activity visualized by FRET-based reporters. *Biochem Biophys Res Commun* **348**, 716–21 (2006).

192. Chen, Y. & Periasamy, A. Intensity Range Based Quantitative FRET Data Analysis to Localize Protein Molecules in Live Cell Nuclei. *J Fluoresc* **16**, 95–104 (2006).
193. Vila Petroff, M. G., Egan, J. M., Wang, X. & Sollott, S. J. Glucagon-like peptide-1 increases cAMP but fails to augment contraction in adult rat cardiac myocytes. *Circ. Res.* **89**, 445–452 (2001).
194. Vittone, L., Mundiña-Weilenmann, C., Said, M. & Mattiazzi, A. Mechanisms Involved in the Acidosis Enhancement of the Isoproterenol-induced Phosphorylation of Phospholamban in the Intact Heart. *J. Biol. Chem.* **273**, 9804–9811 (1998).
195. Hoffmann, C., Leitz, M. R., Oberdorf-Maass, S., Lohse, M. J. & Klotz, K.-N. Comparative pharmacology of human beta-adrenergic receptor subtypes--characterization of stably transfected receptors in CHO cells. *Naunyn Schmiedebergs Arch Pharmacol* **369**, 151–9 (2004).
196. Metra, M. *et al.* Differential Effects of β -Blockers in Patients With Heart Failure: A Prospective, Randomized, Double-Blind Comparison of the Long-Term Effects of Metoprolol Versus Carvedilol. *Circulation* **102**, 546–551 (2000).
197. Shin, J. & Johnson, J. β -Blocker pharmacogenetics in heart failure. *Heart Failure Reviews* doi:10.1007/s10741-008-9094-x
198. Harding, S. E. *et al.* Isolated ventricular myocytes from failing and non-failing human heart; the relation of age and clinical status of patients to isoproterenol response. *Journal of Molecular and Cellular Cardiology* **24**, 549–564 (1992).
199. Roth, D. M. *et al.* Cardiac-Directed Adenylyl Cyclase Expression Improves Heart Function in Murine Cardiomyopathy. *Circulation* **99**, 3099–3102 (1999).
200. Reinkober, J. *et al.* Targeting GRK2 by gene therapy for heart failure: benefits above β -blockade. *Gene Therapy* **19**, 686–693 (2012).
201. Yang, J. H. & Saucerman, J. J. Phospholemman is a negative feed-forward regulator of Ca^{2+} in β -adrenergic signaling, accelerating β -adrenergic inotropy. *Journal of Molecular and Cellular Cardiology* **52**, 1048–1055 (2012).
202. Saucerman, J. J., Healy, S. N., Belik, M. E., Puglisi, J. L. & McCulloch, A. D. Proarrhythmic consequences of a KCNQ1 AKAP-binding domain mutation: computational models of whole cells and heterogeneous tissue. *Circ. Res.* **95**, 1216–1224 (2004).
203. Poole-Wilson, P. A. *et al.* Comparison of carvedilol and metoprolol on clinical outcomes in patients with chronic heart failure in the Carvedilol Or Metoprolol European Trial (COMET): randomised controlled trial. *The Lancet* **362**, 7–13 (2003).
204. Kveiborg, B., Major-Petersen, A., Christiansen, B. & Torp-Pedersen, C. Carvedilol in the treatment of chronic heart failure: Lessons from The Carvedilol Or Metoprolol European Trial. *Vasc Health Risk Manag* **3**, 31–37 (2007).
205. Kindermann, M. *et al.* Carvedilol but not metoprolol reduces beta-adrenergic responsiveness after complete elimination from plasma in vivo. *Circulation* **109**, 3182–3190 (2004).
206. Johnson, J. A. & Liggett, S. B. Cardiovascular Pharmacogenomics of Adrenergic Receptor Signaling: Clinical Implications and Future Directions. *Clin Pharmacol Ther* **89**, 366–378 (2011).
207. Zamah, A. M., Delahunty, M., Luttrell, L. M. & Lefkowitz, R. J. PKA-mediated phosphorylation of the beta 2-adrenergic receptor regulates its coupling to Gs and Gi: Demonstration in a reconstituted system. *J. Biol. Chem.* M202753200 (2002). doi:10.1074/jbc.M202753200
208. Bristow, M. R., Feldman, A. M., Adams Jr., K. F. & Goldstein, S. Selective versus nonselective β -blockade for heart failure therapy: are there lessons to be learned from the COMET trial? *Journal of Cardiac Failure* **9**, 444–453 (2003).
209. Cohn, J. N. *et al.* Plasma norepinephrine as a guide to prognosis in patients with chronic congestive heart failure. *N. Engl. J. Med.* **311**, 819–823 (1984).

210. Goldstein, D. S., McCarty, R., Polinsky, R. J. & Kopin, I. J. Relationship between plasma norepinephrine and sympathetic neural activity. *Hypertension* **5**, 552–559 (1983).
211. Lohse, M. J., Engelhardt, S. & Eschenhagen, T. What Is the Role of {beta}-Adrenergic Signaling in Heart Failure? *Circ Res* **93**, 896–906 (2003).
212. Kubo, H., Margulies, K. B., Piacentino, V., 3rd, Gaughan, J. P. & Houser, S. R. Patients with end-stage congestive heart failure treated with beta-adrenergic receptor antagonists have improved ventricular myocyte calcium regulatory protein abundance. *Circulation* **104**, 1012–1018 (2001).
213. Iaccarino, G. *et al.* Elevated myocardial and lymphocyte GRK2 expression and activity in human heart failure. *Eur Heart J* **26**, 1752–1758 (2005).
214. Meyer, M. *et al.* Alterations of sarcoplasmic reticulum proteins in failing human dilated cardiomyopathy. *Circulation* **92**, 778–784 (1995).
215. Lou, Q., Janardhan, A. & Efimov, I. R. Remodeling of calcium handling in human heart failure. *Adv. Exp. Med. Biol.* **740**, 1145–1174 (2012).
216. Ogletree-Hughes, M. L. *et al.* Mechanical unloading restores beta-adrenergic responsiveness and reverses receptor downregulation in the failing human heart. *Circulation* **104**, 881–886 (2001).
217. Amanfu, R. K. & Saucerman, J. J. Cardiac models in drug discovery and development: a review. *Crit Rev Biomed Eng* **39**, 379–395 (2011).
218. Gjuvsland, A. B., Vik, J. O., Beard, D. A., Hunter, P. J. & Omholt, S. W. Bridging the genotype-phenotype gap: what does it take? *J. Physiol. (Lond.)* **591**, 2055–2066 (2013).
219. Britton, O. J. *et al.* Experimentally calibrated population of models predicts and explains intersubject variability in cardiac cellular electrophysiology. *Proc Natl Acad Sci U S A* **110**, E2098–E2105 (2013).
220. Walmsley, J. *et al.* mRNA Expression Levels in Failing Human Hearts Predict Cellular Electrophysiological Remodeling: A Population-Based Simulation Study. *PLoS ONE* **8**, e56359 (2013).
221. CardioGenomics: Homepage. at <<http://cardiogenomics.med.harvard.edu/home>>
222. Duan, D. Phenomics of cardiac chloride channels: the systematic study of chloride channel function in the heart. *J. Physiol. (Lond.)* **587**, 2163–2177 (2009).
223. Ziolo, M. T. *et al.* Myocyte Nitric Oxide Synthase 2 Contributes to Blunted β -Adrenergic Response in Failing Human Hearts by Decreasing Ca^{2+} Transients. *Circulation* **109**, 1886–1891 (2004).
224. Spann, J. F., Bove, A. A., Natarajan, G. & Kreulen, T. Ventricular performance, pump function and compensatory mechanisms in patients with aortic stenosis. *Circulation* **62**, 576–582 (1980).
225. Davies, C. H. *et al.* Reduced Contraction and Altered Frequency Response of Isolated Ventricular Myocytes From Patients With Heart Failure. *Circulation* **92**, 2540–2549 (1995).
226. Beuckelmann, D. J., Näbauer, M. & Erdmann, E. Intracellular calcium handling in isolated ventricular myocytes from patients with terminal heart failure. *Circulation* **85**, 1046–1055 (1992).
227. Bers, D. M., Eisner, D. A. & Valdivia, H. H. Sarcoplasmic Reticulum Ca^{2+} and Heart Failure Roles of Diastolic Leak and Ca^{2+} Transport. *Circulation Research* **93**, 487–490 (2003).
228. Movsesian, M. A., Karimi, M., Green, K. & Jones, L. R. Ca^{2+} -transporting ATPase, phospholamban, and calsequestrin levels in nonfailing and failing human myocardium. *Circulation* **90**, 653–657 (1994).
229. Schwinger, R. H. *et al.* Unchanged protein levels of SERCA II and phospholamban but reduced Ca^{2+} uptake and Ca^{2+} -ATPase activity of cardiac sarcoplasmic reticulum from dilated cardiomyopathy patients compared with patients with nonfailing hearts. *Circulation* **92**, 3220–3228 (1995).

230. Margulies, K. B. & Houser, S. R. in *Heart Failure: A Companion to Braunwald's Heart Disease (Second Edition)* (Mann, D. L.) 32–47 (W.B. Saunders, 2011). at <<http://www.sciencedirect.com/science/article/pii/B9781416058953100038>>
231. Schillinger, W. *et al.* Influence of SR Ca²⁺-ATPase and Na⁺-Ca²⁺-exchanger on the force-frequency relation. *Basic Research in Cardiology, Supplement* **93**, 38–45 (1998).
232. Chaudhary, K. W. *et al.* Altered myocardial Ca²⁺ cycling after left ventricular assist device support in the failing human heart. *J. Am. Coll. Cardiol.* **44**, 837–845 (2004).
233. Sarkar, A. X. & Sobie, E. A. Regression analysis for constraining free parameters in electrophysiological models of cardiac cells. *PLoS Comput. Biol* **6**, e1000914 (2010).
234. Bousette, N. *et al.* Large-scale characterization and analysis of the murine cardiac proteome. *J. Proteome Res.* **8**, 1887–1901 (2009).
235. Shannon, T. R., Wang, F., Puglisi, J., Weber, C. & Bers, D. M. A mathematical treatment of integrated Ca dynamics within the ventricular myocyte. *Biophys. J.* **87**, 3351–3371 (2004).
236. Niederer, S. A., Fink, M., Noble, D. & Smith, N. P. A meta-analysis of cardiac electrophysiology computational models. *Experimental Physiology* **94**, 486–495 (2009).
237. Poole-Wilson, P. A. *et al.* Comparison of carvedilol and metoprolol on clinical outcomes in patients with chronic heart failure in the Carvedilol Or Metoprolol European Trial (COMET): randomised controlled trial. *Lancet* **362**, 7–13 (2003).
238. Remme, W. J. *et al.* Carvedilol Protects Better Against Vascular Events Than Metoprolol in Heart Failure: Results From COMET. *Journal of the American College of Cardiology* **49**, 963–971 (2007).
239. NOBLE, D. A modification of the Hodgkin--Huxley equations applicable to Purkinje fibre action and pace-maker potentials. *J. Physiol. (Lond.)* **160**, 317–352 (1962).
240. Ahmet, I. *et al.* Cardioprotective and Survival Benefits of Long-term Combined Therapy with β_2 AR Agonist and β_1 AR Blocker in Dilated Cardiomyopathy Post-Myocardial Infarction. *J Pharmacol Exp Ther* jpet.107.135335 (2008). doi:10.1124/jpet.107.135335
241. Kjelsberg, M. A., Cotecchia, S., Ostrowski, J., Caron, M. G. & Lefkowitz, R. J. Constitutive activation of the alpha 1B-adrenergic receptor by all amino acid substitutions at a single site. Evidence for a region which constrains receptor activation. *J. Biol. Chem* **267**, 1430–1433 (1992).
242. Engelhardt, S., Grimmer, Y., Fan, G. H. & Lohse, M. J. Constitutive activity of the human beta(1)-adrenergic receptor in beta(1)-receptor transgenic mice. *Mol. Pharmacol* **60**, 712–717 (2001).